Titre: Title:	Dynamic Modeling, Monitoring and Control of Staged Microbial Fuel Cells
Auteur: Author:	Didac Recio Garrido
Date:	2016
Type:	Mémoire ou thèse / Dissertation or Thesis
Référence: Citation:	Recio Garrido, D. (2016). Dynamic Modeling, Monitoring and Control of Staged Microbial Fuel Cells [Thèse de doctorat, École Polytechnique de Montréal]. PolyPublie. https://publications.polymtl.ca/2356/

UNIVERSITÉ DE MONTRÉAL

DYNAMIC MODELING, MONITORING AND CONTROL OF STAGED MICROBIAL FUEL CELLS

DIDAC RECIO GARRIDO

DÉPARTEMENT DE GÉNIE CHIMIQUE

ÉCOLE POLYTECHNIQUE DE MONTRÉAL

THÈSE PRÉSENTÉE EN VUE DE L'OBTENTION

DU DIPLÔME DE PHILOSOPHIAE DOCTOR

(GÉNIE CHIMIQUE)

OCTOBRE 2016

UNIVERSITÉ DE MONTRÉAL

ÉCOLE POLYTECHNIQUE DE MONTRÉAL

Cette thèse intitulée:

DYNAMIC MODELING, MONITORING AND CONTROL OF STAGED MICROBIAL FUEL CELLS

présentée par : RECIO GARRIDO Didac

en vue de l'obtention du diplôme de : Philosophiae Doctor

a été dûment acceptée par le jury d'examen constitué de :

M. HENRY Olivier, Ph. D., président

M. PERRIER Michel, Ph. D., membre et directeur de recherche

M. TARTAKOVSKY Boris, Ph. D., membre et codirecteur de recherche

M. SRINIVASAN Bala, Ph. D., membre

M. BUDMAN Hector, Ph. D., membre

DEDICATION

This thesis is dedicated to

My parents,

Diego Recio Galán & Rosa Garrido Rodríguez

ACKNOWLEDGEMENTS

The completion of this thesis would not have been possible without the invaluable support of my supervisors, Professor Michel Perrier and Boris Tartakovsky, to whom I am immensely grateful for their effort and dedication. Your knowledge, guidance, persistence, patience and motivation have been fundamental to my training as a researcher.

Merci aux institutions, l'École Polytechnique de Montréal et le Conseil National de Recherches Canada, pour permettre aux étudiants d'encadrer ses études au doctorat dans une collaboration université-organisme de recherche gouvernemental. Merci, encore une fois, Boris et Michel, pour la rendre possible et avoir vécu une expérience très enrichissante et inoubliable.

All the colleagues from NRC, Michelle, Ruxandra, Javier, Charles-David, Caroline and Fred, thanks for your valuable comments and technical expertise. Also a special thanks to Azfar, Ademola and Wassila, fellow Ph.D. sufferers.

Je tiens également à remercier Guillaume, Srini et Michel de me faire confiance pour être plusieurs fois chargé de TD de dynamique des systèmes ainsi que d'opérations unitaires. J'ai beaucoup appris de l'expérience et je me suis aussi amusée.

I would also like to extend my gratitude and friendship to the students from GERAD, Elspeth, Trish and Thibault. Y, por supuesto, gracias a todos los compañeros de fatigas que están ahí des del principio, Nury, Juan y Álvaro. Y también a los que se incorporaron más tarde, Jesús, Manuel, Jaime, Sandra, Richard, Shirley, Pau y Mar. Espero que la amistad perdure independientemente de lo que nos depare el futuro.

Finalment, agraïr-li al meu pare el seu continu recolzament durant aquests darrers quatre anys i mig a Montreal. Tot i la gran llunyania, encara saps quan cal esbroncar-me per tal de fer-me rumiar i redreçar-me pel bon camí. Un fort agraïment també als meus oncles i cosins per les seves continues paraules d'afecte que em fan seguir endavant. I, per últim, no em vull oblidar tampoc de donar les gràcies a la Carme i a la seva familia per la seva afectuosa acollida. M'omple de joia veure que mon pare es troba en tant bona companyia durant la meva llarga absència.

RÉSUMÉ

Le développement humain est étroitement lié à la disponibilité d'énergie et, dans la même mesure, d'eau. La demande croissante de la production d'énergie consomme de grandes quantités d'eau, ainsi des quantités importantes d'énergie sont nécessaires pour le traitement des eaux usées. En prenant en considération le fait que les piles à combustible microbiennes (PCMs) sont capables de la production directe d'électricité à partir de déchets organiques dilués, elles présentent une excellente occasion pour développer une nouvelle technologie de traitement des eaux usées qui pourrait contribuer à résoudre ce dilemme. La polyvalence des PCMs pour fonctionner en utilisant une grande variété d'eaux usées industrielles et domestiques résulte de l'activité biocatalytique de leur biofilm. Les bactéries anaérobies électricigènes qui peuplent le compartiment anodique, transfèrent des électrons issus de l'oxydation de la matière organique à un accepteur d'électrons externe, l'anode. Lorsqu'on alimente les PCMs avec les eaux usées, l'électricité est récupérée à partir de la consommation de la matière organique dans le compartiment anodique, conduisant ainsi à un processus de traitement des eaux usées qui produit de l'énergie.

Plusieurs études récentes ont démontré la grande capacité de stockage de charge dans les biofilms électrochimiques. Par exemple, le fonctionnement des PCMs avec modulation de la période de pulsation (*pulse width modulation:* PWM) ou d'une connexion intermittente de la résistance externe ont démontré que la capacité interne de biofilms anodiques conduit à un comportement non-linéaire complexe, qui combine charge/décharge avec une dynamique rapide, c'est-à-dire, avec des constantes de temps dans l'ordre de quelques millisecondes, avec une dynamique beaucoup plus lente de la croissance et de la décomposition du biofilm microbien, c'est-à-dire, avec des constantes de temps de l'ordre d'heures à quelques jours. Deux modèles déjà existants, dont les circuits électriques équivalents (CEE) décrivent la dynamique rapide électrique du biofilm anodique et dont les modèles bioélectrochimiques décrivent la dynamique lente de croissance de la biomasse et de la consommation de substrat. Cependant, aucun ne décrit les dynamiques complexes combinés causées par l'opération électrique intermittente. Des nouvelles méthodes de gestion de la puissance exploitent la capacité interne des PCMs de surmonter les pertes de puissance importantes causées par une inadéquation entre les résistances internes et externes. Pourtant, il y a un manque évident de stratégies de contrôle capables de répondre aux dynamiques multi-échelles liées à la double

nature biologique et électrique des PCMs. On peut toutefois supposer que l'un des motifs implique l’absence de mesures en temps réel de la concentration du substrat dans l'effluent.

Visant à évaluer l'impact du stockage de charge sur la performance des PCMs, la première contribution de cette thèse consiste au développement d'un modèle combiné bioélectrochimique-électrique (CBE) d'une PCM. En plus de décrire le stockage de la charge, le modèle CBE est aussi en mesure de décrire la dynamique multi-échelles non linéaire des PCMs en fusionnant des bilans de masse et d'électrons avec des équations décrivant un circuit électrique équivalent. La validation expérimentale et l'estimation des paramètres ont été effectuées en utilisant les résultats d’opération des PCMs avec une connexion PWM de la résistance externe. Le modèle CBE montre une précision acceptable pour décrire le comportement dynamique rapide et lent qui est observée dans la tension électrique produite par la PCM, tout en étant capable de prédire de manière adéquate la concentration du substrat à la sortie du réacteur. En outre, le modèle CBE est utilisé pour étudier qualitativement l'effet du cycle de service et la fréquence de commutation sur la performance des PCMs. L'augmentation de la fréquence de commutation du PWM favorise la population des bactéries électricigènes sur les méthanogènes pour des valeurs plus élevées de la résistance externe apparente. Ainsi, la puissance maximale présente un plateau allant de 100% à des valeurs du rapport cyclique inférieurs (environ 90%) ce qui confirme l'effet positif du fonctionnement intermittent de la résistance extérieure à la production d'électricité, même pendant des écarts avec la valeur de la résistance interne.

La deuxième contribution de cette thèse est le développement de stratégies pour la surveillance de la qualité de l’effluent à partir de la mesure en temps réel des variables électriques. Une première approche consiste à simplifier le modèle CBE à une seule équation qui intègre le courant électrique comme une entrée dans le bilan de masse du substrat. Cette approche dynamique est valable dans toute la gamme des concentrations de l’effluent et nécessite l'estimation d'un seul paramètre qui relie le courant produit à la vitesse de substrat consommé. Pourtant, il faut que la concentration du substrat à l’entrée du réacteur soit connue. La seconde approche permet de surmonter cette limitation en décrivant le courant électrique en fonction de la concentration du substrat de l'effluent. La cinétique du modèle CBE suggère une expression type Monod avec l'ajout d'un terme limitant à des faibles concentrations de substrat dans l'effluent. Dans ce cas, trois paramètres doivent être estimés ce qui nécessite des mesures historiques. Des approximations à des faibles concentrations de l'effluent qui nécessitent l'estimation d'un seul paramètre sont également suggérées.

Malheureusement, puisque toutes les stratégies sont basées sur des estimations en boucle ouverte, la convergence à la valeur réelle n’est pas garantie.

Enfin, la troisième contribution de cette thèse propose une configuration de contrôle centralisé adapté pour le contrôle de la qualité des effluents en deux PCMs en série. La configuration des réacteurs en série est une technique largement répandue dans le cadre du traitement des eaux usées. Elle est utilisée pour augmenter les taux de consommation de la source de carbone et réduire les limitations de source de carbone liées à la cinétique microbienne. La commande centralisée proposée est constituée d'un régulateur PID pour commander le débit d'écoulement, et un dispositif de commande ON/OFF pour ajuster la connexion de la résistance externe de la première PCM. La comparaison avec une configuration de contrôle décentralisé qui utilise PIDs en cascade pour le contrôle du débit est aussi montrée. Dans les deux cas, l’opération électrique des PCMs en série est maintenue indépendante entre les cellules. Les résultats expérimentaux montrent un grand dépassement dans le débit manipulé lors de l'utilisation des PIDs en cascade décentralisées. En comparaison, les simulations du PID avec ON/OFF de la configuration de contrôle centralisé montrent un contrôle du débit plus rapide et sans dépassement, tout en étant capable de faire face à des perturbations dans la concentration à l’entrée du réacteur. De plus, la concentration du substrat dans l'effluent est maintenu dans des tolérances acceptables. Fondamentalement, le dispositif de commande ON/OFF utilise la résistance externe comme un équivalent électrique pour contourner hydrauliquement le premier réacteur lorsque des conditions de substrat sont trop faibles dans le deuxième réacteur.

ABSTRACT

Human development is intricately linked to both energy and water availability. Increasing demands for energy production require vast amounts of water consumption. At the same time, significant amounts of energy are required for wastewater treatment. With this respect, microbial fuel cells (MFCs), which are capable of direct electricity production from diluted organic wastes, present an excellent opportunity to develop a novel wastewater treatment technology that could contribute to resolving this dilemma. MFCs' versatility to operate using a wide variety of industrial and domestic wastewaters arises from their biofilm biocatalytic activity. Anaerobic exoelectricigenic bacteria that populate the anodic compartment, transfer electrons derived from the oxidation of organic matter to an external electron acceptor, the anode. When feeding MFCs with wastewater, electricity is recovered from the consumption of the organic matter in the anodic compartment, thus resulting in an energy-producing wastewater treatment process.

Several recent studies demonstrated significant charge storage capacity in electrochemical biofilms. For instance, MFC operation with pulse-width modulated (PWM) or intermittent connection of the external resistance demonstrated that internal capacitance of anodic biofilms leads to complex non-linear behavior. Such behavior combines fast charge/discharge dynamics, i.e., with time constants in the order of milliseconds, with much slower dynamics of microbial biofilm growth and decay, i.e. with time constants in the order of hours to days. Already existent electrical equivalent circuit (EEC) models describe fast electrical dynamics of the anodic biofilm and bioelectrochemical models describe slow biomass growth and substrate consumption dynamics. However, none is able to describe the combined complex dynamics. Meanwhile, novel power management methods exploit such internal MFC capacitance to overcome the significant power losses caused by a mismatch between the external and internal resistances. Yet, there is an obvious lack of control strategies capable of addressing the multi-scale dynamics linked to the dual biological and electrical nature of MFCs. Presumably, one of the reasons involves the difficulty of real time measurements of the effluent substrate concentration.

Aiming to evaluate the impact of charge storage on MFC performance, the first contribution of this thesis consists in the development of a combined bioelectrochemical–electrical (CBE) model of an MFC. In addition to charge storage, the CBE model is able to describe the multi-scale nonlinear

dynamics of MFCs by merging mass and electron balances with equations describing an equivalent electrical circuit. Experimental validation and parameter estimation were performed using results of MFC operation with PWM connection of the external resistance. The CBE model shows an acceptable accuracy when describing both fast and slow dynamic behavior observed in the electric voltage produced by the MFC, while also being able to adequately predict the output substrate concentration. Furthermore, the CBE model is used to qualitatively study the effect of duty cycle and switching frequency on MFC performance. Increasing the switching frequency favors the exoelectricigenic over the methanogenic population for higher values of the apparent external resistance. Thus, maximum power presents a plateau ranging from 100 % to lower duty cycles (around 90 %) which corroborates the positive effect of the intermittent operation of the external resistance on the electricity production even during mismatch with the internal resistance value.

The second contribution of this PhD thesis is the development of strategies for MFC effluent quality monitoring from the real time measurement of the electrical variables. A first approach simplifies the CBE model to a single equation that incorporates the electric current as an input into the substrate mass balance. This dynamic approach is valid in the whole range of effluent concentrations and requires the estimation of a single parameter relating the current produced to the rate of substrate consumed. Yet, it requires for the influent substrate concentration to be known. The second approach overcomes such limitation by describing the electric current as a function of the effluent substrate concentration. Kinetics of the CBE model suggest a Monod expression with the addition of a limiting term at low effluent concentrations. In this case, three parameters need to be estimated and therefore, it necessitates information from historical records. Approximations at low effluent concentrations are also suggested that only require the estimation of a single parameter. Unfortunately, because all the strategies are based on open-loop estimations, convergence to the true value is not guaranteed.

Finally, the third contribution of this thesis proposes a centralized control configuration suitable for effluent quality control in two staged MFCs. Reactor staging is a technique widely used in the context of wastewater treatment. It is used to increase carbon source consumption rates and reduce carbon source limitations related to microbial kinetics. The centralized control configuration consists of a PID to control the flow rate and an ON/OFF controller to adjust the connection of the external resistance in the first MFC. A comparison is made with a decentralized control configuration that uses PIDs in cascade for the control of the flow rate. In both cases, the electrical

operation of the staged MFCs is kept independent between the cells. Experimental results show a big overshoot in the manipulated flow rate when using the decentralized cascade PIDs. Meanwhile simulations of the centralized PID-ON/OFF control configuration result in a quicker flow rate control with no overshoot and the ability to cope with disturbances in the influent concentration whilst keeping the effluent concentration within acceptable tolerances. Basically, the ON/OFF controller uses the external resistance as an electrical equivalent to hydraulically bypassing the first cell when substrate deplete conditions occur in the second cell.

TABLE OF CONTENTS

DEDICATION III

ACKNOWLEDGEMENTS IV

RÉSUMÉ V

ABSTRACT VIII

TABLE OF CONTENTS XI

LIST OF FIGURES XIV

LIST OF TABLES XVI

LIST OF SYMBOLS XVII

LIST OF ABBREVIATIONS XXI

LIST OF APPENDICES XXII

CHAPTER 1 INTRODUCTION 1

1.1 Motivation 1

1.2 Problem definition 2

1.3 Objectives 4

1.4 Thesis structure 4

CHAPTER 2 STATE OF THE ART IN MODELING, OPTIMIZATION AND CONTROL OF BIOELECTROCHEMICAL SYSTEMS 6

2.1 Dynamic modeling 7

2.1.1 Single-species ideal mixing modeling 7

2.1.2 Simplified biofilm modeling 10

2.1.3 Reaction-diffusion biofilm modeling 11

2.1.4 Equivalent electrical circuit modeling 13

2.1.5 Model comparison 15

2.2 Control and optimization of BESs 17
2.2.1 Energy harvesting and power control approaches 18
2.2.2 Model-based optimization and control strategies 21
2.3 Perspectives 25
CHAPTER 3 MATERIALS AND METHODS 26
3.1 MFC design and operation 26
3.2 Analytical methods, inoculum and media composition 28
3.3 Numerical methods and calculations 28
CHAPTER 4 COMBINED BIOELECTROCHEMICAL-ELECTRICAL MFC MODEL 31
4.1 Model formulation and structure 31
4.2 Sensitivity analysis 36
4.3 Parameter estimation 38
4.4 Conclusion 43
CHAPTER 5 EFFECT OF PERIODIC CONNECTION OF THE EXTERNAL RESISTANCE ON MFC PERFORMANCE 45
5.1 Anode capacitance impact on MFC operation 45
5.2 Effect of Duty Cycle and Switching Frequency 47
5.3 Conclusion 50
CHAPTER 6 EFFLUENT QUALITY ESTIMATION 51
6.1 Simplified mass balance 51
6.2 Algebraic expression for the electric current 52
6.3 Importance of R_{ext} operation 57
6.4 Online effluent estimation from the electric current 58
6.5 Conclusion 60

CHAPTER 7 STAGED MFCS FOR WASTEWATER TREATMENT 62

7.1 Dynamic modeling using the CBE model 62

7.2 Effluent quality monitoring 68

7.3 Effluent quality control 72

7.4 Conclusion 77

CHAPTER 8 CONCLUSION, SCIENTIFIC CONTRIBUTION AND PERSPECTIVES 79

8.1 Conclusion 79

8.2 Scientific contribution 81

8.3 Perspectives and recommendations 83

BIBLIOGRAPHY 86

APPENDIX A 95

LIST OF FIGURES

Figure 2.1: MFC modeling approaches....9

Figure 2.2: Regions with the largest treatment capacity in two staged MFCs....22

Figure 3.1: Experimental setup 27

Figure 4.1: Schematic diagram of the CBE model....32

Figure 4.2: Structure for the two CBE model implementations....36

Figure 4.3: Sensitivity profiles for the estimated parameters....37

Figure 4.4: 95 % ellipses of confidence for the CBE model....40

Figure 4.5: Results for the CBE “simulation” model....42

Figure 4.6: Results for the CBE “parameter observer based” model.....43

Figure 5.1: MFC power output estimated for three modes of operation....46

Figure 5.2: Effect of duty cycle and switching frequency on the effluent carbon source....48

Figure 5.3: Effect of duty cycle and switching frequency on the electrical performance....49

Figure 6.1: Electric current and I_{max} dependence on the effluent substrate concentration....54

Figure 6.2: Dependence of the electrical variables with respect to the effluent concentration....55

Figure 6.3: Approximations of the simulated electric current at low effluent concentrations.....56

Figure 6.4: Variations in the electric current and effluent substrate concentration profile....57

Figure 6.5: Simulation of effluent substrate concentration estimation from the electric current...59

Figure 7.1: Results for the CBE “simulation” model for two staged MFCs....64

Figure 7.2: Results for the CBE “parameter observer based” model for two staged MFCs....65

Figure 7.3: Online estimation values for the electrical variables for the two staged MFCs....66

Figure 7.4: Experimental online effluent substrate concentration monitoring in staged MFCs 69

Figure 7.5: Experimental values of electric current as a function of the effluent concentration ...71

Figure 7.6: Block diagram for the hydraulic cascade control configuration.....73

Figure 7.7: Performance of staged MFCs operated with P/O and a PID cascade control 74

Figure 7.8: Simple effluent quality control strategy for staged MFCs.....75

Figure 7.9: Block diagram for the PID and ON/OFF control configuration.....76

Figure 7.10: Comparison of the effluent quality control performance on two staged MFCs 77

LIST OF TABLES

Table 2.1: Summary of the current BES dynamic models in the literature. 16

Table 2.2: Summary of the optimization and control strategies applied to BESs.....24

Table 4.1: CBE model parameters 39

Table 7.1: CBE model parameters for the staged MFCs.....67

LIST OF SYMBOLS

Symbol	*Physical quantity*	*Units*
a	Parameter from the cubic approximation (5.6)	mg-S^3 L^{-3}
b	Parameter for the third order hyperbolic approximation (5.8)	[-]
C	Electric capacitance	F
C_{max}	Highest electric capacitance value	F
C_{min}	Lowest electric capacitance value	F
D	Dilution rate	d^{-1}
DC	Duty cycle	%
e	Error between the output and the desired reference in the PID	-
E_{max}	Highest open circuit voltage value	V
E_{min}	Lowest open circuit voltage value	V
E_{OC}	Open circuit voltage	V
F	Faraday constant	A s mol-e^{-1}
$\mathcal{F}$	Fisher information matrix	-
F_{in}	Input flow rate	L d^{-1}
I_{cell}	Electric current produced by the cell	A
I_{max}	Electric current asymptote in Monod equation (5.3)	A
I'_{max}	Electric current asymptote in inhibited Monod equation (5.5)	A
I''_{max}	Electric current asymptote in cubic Monod equation (5.9)	A
K_c	Constant gain in the PID	-
$K_{d,e}$	Decay rate for exoelectricigenic population	d^{-1}
$K_{d,m}$	Decay rate for methanogenic population	d^{-1}
K_i	Limiting term in equation (5.5)	mg-S^3 L^{-3}

K_M	M_{ox} Monod half constant for exoelectricigenic kinetics	mg-M L^{-1}
K_S	Monod half constant in Monod equation (5.3)	mg-S L^{-1}
K_S'	Monod half constant in inhibited Monod equation (5.5)	mg-S L^{-1}
K_S''	Monod half constant in cubic Monod equation (5.9)	mg-S L^{-1}
$K_{S,e}$	Substrate Monod half constant for exoelectricigenic kinetics	mg-S L^{-1}
$K_{S,m}$	Substrate Monod half constant for methanogenic kinetics	mg-S L^{-1}
K_r	Steepness factor in equations (3.15) to (3.18)	L mg-X^{-1}
K_X	Steepness factor in equation (3.10)	L mg-X^{-1}
m	Number of electrons transferred per mole of mediator	mol-e^{-1} mol-M^{-1}
M_{ox}	Intracellular mediator concentration in oxidized form	mg-M L^{-1}
M_{red}	Intracellular mediator concentration in reduced form	mg-M L^{-1}
M_{Tot}	Total mediator weight per exoelectricigenic microorganism	mg-M mg-X^{-1}
N	Total number of measurements	[-]
P_{cell}	Electric power generated by the MFC	W
Q	Rate of methane production	mL-CH_4 d^{-1}
$q_{max,e}$	Substrate consumption rate for exoelectricigenic population	mg-S mg-X^{-1} d^{-1}
$q_{max,m}$	Substrate consumption rate for methanogenic population	mg-S mg-X^{-1} d^{-1}
R	Ideal gas constant	J K^{-1} mol^{-1}
R_1	Internal resistance (related to ohmic overpotential)	Ω
R_2	Internal resistance (related to activation overpotential)	Ω
R_{ext}	External resistance	Ω
R_{int}	Total value for the internal resistance	Ω
R_{max}	Highest value for R_1 and R_2	Ω
$R_{min,1}$	Lowest value for R_1	Ω

$R_{min,2}$	Lowest value for R_2	Ω
$\bar{s}$	Normalized sensitivity function	-
$\bar{S}$	Normalized sensitivity matrix	-
S	Substrate (or acetate or carbon source) concentration	mg-S L^{-1}
$\hat{S}_i$	Estimated effluent substrate concentration for the ith MFC	mg-S L^{-1}
S_i^{ref}	Desired effluent substrate concentration for the ith MFC	mg-S L^{-1}
S_{in}	Influent substrate concentration	mg-S L^{-1}
t	Time	d
T	Anode Temperature	K
u	Vector of inputs	-
V	Anode volume	L
V_c	Voltage at the capacitor	V
V_{cell}	Electric voltage generated by the MFC	V
x	Vector of state variables	-
X_e	Concentration of exoelectricigenic bacteria	mg-X L^{-1}
X_m	Concentration of methanogenic archaea	mg-X L^{-1}
$X_{max,e}$	Maximal attainable concentration, exoelectricigenic population	mg-X L^{-1}
$X_{max,m}$	Maximal attainable concentration, methanogenic population	mg-X L^{-1}
y	Vector of outputs	-
Y	Yield for M_{ox} balance	mg-M mg-S^{-1}
Y_{CH4}	Methane yield	mL-CH_4 mg-S^{-1}
$\bar{y}_{i,j}^{exp}$	Normalized experimental i^{th} output at the j^{th} sampling time	-
$\bar{y}_{i,j}^{sim}$	Normalized model i^{th} output at the j^{th} sampling time	-

Symbol	*Physical quantity*	*Units*
α_e	Biomass retention parameter for exoelectricigenic population	[-]
α_m	Biomass retention parameter for methanogenic population	[-]
β	Relation current and substrate consumption rate in equation (5.1)	mg-S L^{-1} d^{-1} A^{-1}
γ	Mediator molar mass	mg-M mol-M^{-1}
ε	Half constant for the Monod term limiting current production	mg-M L^{-1}
η_{conc}	Concentration overpotential	V
θ	Vector of parameters	-
$\mu_{max,e}$	Growth rate for exoelectricigenic population	d^{-1}
$\mu_{max,m}$	Growth rate for methanogenic population	d^{-1}
ξ	Substrate Monod half constant for equations (3.16) to (3.18)	mg-S L^{-1}
τ_I	Integral time constant in the PID	min
τ_D	Derivative time constant in the PID	min

LIST OF ABBREVIATIONS

BES	Bioelectrochemical system
BOD_5	Biological oxygen demand (5-day test)
CBE	Combined bioelectrochemical-electrical MFC dynamic model
CSTR	Continuous stirred tank reactor
COD	Chemical oxygen demand
EEC	electrical equivalent circuit
HRT	Hydraulic retention time
MEC	Microbial electrolysis cell
MET	microbial electrochemical technology
MFC	Microbial fuel cell
MPC	Model predictive control
MPPT	Maximum power point tracking
MSE	Mean squared error
PID	Proportional, integral, derivative controller
PWM	Pulse-width modulated operation
P/O	Perturb and observe algorithm
R-PWM	Pulse-width modulated operation of the external resistance

LIST OF APPENDICES

Appendix A – Online parameter estimation procedure for the equivalent electrical circuit.....95

CHAPTER 1 INTRODUCTION

Microbial fuel cells (MFCs) are bioelectrochemical devices designed for direct electricity production from organic matter. The main difference with respect to a conventional fuel cell is that the MFC anode benefits from the biocatalytic activity of exoelectricigenic bacteria, which transfer electrons derived from the oxidation of organic matter to the anode. Similar to fuel cells, the released electrons flow through the external electrical circuit while protons migrate to the cathode in order to reduce oxygen and form water (Logan, 2008).

1.1 Motivation

Owing to the broad selectivity of microbial enzymes and mixed microbial communities capable of oxidizing a wide range of organic molecules, MFCs can be used for energy recovery from diluted organic wastes such as wastewater (Du, Li, & Gu, 2007; Lefebvre, Uzabiaga, Chang, Kim, & Ng, 2011). Such ability for energy recovery provides an excellent opportunity to develop a novel wastewater treatment technology (Du, Li, & Gu, 2007). In comparison with widely used conventional aerobic technologies such as activated sludge, using MFCs for wastewater treatment would present several advantages. In terms of operational costs, the lack of pumping and aeration would save around 21 % and 30-55 % of the total treatment energy demand, respectively (Oh et al. 2010). Additional savings would come from the fact that MFCs generate less sludge and are able to work at temperatures below 20 ºC where traditional anaerobic digestion generally ceases to function (Logan, 2008).

In such context of wastewater treatment, reactor staging is widely used where treatment norms are achieved by connecting two or more reactors in series with the first reactor operating at high carbon source loads and the last reactor performing the final polishing. Such novel technology perfectly fits future scenarios of renewable energy production, where a significant part of the energy comes from renewable sources to sustain increased energy demands (Logan & Regan, 2006). Recent advances in the understanding of MFC microbiology and improved reactor design have led to orders-of-magnitude increase in MFC volumetric power density. Yet, volumetric performance should be further improved to enable commercial applications of microbial electrochemical technologies (METs). Model-based reactor design as well as advanced monitoring and control

strategies play an important role in these efforts with mathematical models representing an important tool for portraying process dynamics, understanding fundamental properties of MFCs, and developing software sensors for advanced process control strategies (Oh et al., 2010).

1.2 Problem definition

Several existing MFC dynamic models are able to adequately describe relatively slow dynamics of biomass growth and carbon source consumption. Some models consider a single microbial population (Picioreanu, Katuri, van Loosdrecht, Head, & Scott, 2007; Oliveira, Simões, Melo, & Pinto, 2013b; Zeng, Choo, Kim, & Wu, 2010; Zhang & Halme, 1995), while others were expanded to describe mixed microbial populations required for degrading complex carbon sources such as wastewater (Picioreanu, Katuri, Head, van Loosdrecht, & Scott, 2008; Pinto, Srinivasan, Manuel, & Tartakovsky, 2010) and to enable calculation of pH gradients in anodophilic biofilms (Picioreanu, van Loosdrecht, Curtis, & Scott, 2010). In another approach, electrochemical biofilms were described as a one-dimensional conductive matrix (Kato Marcus, Torres, & Rittmann, 2007). More complex models are able to describe the evolution in time and space of several key variables, such as current, charge, voltage, power output and consumption of substrates (carbon sources) for several microbial populations (Picioreanu, Head, Katuri, van Loosdrecht, & Scott, 2007). However, the high complexity of some models makes them unsuitable for developing software sensors or model-based control oriented strategies for the MFCs.

Furthermore, recent experiments demonstrated significant charge storage capacity of bioelectrochemical biofilms (Schrott, Bonanni, Robuschi, Esteve-Nuñez, & Busalmen, 2011). MFC operation with pulse-width modulated (PWM) or intermittent connection of the external resistance (Coronado, Perrier, & Tartakovsky, 2013; Grondin, Perrier, & Tartakovsky, 2012) demonstrated that internal capacitance of anodic biofilms leads to complex non-linear behavior. Such behavior combines fast charge/discharge dynamics, i.e., with time constants in the order of milliseconds, with much slower dynamics of microbial biofilm growth and decay, i.e. with time constants in the order of hours to days. While an electrical equivalent circuit (EEC) model is able to describe fast electrical dynamics of the anodic biofilm (Coronado, Tartakovsky, & Perrier, 2013), this simplified approach does not allow for describing biomass growth and substrate consumption dynamics resulting in a very limited predictive capacity of the EEC model. On the other hand, such biomass-related dynamics can be well described by a bioelectrochemical model.

Besides modeling, another prevailing research topic in MFCs concerns its electrical operation. As any other electrical voltage source, the electrical power produced by the MFCs suffers dramatic losses when the external resistance does not match the value of the internal resistance of the reactor. For this reason, research has been devoted to tracking internal resistance in MFCs by adjusting the external resistance (Woodward, Perrier, Srinivasan, Pinto, & Tartakovsky, 2010). However, the external resistance cannot be changed in practical applications. Recent works have demonstrated that intermittent connection counteracts considerable losses in power output as compared to MFC operation with fixed external resistance (Grondin, Perrier, & Tartakovsky, 2012), particularly when operating at values of the external resistance which were below the internal resistance. While previous works study the effect of time connection and switching frequency experimentally (Coronado, Perrier, & Tartakovsky, 2013; Gardel, Nielsen, Grisdela, & Girguis, 2012; Grondin, Perrier, & Tartakovsky, 2012), there is still a lack of an engineering tool useful to further extend the understanding of the periodic operation effect on MFC performance. Very few studies have considered the effect of the connection time and switching frequency in the MFC performance and microbial structure. In this way, MFC dynamic modelling could shed some light in the subject and be used for developing MFC-based treatment systems with high volumetric power output.

The vast majority of the control and optimization studies found in literature are aimed at regulating MFC voltage or maximizing power output, i.e. they address fast electrical dynamics (Wang, Park, & Ren, 2015). Yet, successful MFC commercialization necessitates reliable process control strategies. There is an obvious lack of control strategies capable of addressing the multi-scale dynamics linked to the dual biological and electrical nature of MFCs. Probably one of the main reasons for disregarding the biological nature of MFCs in the control strategies involves the difficulty of real time measurements of the effluent concentration. Current techniques for effluent estimation such as chemical oxygen demand (COD) and biological oxygen demand (BOD_5) do not represent a viable online technique for effluent quality monitoring. Thus, real-time monitoring of the organic load required to comply with regulatory norms still represents a challenge. Benefiting from the electrochemical nature of MFCs, continuous estimations of the biologically consumable organic fraction in wastewater could be obtained from the electrical measurements in MFCs (Chouler & Di Lorenzo, 2015).

1.3 Objectives

The general objective of this thesis is to study the dynamic behavior and performance of staged MFCs.

Furthermore, in light of the current limitations of the existing MFC models to describe recently observed dynamics and the lack of control strategies dealing with the dual biological and electrical nature of MFCs, the specific objectives, in order of importance, are to:

1. Develop a combined bioelectrochemical-electrical (CBE) model of a MFC able to describe the anodic capacitance behavior recently observed during pulsed width modulated (PWM) connection of the external resistance.
2. Develop monitoring strategies for the continuous estimation of the effluent concentration from the measurement of the electrical variables in MFCs and analyse the monitoring capabilities of the CBE model for applications in wastewater treatment.
3. Qualitatively study the effect of the PWM operation of the external resistance on MFC performance using the CBE model, with duty cycle and switching frequency the two operational variables of interest.
4. Carry out experiments to sustain the operation of two MFCs hydraulically connected in series fed with acetate. Use the CBE model to describe the behavior of the two staged MFCs and present a simple control strategy suitable for wastewater treatment applications.
5. Present an exhaustive overview in the current dynamic modeling trends and the process control approaches in bioelectrochemical systems highlighting their main characteristics and limitations.

1.4 Thesis structure

This document is organized into six chapters. Chapter 2 thoroughly reviews the current state of modeling, optimization and control of BESs systems, highlighting their main characteristics and limitations in order to expose new research opportunities. Chapter 3 presents the materials and methods used during MFC experiments and the methodology of parameter estimation and validation used in this thesis. In addition, the experimental setup for the control of staged MFCs is shown. Chapter 4 describes the structure and parameter identification of the dynamic CBE model.

Two possible modeling approaches are introduced, first a “simulation” CBE model that can be used to predict MFC output voltage, carbon source effluent concentration, and the distribution of microbial populations under various operating conditions. Second, a “parameter observer-based” CBE model that runs concurrently with the experiment and the electrical parameters related to the EEC are replaced by their online estimations obtained in real time. Subsequently, chapter 5 uses the CBE “simulation” model to qualitatively study the effect of duty cycling and switching frequency on the overall MFC performance. Then, chapter 6 presents two monitoring approaches for the online estimation of the effluent concentration, one based on the simplified dynamic mass balance of the substrate concentration and the second based on a Monod expression with limitation at low effluent concentrations obtained from the kinetics of the exoelectricigenic bacteria. Finally, chapter 7 gathers all the concepts from previous chapters and applies them to staged MFCs. The CBE model is used to describe the dynamics of the two staged MFCs under PWM operation, the online estimation procedures are experimentally validated for the effluent quality monitoring of the two reactors and a simple centralized control configuration for the effluent quality control based on a PID and an ON/OFF controller is presented.

CHAPTER 2 STATE OF THE ART IN MODELING, OPTIMIZATION AND CONTROL OF BIOELECTROCHEMICAL SYSTEMS

Human development is intricately linked both to energy and water availability. The International Energy Agency estimates that energy production requires about 15% of world's total water consumption (IEA, 2012). At the same time, significant amounts of energy are needed for wastewater treatment. With this respect, bioelectrochemical systems (BESs) such as Microbial Fuel Cells (MFCs) and Microbial Electrolysis Cells (MECs), which are capable of producing energy from wastewater, represent a promising new technology that could contribute to resolving this dilemma (Logan & Regan, 2006; Logan et al., 2008; Lovley, 2008).

MFCs and MECs exploit the ability of anodophilic (exoelectricigenic) microorganisms for extracellular electron transfer and hence energy production through microbial oxidation of organic matter (Logan, 2009). Both MFCs and MECs can operate using a wide variety of industrial and domestic wastewaters (Kelly & He, 2014; Lefebvre, Uzabiaga, Chang, Kim, & Ng, 2011). Typically, BESs consist of two electrodes connected by an external circuit (Logan, 2008) with the organic matter oxidation taking place at the anode and reduction reactions, such as oxygen reduction reaction in MFCs or hydrogen evolution reaction in MECs, taking place at the cathode. Detailed description of MFC and MEC principles of operation can be found in a number of reviews (Logan, 2008; Lovley, 2008; Schröder, 2007; Yang, Xu, Guo, & Sun, 2012).

Extensive experimental work during the past decade has led to significant advancements in the understanding of BES microbial populations (Logan, 2009; Lovley, 2008), materials (Kundu, Sahu, Redzwan, & Hashim, 2013; Wang et al.,2014), design and operation (Oliveira, Simões, Melo, & Pinto, 2013b). Yet, progress in MFC and MEC scale-up faces a number of challenges, mostly related to low volumetric performance and reactor instability (Janicek, Fan, & Liu, 2014; Logan, 2010). With this in mind, model-based design, control and optimization approaches, which are used in bioprocess engineering (Dochain, 2013), might be instrumental in furthering BES technologies towards commercialization. Previous reviews on MFC modeling include a number of modeling approaches (Oh et al., 2010; Oliveira, Simões, Melo, & Pinto, 2013b; Ortiz-Martínez et al., 2015). These reviews, however, did not focus on fast process dynamics and the emerging area

of BES real-time monitoring, control and optimization, which deals with unpredictable external disturbances and maximizing energy production. To address this gap, we review the existing MFC and MEC dynamic models, the existing control strategies and the energy harvesting configurations. Following this review, model-based methods for control and optimization of MFCs and MECs are discussed.

2.1 Dynamic modeling

The concept of a mediator-less MFC was only introduced about a decade ago (Chaudhuri & Lovley, 2003; Liu, Cheng, & Logan, 2005) while the MEC concept is even more recent (Rozendal, Hamelers, Euverink, Metz, & Buisman, 2006). Accordingly, most of the research is dedicated to experimental studies, with only some studies dedicated to MFC modeling and even fewer to MEC modeling. Two approaches are commonly used in BES modeling. The bioelectrochemical modeling utilizes the knowledge of microbiology and bioelectrochemistry to describe microbial growth and carbon source consumption in BESs, while the approach of electrical equivalent circuit modeling describes BESs as electrical circuits to represent fast (milliseconds to seconds) electrical processes, while neglecting the relatively slow (minutes to days) dynamics of biomass growth and metabolism. A key assumption in the bioelectrochemical models is the mechanism by which the electron transfer from a carbon source to the anode is accomplished. Based on a number of recent experimental studies, direct electron transfer (involving either direct contact or the presence of conducting nanowires) and mediated electron transfer (via exogenous redox mediators or via secondary metabolites) are commonly accepted (Schröder, 2007). The following sections classify BES models based on the complexity of the mass balances (e.g. ideal mixing vs biofilm systems) and the complexity of the transport phenomena (e.g. one-dimensional vs three-dimensional biofilm) and microbial populations considered by the model.

2.1.1 Single-species ideal mixing modeling

A relatively simple approach to describe BES dynamics involves single population modeling. Also, to further simplify material balances the mass transport processes are assumed to be fast compared with the biochemical and redox reactions, such that the concentration of reactants in the bulk solution, inside the bacteria and on the anode surface are considered to be equal. In essence, such models consider the anodophilic microorganisms to be suspended in the anodic liquid.

The first such model was proposed by Zhang and Halme (1995) to describe an MFC. This model was developed before the recent concept of mediator-less MFCs was introduced (Chaudhuri & Lovley, 2003). Accordingly, the model described an MFC with an external mediator (2-hydroxy1,4 naphthoquinone or HNQ), which was used in the experiment to facilitate electron transfer (Figure 2.1 A). Model dynamics was based on the electrochemical and mass balances of a batch reactor. Carbon source consumption was modeled by Monod-type kinetics, while first order redox reactions at the anode and between the metabolites and the mediator were assumed. The electrochemical balance used the Nernst's equation to describe the open-circuit voltage, the Tafel approximation to calculate the activation overpotential, and Ohm's law to describe the ohmic overpotential. The concentration overpotential was assumed to be negligible. Finally, the output current of the cell was given by Faraday's law of electrolysis. The model assumed constant biomass density thus lacking dynamics of microbial growth. In spite of this and other limitations, this model presented the main principles of bioelectrochemical modeling, which were utilized in a number of subsequent models.

The development of modern mediator-less MFCs (Chaudhuri & Lovley, 2003; Lovley, 2008) necessitated an updated version of the ideal-mixing model, which was developed by Zeng, Choo, Kim and Wu (2010). This is the only work that considers both the anode and cathode compartments. Mass balances were obtained assuming an ideally stirred tank reactor (STR) with Butler–Volmer expressions incorporated into the reaction kinetics to simulate the electrochemical balance. A sensitivity analysis of the parameters with respect to the power output of the MFC revealed the electron transfer coefficient of the cathode as the most significant factor limiting the performance of the MFCs. The model was used to describe MFC operation on acetate and synthetic wastewater. While the model adequately described MFC operation on acetate, the discrepancies observed when operating the MFC on synthetic wastewater might be related to the limitations of the single-species model.

Picioreanu, Katuri, van Loosdrecht, Head and Scott (2010) also proposed a single-species ideal mixing MFC model. Oxidation of the carbon source by suspended cells using the oxidized form of an external mediator was assumed to take place in the bulk liquid, while the reduced form of the external mediator was assumed to be oxidized at the anode surface. Although biofilm formation was not considered, a diffusion layer was assumed to be adjacent to the anode surface. Therefore, steady-state one-dimensional mass balance equations applied to the diffusion layer were needed to

calculate the concentrations on the anode surface. Unlike the previous models, the electrochemical balance considered the activation and ohmic overpotentials.

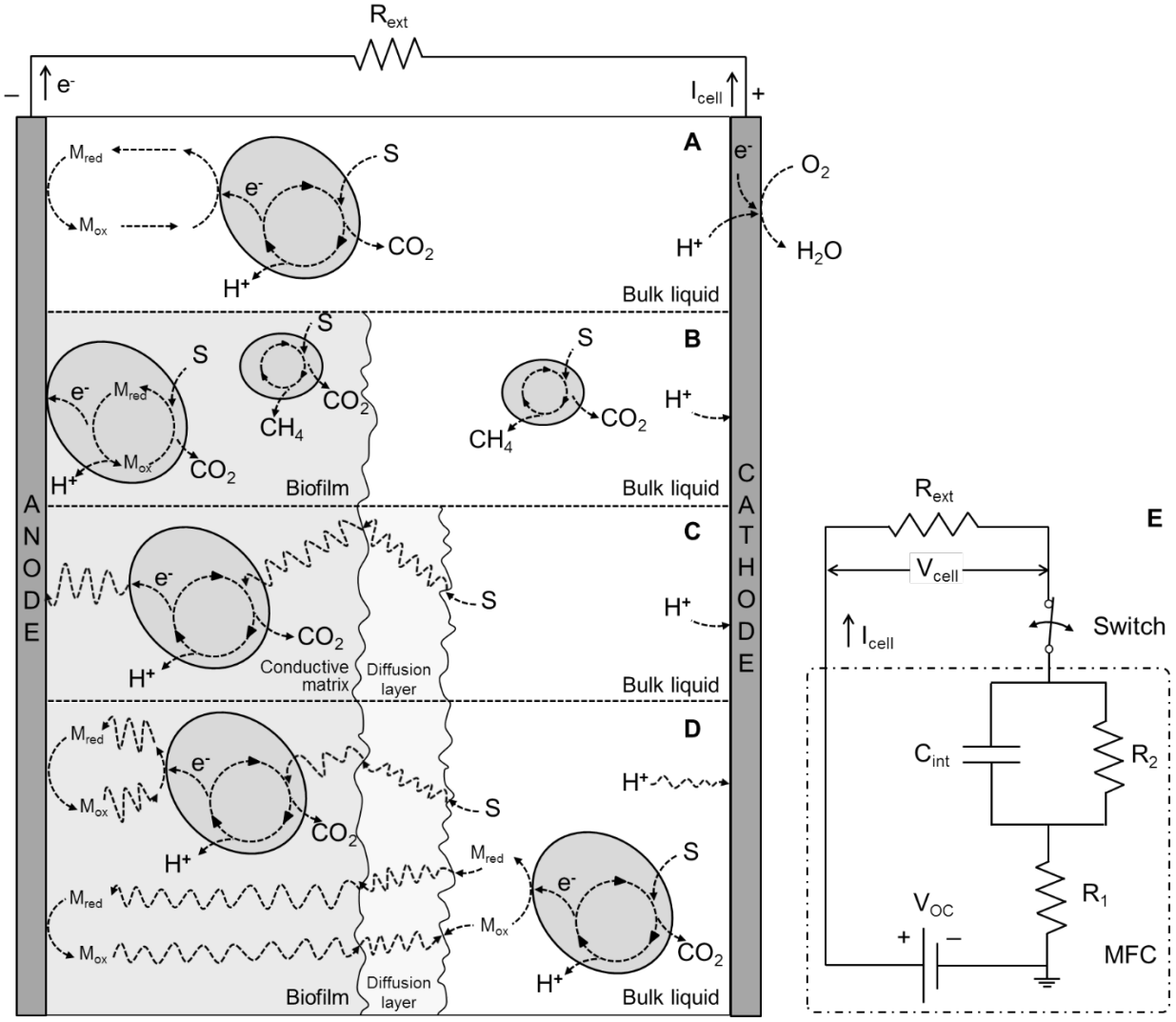

Figure 2.1: MFC modeling approaches: (A) Ideal mixing model; (B) simplified biofilm model; (C) solid conductive matrix biofilm model; (D) three dimensional (3D) biofilm model; (E) electrical equivalent circuit (EEC) model.

Due to the simplicity of the single species ideal mixing models, this modeling approach inherently featured a number of limitations. In particular, the presence of methanogens was often observed, even when BESs were operated on a single carbon source such as acetate (Logan et al., 2008; Picioreanu, Kreft, & van Loosdrecht, 2004; Pinto, Srinivasan, Manuel, & Tartakovsky, 2010).

Also, formation of electrochemically active biofilms was observed on one or both electrodes (Babauta, Renslow, Lewandowski, & Beyenal, 2012; Ramasamy, Ren, Mench, & Regan, 2008). Biomass retention and mass transfer limitations related to the existence of these biofilms need to be taken into consideration for more accurate modeling, which gave rise to a number of biofilm models described below.

2.1.2 Simplified biofilm modeling

The complex nonlinear dynamics of BESs can be better described by accounting for the presence of anodophilic biofilm. Here, a number of simplifying assumptions can be used to avoid the complexity of reaction–diffusion material balances, e.g. by disregarding carbon source diffusion in the biofilm. Such a model, which also described the co-existence of the anodophilic and methanogenic microbial populations in the anodic compartment of a MFC (Figure 2.1 B), was developed by Pinto, Srinivasan, Manuel and Tartakovsky (2010). In this model, charge transfer mechanism from the carbon source to the anode was assumed to involve an intracellular mediator. Also, extracellular electron transfer through nanowires or direct contact with the anode was assumed. Multiplicative Monod kinetics was used to describe species competition for the carbon source. Current production was related to the amount of oxidized mediator by means of Faraday's law of electrolysis. Concentration losses were calculated using the Nernst equation, while the intracellular mediator concentration and the activation losses were calculated by the linear approximation of the Butler–Volmer equation. Finally, biofilm formation and retention was described by a two-phase growth washout model. Parameter estimation and sensitivity analysis of this model were carried out using experimental results obtained in continuous flow MFCs. The model was used to demonstrate the impact of the organic load and the external resistance on the equilibrium between the methanogenic and anodophilic microbial populations. The methanogenic microorganisms were shown to proliferate at high external resistance values, while the anodophilic microorganisms were predicted to proliferate at the external resistance equal or below the internal resistance value.

The model of Pinto, Srinivasan, Manuel and Tartakovsky (2010) was further extended to describe operation of a MEC on a complex carbon source (Pinto, Srinivasan, Escapa, & Tartakovsky, 2011). Accordingly, the extended model included fermentative, anodophilic, methanogenic acetoclastic, and methanogenic hydrogenophilic microbial populations. After parameter estimation, the model

adequately described hydrogen production from synthetic wastewater. This model was further modified to develop a unified (MxC) model describing both MFC and MEC operation (Pinto, Tartakovsky, & Srinivasan, 2012).

2.1.3 Reaction-diffusion biofilm modeling

Detailed description of the distribution of microbial populations and carbon sources within the biofilm can be only obtained by using reaction–diffusion material balances. Kato Marcus, Torres and Rittmann (2007) developed the first one-dimensional (1D) biofilm model of a MFC (Figure 2.1 C). This work considered anodophilic biofilm as a conductive solid matrix characterized by its ability to transfer electrons from the anodophilic bacteria to the anode. In addition to the conductive solid matrix, a diffusive non-conductive layer was considered between the conductive matrix and the bulk anodic liquid. Also, the model considered active and inactive biomass competing for space within the biofilm. The conductivity of the matrix was linked to the current density and local voltages along the biofilm depth. Steady state assumption was used for carbon source and electron transport calculations. A Nernst–Monod equation was derived to describe the relationship between the rate of carbon source consumption, its concentration, and the electrical potential. Simulations revealed that the limiting factors at the anodic biofilm change from potential limitations at low conductivity, to dual potential and carbon source transfer limitations at a moderate conductivity, to only mass transfer limitations at high conductivity.

The originality of this model lies in considering the anodophilic biofilm as a conductive solid matrix. However, this model did not consider diffusion limitations or the existence of several microbial populations. Sedaqatvand, Esfahany, Behzad, Mohseni and Mardanpour (2013) extended the model of Kato Marcus, Torres and Rittmann (2007) to describe a single-chamber MFC fed with dairy wastewater. Only three parameters were estimated, including the biofilm conductivity. Notably, the Nernst–Monod equation was experimentally validated by Torres, Marcus, Parameswaran and Rittmann (2008) demonstrating its ability to predict anode potential losses. On the other hand, the work of (Hamelers, Ter Heijne, Stein, Rozendal, & Buisman, 2011) demonstrated that a Butler–Volmer– Monod equation to express the kinetics of the anodophilic bacteria provides better description of the experimentally acquired polarization curves than the Monod–Nernst equation proposed by Kato Marcus, Torres and Rittmann (2007).

Oliveira, Simões, Melo and Pinto (2013a) developed a 1D steady state MFC model describing heat, charge and mass transfer processes in a double chamber MFC. The model assumed Fick's laws of diffusion to dominate the heat and mass transfer, while convection was neglected. Fourier's law was used for the thermal energy model, while Tafel and Monod equations described the anode and cathode kinetics. Simulations showed the effects of acetate concentration and temperature on polarization and power curves as well as on the biofilm thickness. This model provided adequate description of polarization test data from Zeng, Choo, Kim and Wu (2010).

Sirinutsomboon (2014) presented another 1D model for a membrane-less single-chamber MFC fed with molasses. In this model, Fick's second law was used to describe oxygen diffusion from the cathode to the anode, sucrose diffusion from the bulk liquid to the biofilm, and proton diffusion through the anode. Once again, biofilm modeling was based on the Nernst–Monod equation from Kato Marcus, Torres and Rittmann (2007). The Monod equation combined with Butler–Volmer and Nernst equations were used to model anode and cathode reactions. Simulations showed the sucrose concentration over time in the bulk liquid and within the biofilm, open circuit voltage dependence on anode and cathode thickness, and finally, the oxygen concentration profile within the cathode layer. However, model predictions were not compared to experimental results.

Spatial heterogeneity of biofilms in MFCs is essential for improved representation of the biofilm processes. By modifying the model of Kato Marcus, Torres and Rittmann (2007), Jayasinghe, Franks, Nevin, & Mahadevan (2014) developed a two-dimensional (2D) MFC model capable of improved biofilm simulation. This model combined extracellular processes and intracellular metabolism of the microorganisms. Also, it considered active, inactive, and respiring biomass. A flux balance analysis predicted the change in yields, which enabled biofilm growth and metabolism simulations. These modeling results suggested that biofilm conductivity was not a limiting factor in the conduction based model of Kato Marcus, Torres and Rittmann (2007).

Another 2D model was developed by Merkey and Chopp (2012) to explore the impact of anode density and arrangement on current production in an MFC. This biofilm model was also based on the work of Kato Marcus, Torres and Rittmann (2007). Several regions were considered such as bulk liquid, biofilm and solid electrode. The model was used to study the effect of multiple anodes and their spatial distribution on current production. The main limiting factor affecting current production was found to be carbon source delivery to the entire biofilm surface.

Picioreanu, Head, Katuri, van Loosdrecht and Scott (2007) presented a three dimensional (3D) biofilm model (Figure 2.1 D). This MFC model was based on diffusion–reaction mass balances for chemical species coupled with microbial growth and spreading of biomass represented by hard spherical particles. The model considered the existence of methanogenic and anodophilic microorganisms with the growth of anodophilic microorganisms assumed to be limited by acetate and oxidized mediator concentrations, which were modeled using double Monod kinetics. Bulk liquid mass balances were used to determine substrate and suspended biomass concentrations while the biofilm was modeled using the particle-based approach. The resulting model featured significant computational times (around 14 h for one 3D simulation) and a large number of parameters. Subsequently, Picioreanu, van Loosdrecht, Curtis and Scott (2010) adapted this model to describe MFC operation on wastewater. This modification used the International Water Association (IWA) anaerobic digestion model number 1 (ADM1) (Batstone et al., 2002). Six microbial populations were considered and the external redox mediators were assumed to be present in the bulk liquid. Furthermore, the same research group extended the original multi-dimensional model to include pH calculations and variations in the electrode geometry (Picioreanu, Katuri, van Loosdrecht, Head, & Scott, 2010). Spatial pH distribution was calculated by using Nernst–Planck fluxes of ions with ionic charge balance instead of molecular diffusion. The model simulated single-species electroactive biofilm on a planar and porous electrode, and multi-species electroactive and fermentative biofilm on a planar electrode. However, model predictions were not validated using experimental results.

2.1.4 Equivalent electrical circuit modeling

In electrochemical systems the layer at the interface between the electrode and the electrolyte stores electrical charge. In such systems, an abrupt change of current results in a fast change of voltage followed by a slow transition towards equilibrium. A simple approach to modeling the double layer capacitance can be based on an equivalent electrical circuit (EEC), with the charge storage represented by an electrical capacitor (Figure 2.1 E).

Wagner (2002) used the electrochemical impedance spectroscopy to characterize polymer electrolyte membrane (PEM) fuel cells by means of EECs based on ohmic (R) and capacitive (C) elements. Connections of those elements in parallel or in series represented subsequently or simultaneously occurring processes. The same technique was applied to study the impact of biofilm

growth on the MFC anode impedance (Ramasamy, Ren, Mench, & Regan, 2008), and also to measure the overall internal resistance of an upflow MFC (He, Wagner, Minteer, & Angenent, 2006). R/C elements connected in parallel represented the charge transfer resistance (due to the activation overvoltage) and the double layer capacitance effect. A resistance connected in series with the R/C element represented ohmic resistance of the electrolytes and the membrane (Figure 2.1 E). Adding more R/C elements to the basic circuit allowed a more detailed description of the fuel cell.

The two works mentioned above fitted the outputs of the EEC to the static polarization curves (voltage against current) and the Nyquist plots obtained in the electrochemical impedance spectroscopy tests to estimate the contribution of various intrinsic resistances to the overall internal MFC impedance. Pathapati, Xue and Tang (2005) included the dynamic equation of the capacitor resulting from applying Kirchhoff circuit laws to the mass balances of a hydrogen fuel cell in order to describe the capacitance effect of the system. Parameter estimation of this model was performed by fitting the dynamic voltage values obtained experimentally. Later, Ha, Moon, Kim, Ng and Chang (2010) used the same methodology to describe the current generated by an MFC during a step change in the external load.

Coronado, Perrier and Tartakovsky (2013) used the same basic EEC shown in figure 2.1 E to model the fast voltage dynamics observed in MFCs. Model parameters were estimated by fitting the model outputs to the measured voltage of the MFC operated with a pulse-width modulated connection of the external resistance, R_{ext}. Furthermore, Coronado, Tartakovsky and Perrier (2013) developed an on-line parameter identification method which required MFC operation at low (0.1 Hz) and high frequencies (100 Hz) of the external resistance connection/disconnection. This online parameter estimation procedure used the analytical solution of the equivalent circuit model to estimate the internal resistances, R_1 and R_2, related to the ohmic and activation losses, respectively, the open circuit voltage, E_{oc}, and the internal capacitance, C (Figure 2.1 E).

To summarize, EEC models only describe fast electrical dynamics but are lacking the predictive capacity of the bioelectrochemical models. Typical applications of EEC models include design of Power Management Systems, as described below.

2.1.5 Model comparison

Table 2.1 compares the models reviewed above based on the considered material balances, microbial populations, and the complexity of kinetic equations. Although not a comprehensive guide to model selection, this comparison could be useful in deciding on the model type suitable for a particular application (e.g. process design vs process control) and to reveal shortcomings of the existing models. For example, in bioelectrochemical systems with mature biofilms the ideal mixing models might be capable of adequately describing the dominant (anodophilic) microbial population, while requiring relatively short computational times for numerical solutions. Although periodic parameter re-estimation might be required to account for population shifts, these models might be suitable for real-time process monitoring and control applications. Here, simple voltage and current measurements could be used for model-based estimations of the effluent carbon source concentrations by means of soft sensors (Dochain, 2003).

As compared to the ideal mixing models the simplified biofilm models feature an improved prediction accuracy, in particular when attempting to model biofilm growth (e.g. during BES startup) or decay (e.g. during carbon-deplete conditions). By overlooking detailed biofilm structure, the simplified biofilm models can be conveniently adapted to describe various types of bioelectrochemical reactors while requiring reasonable computational times. With further development and scale-up of BESs, both ideal mixing and simplified biofilm models might be suitable for real-time process monitoring and control applications.

Finally, the reaction–diffusion biofilm models provide the most accurate description of biofilm-based BESs and could be recommended for rigorous performance analysis and design. For example, a recently discussed approach for combining several MFCs and MECs to achieve hydrogen production without an external energy input (Sun et al., 2009) could be refined with this modeling approach. Also, to save time and effort, the control and monitoring strategies needed for operating full-scale MFCs and MECs could be tuned using such comprehensive models. Yet, owing to the complexity and long computational times the use of the reaction–diffusion models might be limited to modeling experts.

Table 2.1: Summary of the current BES dynamic models in the literature.

Reference	Modeling approach	Populations	Electron transfer	Reaction model	Electrode modeling
Zhang and Halme (1995)	Ideal mixing	Single	External mediator	Monod, Nernst, Tafel	Anode
Picioreanu, Katuri, van Loosdrecht, Head and Scott (2010)	Ideal mixing	Single	External mediator	Monod, Nernst	Anode
Zeng, Choo, Kim and Wu (2010)	Ideal mixing	Single	Direct	Monod, Butler Volmer	Anode, cathode
Pinto, Srinivasan, Manuel and Tartakovsky (2010)	Simplified biofilm	Two species	Direct, intracellular mediator	Double Monod, Nernst, Butler Volmer	Anode
Pinto, Srinivasan, Escapa and Tartakovsky (2011)	Simplified biofilm	Two species	Direct, intracellular mediator	Double Monod, Nernst, Butler Volmer	Anode
Kato Marcus, Torres and Rittmann (2007)	1D	Active, inactive	Conduction	Monod-Nernst	Anode
Oliveira, Simões, Melo and Pinto (2013a)	1D	Single	Direct	Monod, Tafel	Anode, cathode
Sirinutsomboon (2014)	1D	Single	Conduction	Monod, Nernst, Butler Volmer + Monod-Nernst	Anode, cathode
Jayasinghe, Franks, Nevin and Mahadevan (2014)	2D	Active, inactive, respiring	Conduction	Genome-scale metabolic model + Monod-Nernst	Anode
Merkey and Chopp (2012)	2D	Active, inactive	Conduction	Monod-Nernst	Anode
Picioreanu, Head, Katuri, van Loosdrecht and Scott (2007)	3D	Multi species	External mediator	Double Monod, Nernst, Butler Volmer	Anode
Picioreanu, Katuri, Head, van Loosdrecht and Scott (2008)	3D	Multi species	External mediator	Double Monod, Nernst, Butler Volmer	Anode
Picioreanu, van Loosdrecht, Curtis and Scott (2010)	3D	Multi species	External mediator	Double Monod, Nernst, Butler Volmer	Anode
Ha, Moon, Kim, Ng and Chang (2010)	Electrical equivalent circuit	-	-	-	Anode
Coronado, Perrier and Tartakovsky (2013)	Electrical equivalent circuit	-	-	-	Anode
Recio-Garrido, Perrier and Tartakovsky (2016)	Simplified biofilm + electrical equivalent circuit	Two species	Direct, intracellular mediator	Double Monod, Nernst, Butler Volmer	Anode

The comparison also highlights future directions in BES model development. In particular, it can be noted that most of the reviewed models do not consider charge storage in anodophilic biofilms, although this phenomenon is well documented (Fradler et al., 2014; Ha, Moon, Kim, Ng, & Chang, 2010). While an EEC model can be used for charge storage modeling, this model does not account for bioelectrochemical processes in biofilms, i.e. each of the two approaches has certain shortcomings. With this regard, a recently proposed combined bioelectrochemical-electrical (CBE) model (Recio-Garrido, Perrier, & Tartakovsky, 2016) resolves this limitation by combining the bioelectrochemical and electrical equivalent circuit equations. Accordingly, this model is capable of describing both fast electrical dynamics and slow microbial growth.

Other opportunities for improved predictive capacity of BES models include cathodic reaction modeling, and modeling of oxygen diffusion through the air-breezing cathode. Also, while some models describe electrochemical reactions associated with Me-based catalysts, none consider biocathodes or microbially catalyzed electrosynthesis. This lack of cathode (bio)reaction modeling becomes more important with the advance of microbial electrosynthesis (Wang, & Ren, 2013). Finally, it might be noted that most of the existing models are dedicated to MFC modeling, while relatively few MEC models exist.

2.2 Control and optimization of BESs

Successful scale-up of the bioelectrochemical technologies, among other factors, depends on the development of reliable process control and optimization strategies. BESs are often operated on organic wastes such as wastewater. Although these carbon sources are sustainable, they feature significant variability of physical and chemical characteristics. Accordingly, control and optimization strategies may be needed to deal with the rapid variations in the influent stream composition, pH, temperature, conductivity, and other parameters. These variations have been found to result in performance deterioration due to the changes in BES electrical properties (del Campo, Cañizares, Lobato, Rodrigo, & Morales, 2014; Oh & Logan, 2007; Pinto, Srinivasan, Guiot, & Tartakovsky, 2011; Watson, & Logan, 2011) and microbial community (Lyon, Buret, Vogel, & Monier, 2010; Ren, Yan, Wang, Mench, & Regan, 2011).

2.2.1 Energy harvesting and power control approaches

Practical applications require energy harvesting to be performed by dedicated electrical circuits. These circuits comprise power management systems, which convert low voltage produced by MFCs to a usable voltage and accumulate energy to release it in an energy burst. A detailed description of these energy harvesting approaches and the corresponding electrical circuits can be found in Wang et al. (Wang, Park, & Ren, 2015). It is suggested that energy harvesting technologies can be subdivided into capacitor-based systems, charge pump based systems, and boost converter-based systems.

In addition to using external capacitors, recent research demonstrated that internal MFC capacitance can be also used for energy storage (Fradler et al., 2014; Ha, Moon, Kim, Ng, & Chang, 2010; Walter, Greenman, & Ieropoulos, 2014). In particular, Grondin, Perrier and Tartakovsky, (2012) developed an MFC energy harvesting approach in which the external resistance disconnects when the voltage decreases below a predefined minimum voltage threshold and is reconnected when the MFC voltage exceeds a predefined maximum threshold. This approach results in an intermittent electrical load connection, which can be described by its duty cycle (a fraction of time the load is connected over an interval) and an average power output per cycle. Such an intermittent connection was demonstrated to avoid considerable losses in power output as compared to an MFC operation with fixed external resistance, particularly when operating at values of the external resistance which were below the internal resistance.

Gardel, Nielsen, Grisdela and Girguis (2012) demonstrated operation of a sediment MFC with intermittent (periodic) connection of the electrical load. The cycle duration was much longer as compared to the previous work (dozens of minutes vs seconds). This work studied the influence of duty cycle on cumulative charge, current and microbial composition. Experimental results showed that shorter switching intervals lead to more accumulated charge. Interestingly, microbial communities were found to be unaffected by such periodic operation in a broad range of switching frequencies. At the same time, MFC operation at different values of fixed external resistances was observed to affect microbial populations (Lyon, Buret, Vogel, & Monier, 2010).

Coronado, Perrier and Tartakovsky (2013) used pulsed-width modulated connection of the external electrical load (PWM mode of operation) at frequencies ranging from 0.1 Hz to 1000 Hz. This work confirmed that power losses during MFC operation at values of the external resistance below

the internal resistance values can be avoided by using the PWM mode. Furthermore, gradual increase of MFC power output (Coulombic efficiency) was observed after several days of PWM operation.

The effect of duty cycle and switching frequency during PWM operation of an MFC was studied by Wang, Ren and Park (2012). In this study, a boost-converter based energy harvester circuit was used. By using this approach an optimal combination of the duty cycle and switching frequency for a given inductance can be found for certain operating conditions, such as maximum power or maximum current operation. In addition, Premier, Kim, Michie, Dinsdale and Guwy (2011) used a logic-based control of the external resistance considering the gradient of the power against current and the power against time. These gradients were determined measuring the voltage and applying a first order backward finite difference algorithm.

As in any power supply, MFC power output strongly depends on the connected electrical load. In the case of a resistive load, maximum power point is achieved when the internal resistance equals the external resistance (Logan, 2008). Significant power losses were observed when the internal and external electrical resistances mismatch (Pinto, Srinivasan, Guiot, & Tartakovsky, 2011). As mentioned above, the biological nature of MFCs makes electrical characteristics, including the internal resistance, depend on fast changing environmental factors. As a consequence of this dynamic system, periodic adjustment of the external electrical load is required to avoid substantial losses in power production. Similarly, internal resistance might frequently change during MEC operation also requiring periodic adjustments of the applied voltage.

With the exception of Wang, Ren and Park (2012), the control approaches described above do not ensure an optimal operation of the MFCs. A more traditional approach to overcome power losses uses a maximum power point tracking (MPPT) real-time optimization method, which seeks an external resistance that maximizes the power output (Woodward, Tartakovsky, Perrier, & Srinivasan, 2009). Changing the external resistor values is not a practical approach for energy harvesting and thus, similar to electric power sources such as photovoltaic arrays and fuel cells, this problem can be resolved by connecting power sources to a power converter. Then the duty cycle or the current drawn by the converter is optimized using the MPPT method (Esram & Chapman, 2007). MPPT methods have been demonstrated to reduce start-up time by increasing microbial bioelectrochemical activity (Andersen et al. 2013; Boghani, Kim, Dinsdale, Guwy, &

Premier, 2013; Molognoni et al., 2014) or even to increase voltage of an MFC stack and avoid voltage reversal (Boghani et al. 2014).

A comparison of several MPPT methods used for optimal MFC control is given in Woodward, Perrier, Srinivasan, Pinto and Tartakovsky (2010). This work evaluated the perturbation and observation (P/O) method, the gradient method and the multi-unit optimization method. The P/O method was based on step-wise changes of the external resistance with the direction of external resistance change determined by the sign of the power output change. In the gradient method, the power output gradient was evaluated at each step, and then the resistance was changed in the direction of the gradient. The multi-unit method required simultaneous operation of at least two MFCs. The gradient was estimated using an offset in the inputs (external resistance values) as a finite difference between the outputs (power density). Comparison of these three MPPT methods under temperature and substrate disturbances showed that the multiunit method provides the fastest convergence. However, this approach required nearly identical MFCs, an assumption that can hardly be satisfied in practice. Overall, the P/O method, although slow to converge, demonstrated better robustness. Further confirmation of the P/O algorithm robustness was obtained by long-term operation of an MFC fed with synthetic wastewater (Pinto, Srinivasan, Guiot, & Tartakovsky, 2011). This work concluded that the real-time optimization of the external resistance led to significantly higher power outputs and lower methane production as compared to a MFC operated with a fixed external resistance.

Furthermore, Attarsharghi, Woodward and Akhrif (2012) used an extremum seeking control scheme comprising a feedback control loop with an adaptive feedback that optimizes a pre-defined objective function. The optimal solution is reached by following the condition of optimality, i.e., for an unconstrained case, it forces the gradient to zero. Simulations showed that the effect of a carbon source disturbance could be detected only when the effects of such disturbance influence the power output of the MFC, leading to a temporarily suboptimal performance and subsequent power loss. Consequently, a corrective term was added in order to anticipate the effect of such disturbances on the power output and compensate for the loss.

Thus far, very few attempts to optimize MEC performance exist. Tartakovsky, Mehta, Santoyo and Guiot (2011) applied the P/O algorithm to track the minimal apparent resistance by adjusting the applied voltage. The algorithm was tested in laboratory-scale continuous flow MECs fed with

acetate or synthetic wastewater. In all tests, changes in MEC performance caused by the variations in organic load, carbon source properties, and hydraulic retention time were successfully followed by the P/O algorithm resulting in high hydrogen production, while avoiding excessive power consumption.

In another study, Andersen et al. (2013) operated a stack of MECs electrically connected in series using a cell balance system (CBS) that dynamically adapted the applied voltages of each MEC in the stack. The voltage switching approach used to balance stacked BESs relative to individual cell performance was crucial in providing the rapid start-up and sustained performance of stacked BESs.

In summary, the current trend in energy harvesting and power control approaches only considers the electrical nature of BESs. A more promising approach would consider the dual electrical and biochemical nature of BESs in order to improve the predictive accuracy of the models.

2.2.2 Model-based optimization and control strategies

Currently, most of the research efforts in the area of BES optimization and control are focused on the development of effective energy harvesting methods for MFCs using model-free algorithms (Wang, Park, & Ren, 2015). Meanwhile, dynamic models such as those described above enable the development of advanced model-based control strategies. These strategies were applied with success to other biological systems with complex non-linear dynamics (Dochain, 2013). Such strategies include input/output or global linearization, feedback linearization, nonlinear optimal control, and nonlinear model predictive control (MPC). Development of control and optimization strategies for BESs might benefit from these existing methods.

In one of the first examples of model-based BES optimization, Pinto, Tartakovsky, Perrier and Srinivasan (2010) optimized an MFC-based wastewater treatment by using an approach of MFC staging (connection in series). The study considered two MFCs hydraulically connected in series. By analyzing the two population MFC model (Pinto, Srinivasan, Manuel, & Tartakovsky, 2010), the authors demonstrated that the ratio between the methanogenic and anodophilic microbial populations can be controlled by the electric load and that the MFCs connected in series always improve the wastewater treatment efficiency. Furthermore, it was shown that the optimal operating conditions (exoelectricigenic (anodophilic) at low external resistance or methanogenic at high

external resistance) are defined by the influent and effluent carbon source concentrations. Several optimal reactor configurations were identified, as shown in figure 2.2. At high organic loads (high influent wastewater concentration) optimal performance is achieved when both MFCs are operated at high external resistance, i.e. both MFCs are methanogenic. At moderate organic loads treatment performance is maximized if the first MFC is methanogenic and the second MFC is exoelectricigenic. Finally, at low organic loads performance is maximized if both MFCs are exoelectricigenic.

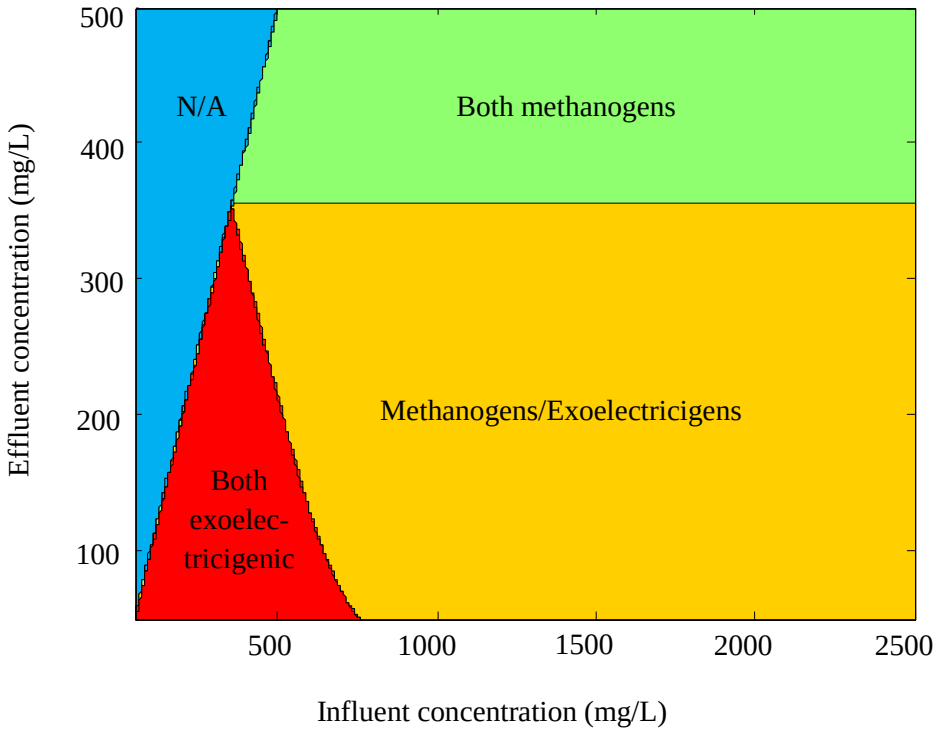

Figure 2.2: Regions with the largest treatment capacity in two staged MFCs. N/A refers to non-feasible region where the effluent concentration is greater than the influent concentration. Adapted from Pinto, Tartakovsky, Perrier and Srinivasan (2010).

In another optimization study, Pinto, Tartakovsky and Srinivasan (2012) used a unified BES (MxC) model (Pinto, Srinivasan, Escapa, & Tartakovsky, 2011) to derive analytical expressions for the optimal current that maximizes power production in MFCs or hydrogen production in MECs. The model analysis showed that the optimal current strongly depends on the internal resistance.

Furthermore, the unified model was used to demonstrate on-line tracking of a varying optimum by the multi-unit optimization method (Woodward, Perrier, Srinivasan, Pinto, & Tartakovsky, 2010).

Yahya, Hussain, Wahab and Khairi (2015) simplified the MEC model of Pinto, Srinivasan, Escapa and Tartakovsky (2011) to facilitate model application for process control purposes. The original three-phase model described above was reduced to a two phase model comprised of an anodic biofilm (layer 1) and a cathodic biofilm (layer 2). The authors then simulated performance of a classical proportional–integral–derivative (PID) controller tuned with an adaptive gain technique to control the production of hydrogen by selecting the optimal current and applied voltage. Also, Yan and Fan (2013) used a fuzzy PID controller to regulate the output voltage of an MFC. Process control simulations were performed using the MFC model of Zeng, Choo, Kim and Wu (2010).

In another study, Fang, Zang, Sun and Yu (2013) optimized the operational conditions of an MFC by considering an integrated modeling approach, which used uniform design, a machine learning approach, and a global genetic searching algorithm to develop the model. The resulting integrated model was used to optimize pH, temperature, ionic strength, and nitrogen concentration.

In terms of advanced model-based control strategies, only a single reference to the linear model predictive controller (MPC) designed by Fan, Zhang and Shi (2015) for the purpose of controlling MFC voltage can be found in the literature. The model used in this study to describe the MFC was based on the work of Zeng, Choo, Kim and Wu (2010). For the MPC controller a simple linear state-space dynamic model was derived based on the approximation of the experimental data using the least squares method. The MPC optimization problem tracked a given reference voltage and was solved by using Laguerre functions.

A summary of the control and optimization methods reviewed above is provided in table 2.2. It can be seen that most of these control and optimization studies were aimed at regulating BES voltage or maximizing power output, i.e. they address fast electrical dynamics. There is an obvious lack of control strategies capable of addressing the multi-scale dynamics linked to the dual biological and electrical nature of BESs. With this respect, the use of model-based controllers could provide a superior performance for both disturbance rejection and optimal operation.

Table 2.2: Summary of the optimization and control strategies applied to BESs.

BES	Reference	Manipulated input	Controlled output	Algorithm/ Controller	Disturbance
MFC	Wang, Park and Ren (2012)	Resistance	Voltage	Intermittent connection	-
	Grondin, Perrier and Tartakovsky, (2012)	Duty cycle	Voltage	Constraints on the voltage	Influent concentration
	Coronado, Perrier and Tartakovsky (2013)	Duty cycle, frequency	Voltage	PWM	Influent concentration
	Gardel, Nielsen, Grisdela and Girguis (2012)	Duty cycle, frequency	Current	PWM	Influent concentration
	Wang, Ren and Park (2012)	Inductance, duty cycle, frequency	Voltage, current	PWM, boost converter	Influent concentration
	Premier, Kim, Michie, Dinsdale and Guwy (2011)	Resistance	Power	Logic-based	Temperature
	Woodward, Tartakovsky, Perrier and Srinivasan (2009)	Resistance	Power	P/O, gradient, multiunit	Temperature, influent concentration
	Woodward, Perrier, Srinivasan, Pinto and Tartakovsky (2010)	Resistance	Power	Multiunit	Temperature, influent concentration
	Attarsharghi, Woodward and Akhrif (2012)	Resistance	Power	ESC	Influent concentration
	Yan and Fan (2013)	Flow rate	Voltage	PID, fuzzy PID	Resistance
	Fang, Zang, Sun and Yu (2013)	pH, temperature, ionic strength, nitrogen concentration	Coulombic efficiency, power	Integrated approach	-
	Fan, Zhang and Shi (2015)	Flow rate	Voltage	MPC	Temperature, influent concentration
MEC	Tartakovsky, Mehta, Santoyo and Guiot (2011)	Voltage	Current	P/O	Input flow rate, influent concentration
	Yahya, Hussain, Wahab andKhairi (2015)	Voltage	Hydrogen production	PID with adaptive gain	Input flow rate, influent concentration
	Andersen et al. (2013)	Frequency	Current	Cell balance system	Influent concentration

2.3 Perspectives

The discovery of mediator-less BESs created an opportunity for developing a number of novel technologies for sustainable energy or resource production from sustainable energy sources such as organic wastes. However, many BES technologies remain in the early development stages with a number of obstacles still to be resolved before progressing towards industrial applications. This transition from discovery to technology implementation can be accelerated by merging the knowledge of BES microbiology, electrochemistry and operating know-how into mathematical models suitable for process design, control and optimization.

Several areas of interest for applying model-based optimization and control techniques can be pointed out. BES models can be used for optimizing design and configuration of MFCs and MECs. Biofilm models, which account for the properties of anodophilic biofilms containing multiple microbial populations, can be most useful in this regard. Other BES optimization studies can address issues of optimal connection of multiple units. Development of software sensors (observers) capable of real-time estimation of key process parameters is another potentially promising research area. On-line monitoring strategies, which provide timely information on the state of BESs might be instrumental in stabilizing performance and averting process failures due to unpredictable variations in the influent stream composition.

CHAPTER 3 MATERIALS AND METHODS

3.1 MFC design and operation

Experiments were conducted in two continuous flow membrane-less air–cathode MFCs with an anodic compartment volume of 50 mL. Each MFC was constructed with a series of polycarbonate plates housing a 10 x 5 cm carbon felt anode with a total thickness of 5 mm (SGL Canada, Kitchener, ON, Canada) and a cathode made of a 10 x 5 cm manganese-based catalyzed carbon E4 electrode (Electric Fuel Ltd, Bet Shemesh, Israel). A nylon cloth separated the two electrodes.

The two MFCs were hydraulically operated in series, i.e. the effluent of the first MFC acted as influent for the second MFC. No pump was required between the two MFCs and liquid mixing inside each reactor was ensured by an external recirculation loop. The recirculation flow rate was kept constant during all the experiments. Choosing it an order of magnitude higher than the influent flow rate allowed for a constant biofilm thickness. A thermocouple was placed inside each anodic chamber and a flow-through heater located in the external recirculation loop was connected to a temperature controller (Model JCR-33A, Shinko Technos Company Ltd., Osaka, Japan) in order to maintain the temperature at a pre-set value of 23ºC for each MFC.

Acetate was used as the sole source of carbon. A highly concentrated acetate stock solution containing around 60 g L^{-1} of acetate was diluted into a trace metal solution in order to obtain the desired influent concentration at every time instant. To do so, two identical peristaltic pumps (model L/S, Masterflex, Cole-Parmer Instrument Company LLC., Chicago, IL, United States) were used to control the feed rates of each solution separately. Nominal value for the trace metals solution flow rate was typically set around 450 mL d^{-1} providing a hydraulic retention time around 2.7 h, and its range of operation was tested between 200 to 800 mL d^{-1}. Nominal value for the influent acetate concentration was typically set to 1000 mg L^{-1} and it was varied from 500 to 1800 mg L^{-1}.

Throughout the tests, the MFCs were electrically operated using pulse-width modulated connection of the external resistor (R-PWM mode) or using a P/O algorithm. In the first case, PWM operation involved connecting the external resistor to MFC terminals with an electronic switch (CMOS

transistor, model ADG801, Analog Devices Inc., Norwood, MA, United States). The switch was computer-controlled using a Labjack U3-LV data acquisition board (LabJack Corp., Lakewood, CO, USA). The data acquisition board was also used to record MFC voltage at a maximum rate of 22,500 scans/ s. In the second case, P/O operation for each MFC was performed using a computer controlled digital potentiometer with a data acquisition board (Innoray, Montreal, QC, Canada) that provided a resistor variation range from 4 to 133 Ω with a step of 1.3 Ω. More details about the two modes of operation are provided elsewhere (Coronado, Perrier, & Tartakovsky, 2013; Woodward, Perrier, Srinivasan, Pinto, & Tartakovsky, 2010). Figure 3.1 shows the experimental setup for the two staged MFCs and a screen print of the interface written in Visual Basic used to control both the hydraulic and electrical variables of the two MFCs. Note that, in the experimental setup, the first MFC is the one placed higher on the right side with respect to the second one placed lower on the left side. No additional pump in between the two MFCs was required for their correct operation.

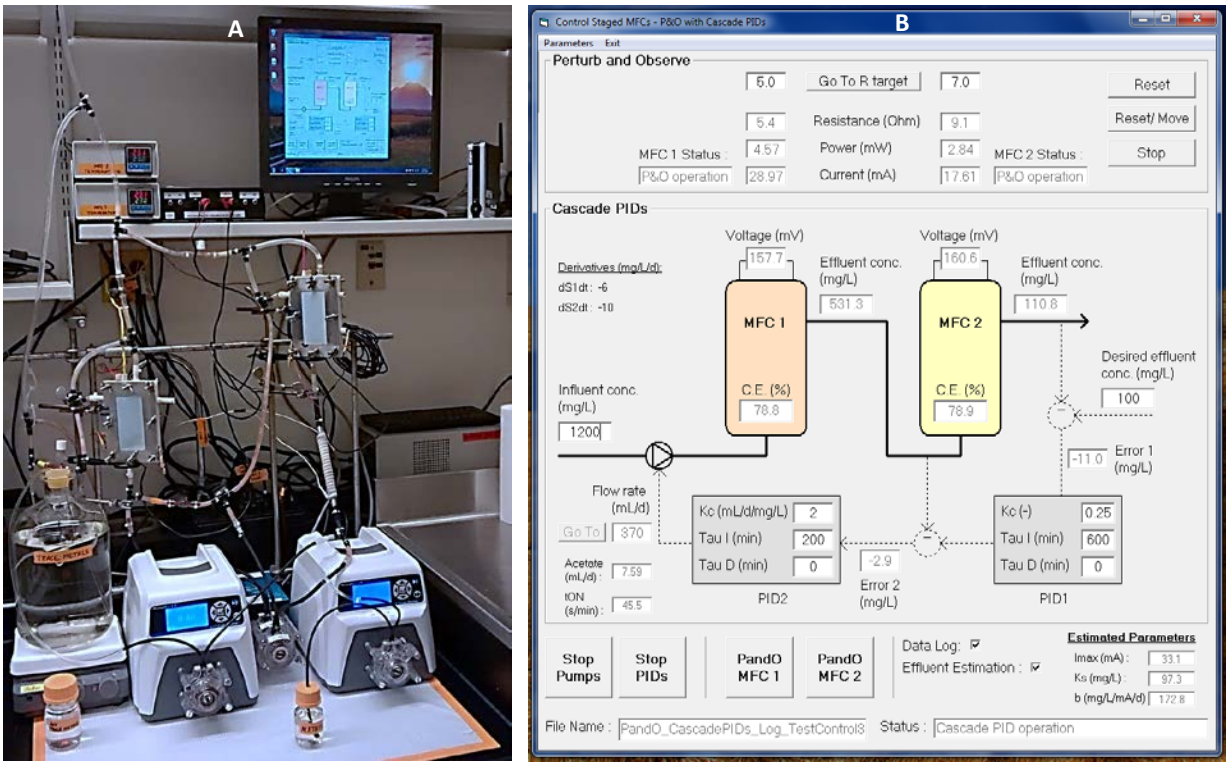

Figure 3.1: Experimental setup of two staged MFCs (A) and Visual Basic interface program showing the control strategy, in this case, P/O with PIDs in cascade (B).

3.2 Analytical methods, inoculum and media composition

Acetate concentration in the anodic liquid was analyzed on an Agilent 6890 gas chromatograph (Wilmington, DE, USA) equipped with a flame ionization detector. Method details are provided in Tartakovsky, Manuel, Neburchilov, Wang and Guiot (2008). Additionally, for some tests, acetate concentration was determined by spectrophotometry (DR3900, Hach, Loveland, CO, United States) using the esterification method provided by the Volatile Acids TNTplus 872 reagent set (Hach, Loveland, CO, United States).

The first MFC was inoculated with 5 mL of homogenized anaerobic sludge (Lassonde Industries, Inc., Rougemont, QC, Canada) with a volatile suspended solids (VSS) content of approximately 40–50 g L^{-1} and 20 mL of effluent from an operating MFC. The second MFC was populated by the bacteria detached from the first MFC with a global startup period of around 6 weeks.

The nutrient feed stock solution was composed of $NaC_2H_3O_2$ (80 g L^{-1}), yeast extract (0.83 g L^{-1}), NH_4Cl (18.7 g L^{-1}), KCl (74.1 g L^{-1}), K_2HPO_4 (32.0 g L^{-1}) and KH_2PO_4 (20.4 g L^{-1}). The concentration of sodium acetate in such solution was around 58.5 g L^{-1} (as CH_3COO^-). 1 mL of a trace elements stock solution was added to 1 L of deionized water, which was fed to the MFCs. On the other hand, the trace metals stock solution was composed of $FeCl_2 \cdot 4H_2O$ (2.053 g L^{-1}), H_3BO_3 (0.052 g L^{-1}), $ZnCl_2$ (0.0512 g L^{-1}), $CuCl_2$ (00396 g L^{-1}), $MnCl_{2.4}H_2O$ (0.0516 g L^{-1}), $(NH_4)_6Mo_7O_{24} \cdot 4H_2O$ (0.051 g L^{-1}), $AlCl_3$ (0.0528 g L^{-1}), $CoCl_2 \cdot 6H_2O$ (0.0532 g L^{-1}), $NiCl_2 \cdot 6H_2O$ (0.093 g L^{-1}), $(HO_2CCH_2)_2NCH_2CH_2N(CH_2CO_2H)_2$ (0.504 g L^{-1}) and HCl (1 mL L^{-1}). The anodic liquid solution conductivity was around 16 mS cm^{-1} and the pH around 6.5.

3.3 Numerical methods and calculations

Matlab R2012a (Mathworks, Natick, MA, USA) was used for all offline calculations. Parameter estimation was performed using the *fminsearch* subroutine of the Matlab Optimization Toolbox and the model equations were solved using a variable order integration method for stiff differential equations (*ode15s*). Online estimations of the electrical parameters from the EEC model were carried out according to the algorithm described by Coronado, Tartakovsky and Perrier (2013). A brief description of this algorithm is provided in the appendix A.

For the purpose of the sensitivity analysis, the sensitivity functions of the outputs with respect to each parameter were calculated. Assuming a general form of a dynamic model defined by its state and output equations as

$$\frac{dx}{dt} = f(t, x, u, \theta) \tag{3.1}$$

$$y(t) = g(t, x, u, \theta) \tag{3.2}$$

where t is the time, x is the vector of state variables, u is the input vector, y is the output vector and θ is the vector of parameters. In order to find the parameters with the highest influence on the model outputs, normalized sensitivity functions of the outputs with respect to each parameter were calculated as described in Kravaris, Hahn and Chu (2013):

$$\frac{d}{dt}\left(\frac{\partial x}{\partial \bar{\theta}}\right) = \frac{\partial f}{\partial x}\left(\frac{\partial x}{\partial \bar{\theta}}\right) + \frac{\partial f}{\partial \bar{\theta}}, \tag{3.3}$$

$$\frac{\partial \bar{y}}{\partial \bar{\theta}} = \frac{d\bar{y}}{dy}\left[\frac{\partial g}{\partial x}\left(\frac{\partial x}{\partial \bar{\theta}}\right) + \frac{\partial g}{\partial \bar{\theta}}\right]. \tag{3.4}$$

The correlation between the sensitivity functions calculated for the selected parameters was evaluated with the Pearson's linear correlation coefficient obtained with the *corr* function in Matlab's Statistics Toolbox. The magnitude of the effect of any parameter on a given output was calculated as the norm of its normalized sensitivity function $\|\bar{s}\|$, where $s = \partial\bar{y}/\partial\bar{\theta}$. The ellipses of confidence and the corresponding confidence intervals were calculated by means of the covariance matrix obtained as the inverse of the Fisher information matrix $\mathcal{F}$ and expressed as:

$$\mathcal{F} = \bar{S}^T \Sigma \bar{S}, \tag{3.5}$$

where $\bar{S} = \left[\bar{s}_1, \ldots, \bar{s}_p\right]$ is the sensitivity matrix for each output and Σ is the matrix containing the scaling factors $1/\sigma^2$ for each output. Here, σ^2 is the mean squared error (MSE) of each model output.

The objective function minimized for the model parameter estimation was formed by summing the MSE of each output as follows:

$$F_{obj} = \sum_i \left[\frac{1}{N_i}\sum_{j=1}^{N}\left(\bar{y}_{i,j}^{\exp} - \bar{y}_{i,j}^{\mathrm{sim}}\right)^2\right], \tag{3.6}$$

where $\bar{y}_{i,j}^{\exp}$ and $\bar{y}_{i,j}^{\mathrm{sim}}$ are the normalized experimental and model (simulated) outputs at the j^{th} sampling time; i is the model output index, and N is the number of measurements.

Visual Basic 6.0 (Microsoft Corporation, Redmon, WA, United States) was used for all online estimations and control of the staged MFCs. The discrete PID incremental form used in the control is the following:

$$\Delta u = K_c \left[\Delta e + \frac{\Delta t}{\tau_I} e_k + \frac{\tau_D}{\Delta t}(e_k - 2\Delta e + e_{k-2})\right] \quad (3.7)$$

where $\Delta u = u_k - u_{k-1}$ is the increment in the manipulated input u for the increment in time, Δt, between time instants k and $k-1$, and $\Delta e = e_k - e_{k-1}$ is the increment in the error e. K_c, τ_I and τ_D represent the proportional gain, and the integral and derivative time constants, respectively.

CHAPTER 4 COMBINED BIOELECTROCHEMICAL-ELECTRICAL MFC MODEL

This chapter addresses the current need for a dynamic MFC model able to describe the double layer capacitance effect and complex non-linear dynamics observed in most recent experiments, in particular tests involving pulse-width modulated connection of the external resistance.

4.1 Model formulation and structure

The CBE model is obtained by merging equations describing microbial, carbon source and electron balances of the bioelectrochemical model developed by Pinto, Srinivasan, Manuel and Tartakovsky (2010) with equations describing the EEC of an MFC (Coronado, Perrier, & Tartakovsky, 2013). Because the CBE model is largely based on such bioelectrochemical model, it inherits its features and assumptions. Consequently, the model accounts for exoelectricigenic (attached) and methanogenic (attached or suspended) microbial communities, which are modeled by a two-phase growth-washout model (Tartakovsky et al., 2008) with multiplicative Monod growth kinetics. Acetate (S) is considered as the sole carbon source. Other assumptions are the following: (1) the CBE material balances only describe the anodic compartment assuming a non-limiting cathode reaction rate; (2) the extracellular electron transfer mechanism from the carbon source to the anode is assumed via nanowires or direct contact with the anode; (3) the intracellular charge transfer mechanism is assumed to involve the oxidized and reduced forms of an intracellular mediator (e.g. NADH/NAD^+) with a constant mediator pool per microorganism. Furthermore, reactor material balances are simplified by assuming: (4) ideal carbon source mixing within the anode compartment; (5) absence of carbon source and microbial gradients within the anodic biofilm; (6) negligible gas transport through the cathode; and, (7) constant temperature and pH. The concept of the CBE model is presented in figure 4.1. Similar to the EEC model, internal resistance (R_1) represents the electrolyte ohmic resistance, while a resistor/capacitor circuit is included to describe the internal capacitance (C) and the activation losses (R_2). Accordingly, MFC internal resistance (R_{int}) is defined as

$$R_{int} = R_1 + R_2. \tag{4.1}$$

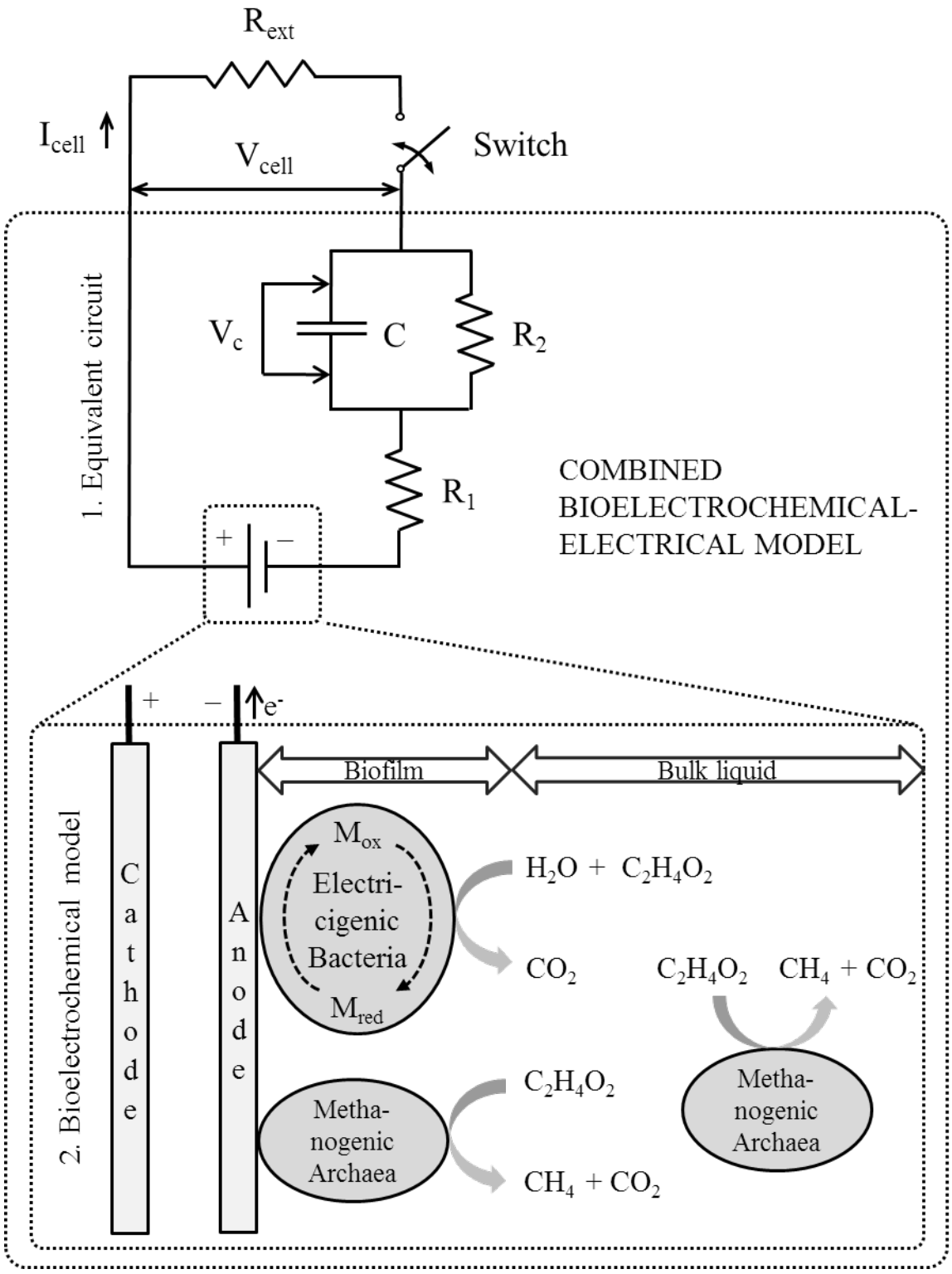

Figure 4.1: Schematic diagram of the CBE model for MFCs.

Based on the assumptions described above, MFC dynamic mass balances are given by the following equations:

$$\frac{dS}{dt} = -q_e X_e \ - q_m X_m + D(S_{in} - S), \tag{4.2}$$

$$\frac{dX_e}{dt} = \left(\mu_e - K_{d,e} - \alpha_e D\right) X_e, \tag{4.3}$$

$$\frac{dX_m}{dt} = \left(\mu_m - K_{d,m} - \alpha_m D\right) X_m, \tag{4.4}$$

$$\frac{dM_{ox}}{dt} = -Y q_e \ + 86\,400\,\gamma \frac{I_{cell}}{mFVX_e}, \tag{4.5}$$

where S is the substrate (acetate) concentration consumed by the exoelectricigenic bacteria, X_e, capable of producing electricity by means of an intracellular mediator, M_{ox}, or by the methanogenic archaea that produce methane, X_m. S_{in} is the input substrate concentration, $D = F_{in}/V$ is the dilution rate with the input flow rate F_{in} and the volume of the anodic compartment V. K_d is the microbial decay rate, Y is the yield of oxidized mediator, γ is the mediator molar mass, m is the number or electrons transferred, F is the Faraday constant and I_{cell} is the current produced by the MFC. The term 86 400 is only a conversion for the time units so that all derivatives are expressed in terms of days. The corresponding microbial growth rates μ and substrate consumption rates q are defined using multiplicative Monod kinetics as follows:

$$\mu_e = \ \mu_{max,e} \left(\frac{S}{K_{s,e}+S}\right) \left(\frac{M_{ox}}{K_M+M_{ox}}\right), \tag{4.6}$$

$$q_e = \ q_{max,e} \left(\frac{S}{K_{s,e}+S}\right) \left(\frac{M_{ox}}{K_M+M_{ox}}\right), \tag{4.7}$$

$$\mu_m = \ \mu_{max,m} \left(\frac{S}{K_{s,m}+S}\right), \tag{4.8}$$

$$q_m = \ q_{max,m} \left(\frac{S}{K_{s,m}+S}\right), \tag{4.9}$$

with K_S and K_M the Monod half rates for the substrate and oxidized mediator terms, respectively.

The biomass retention parameter α used to represent the limiting effect of the biofilm in the microorganisms' concentration is defined by the empirical expression

$$\alpha = \frac{1}{2}\left[1 + tanh[K_x(X_e + X_m - X_{max})]\right], \tag{4.10}$$

where K_x is a steepness factor and X_{max} is the maximum microbial concentration in the biofilm.

The electrochemical balance is given by

$$I_{cell} = \frac{E_{oc} - \eta_{conc} - V_c}{R_{ext} + R_1}\left(\frac{M_{red}}{\varepsilon + M_{red}}\right), \tag{4.11}$$

Where E_{oc} is the open circuit voltage, V_c is the voltage at the capacitor, R_{ext} is the external resistance applied to the MFC, M_{red} is the reduced oxidized mediator concentration and ε is the parameter for the Monod-like term which limits calculated MFC current at low values of M_{red}. The concentration losses η_{conc} are defined as

$$\eta_{conc} = \frac{RT}{mF} ln\left(\frac{M_{Tot}}{M_{red}}\right), \tag{4.12}$$

$$M_{Tot} = M_{ox} + M_{red}. \tag{4.13}$$

with R the ideal gas constant, T the temperature of the MFC and M_{Tot} the total concentration of intracellular mediator. Also, the following dynamic equation is used to describe the voltage at the internal capacitor:

$$\frac{dV_c}{dt} = \frac{86400}{C}\left(I_{cell} - \frac{Vc}{R_2}\right). \tag{4.14}$$

The following empirical expressions were derived based on previously obtained experimental results (Coronado, Tartakovsky, & Perrier, 2013; Grondin, Perrier, & Tartakovsky, 2012; Pinto, Srinivasan, Manuel, & Tartakovsky, 2010) and are used to describe the dependence of the internal resistances R_1 and R_2, the open circuit voltage E_{oc} and the internal capacitance C on the anodic biofilm:

$$R_1 = R_{min1} + (R_{max} - R_{min1})e^{-K_r X_e}, \tag{4.15}$$

$$R_2 = R_{min2} + (R_{max} - R_{min2})e^{-K_r X_e\left(\frac{S}{\xi + S}\right)}, \tag{4.16}$$

$$E_{oc} = E_{min} + (E_{max} - E_{min})e^{\frac{-1}{K_r X_e\left(\frac{S}{\xi + S}\right)}}, \tag{4.17}$$

$$C = C_{min} + (C_{max} - C_{min})e^{\frac{-1}{K_r X_e\left(\frac{S}{\xi + S}\right)}}, \tag{4.18}$$

where K_r is a steepness factor, min and max subindices indicate the minimum and maximum values for the variables and ξ is the parameter for the Monod-like term which links the EEC electrical variables to the substrate concentration.

Output electrical voltage and power are given by the following expressions:

$$V_{cell} = I_{cell} R_{ext}, \tag{4.19}$$

$$P_{cell} = V_{cell} R_{ext}. \tag{4.20}$$

Finally, the rate of methane production, Q, by methanogenic microorganisms is assumed to be proportional, with yield Y_{CH_4}, to the substrate consumption rate by this trophic group

$$Q = Y_{CH_4} q_m X_m V. \tag{4.21}$$

The proposed CBE model is capable of describing both fast and slow MFC dynamics. Notably, the model can be used for two distinctly different types of simulations. A conventional, "simulation" modeling approach is described by equations 4.1 to 4.21. This approach can be used to predict MFC output voltage, carbon source effluent concentration, and the distribution of microbial populations under various operating conditions. This application of the model requires prior knowledge of all the model parameters listed in table 4.1. Since the CBE model shares the microbial kinetics and material balances with the bioelectrochemical model of Pinto, Srinivasan, Manuel and Tartakovsky (2010), the two models predict the same long-term dynamics in the absence of fast external resistance variations.

In addition to offline predictions, a "parameter observer-based" version of the model could be used, where the simulations are carried out concurrently with the experiment and the empirical equations (4.15 to 4.18) are replaced by R_1, R_2, C, and E_{oc} estimations obtained in real time, e.g. using the estimation procedure proposed by Coronado, Tartakovsky and Perrier (2013) as described in the appendix A. This means that the electrical variables, which represent the observable part of the CBE model, are estimated online using the EEC model and are then plugged into the biochemical model, which is non observable. This procedure can be applied to the existing measurements or in real-time. The two approaches to utilizing the model are illustrated in figure 4.2.

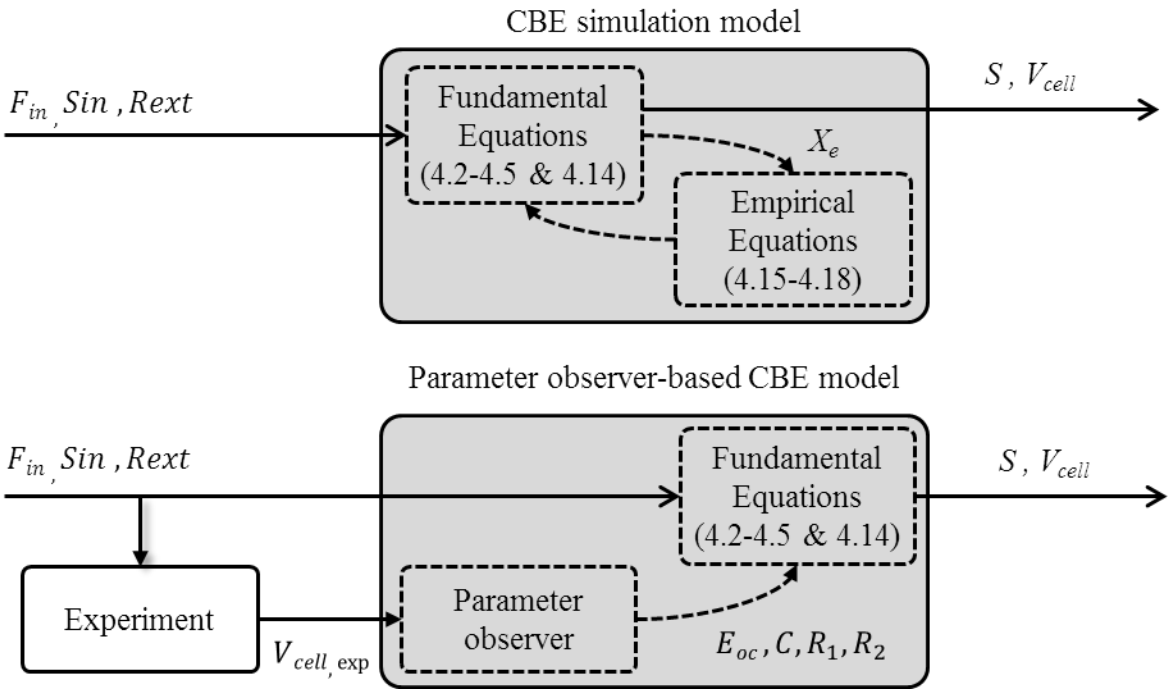

Figure 4.2: Structure for the two CBE model implementations. The inputs are F_{in} (flow rate), S_{in} (influent substrate concentration), and R_{ext}, (external resistance). The outputs are S (effluent carbon source concentration) and V_{cell} (voltage). The ‘‘parameter observer-based’’ CBE model uses instant estimations of the electrical variables such as open circuit voltage (E_{oc}), capacitance (C), and internal resistances ($R_1$and R_2).

4.2 **Sensitivity analysis**

The sensitivity analysis was carried out to reduce the number of model parameters requiring identification. First, the norm of the sensitivity profiles (equation 3.4) for all parameters was computed and arranged from highest to the lowest values. The highest norm indicates the highest impact of the parameter on the selected output. Second, because of the limited number of measurable state variables, the confidence intervals obtained from the Fisher information matrix (equation 3.5), were used to select parameters that can be estimated with an acceptable accuracy.

The influence of all model parameters on the model outputs was evaluated (results not shown) and four parameters (Y, $\mu_{max,e}$, K_r and K_x) with the highest impact were selected for parameter identification. The magnitude of the effect of Y, $\mu_{max,e}$, K_r and K_x on the model outputs (expressed

as the norm of the sensitivity function in equation 3.4) was, respectively, 2.7, 11.5, 0.27 and 1.7 for the output substrate concentration profile and 40.9, 72.1, 598 and 11.8, for the output voltage profile. Accordingly, $\mu_{max,e}$ showed the highest effect on the output substrate concentration while K_r had the greatest impact on voltage output.

Figure 4.3 shows the sensitivity profiles corresponding to these four parameters (Y, $\mu_{max,e}$, K_r and K_x). The profiles were obtained using the same inputs (influent acetate concentration and flow rate profiles) as those used in the experimental data for parameter estimation. Thus, the input flow rate was maintained so that the hydraulic retention time within the MFC was about 7.5 h and the input substrate concentration was subjected to step-wise changes as depicted in figure 4.3 A. Also, the external resistance was set to 12 Ω and controlled using the R-PWM mode of operation.

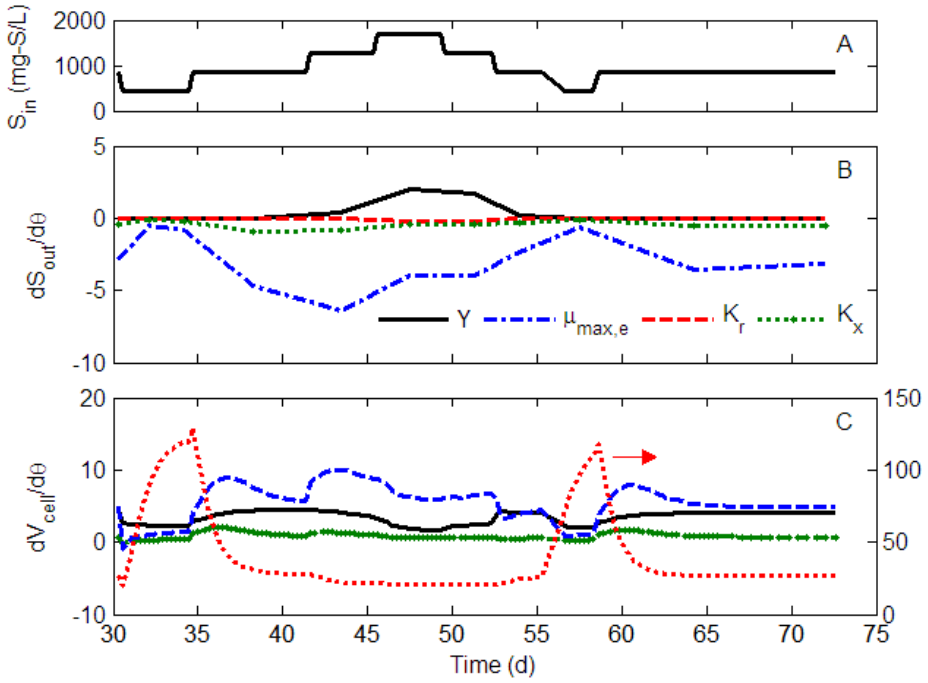

Figure 4.3: Sensitivity profiles for the estimated parameters. Influent substrate concentration profile (A) and sensitivity profiles corresponding to the effluent carbon source concentration (B) and output voltage (C) for the estimated parameters.

It should also be mentioned that in all simulations the profile for the methanogenic microorganisms remained negligible, probably due to the operational conditions favoring growth of the

exoelectricigenic bacteria (Kaur et al., 2014). Accordingly, all the parameters related to the methanogenic population showed little effect on the outputs. Their values were taken from previous experiments where methane production was measurable (Pinto, Srinivasan, Manuel, & Tartakovsky, 2010). Any other remaining parameters were not considered because either they presented negligible effects on the outputs or their values could be assumed (e.g. physical constants) or experimentally measured and did not need to be re-estimated.

4.3 Parameter estimation

To estimate model parameters, the difference between model outputs and the corresponding experimentally measured values (acetate concentrations and MFC voltage) was minimized according to equation (3.6). First, parameters of the "simulation" model described in figure 4.2 were estimated. Only four parameters, suggested by the sensitivity analysis were estimated.

The estimated values of Y, $\mu_{max,e}$, K_r and K_x were 41.3, 1.87, 0.031 and 0.00077, respectively (units are indicated in table 4.1). To visualize the estimation accuracy and the correlations between the estimated parameters, the 95 % confidence ellipses were calculated. All the parameters had low correlations as it can be observed by the ellipses being parallel to the axis, except for the set of parameters $\mu_{max,e} - K_x$ (figure 4.4 A). The lowest Pearson's correlation coefficient was -0.06 for $Y - K_r$ and the highest correlation corresponds to $\mu_{max,e} - K_x$, at 0.86. The highest correlation can be observed by the ellipse being at a certain angle with respect to the axis. The Fisher information matrix (equation 3.5) was invertible with the lowest and highest eigenvalues being 100 and $2.5 \cdot 10^{-6}$, respectively.

With a 95 % confidence level, the intervals of confidence were 4.3, 4.1, 0.2 and 25.7 % for Y, $\mu_{max,e}$, K_r and K_x, respectively, i.e., the accuracy of K_x estimation was the lowest. Also, the sensitivity analysis shows that K_x has low impact on the effluent acetate concentration (figure 4.3 B) and the MFC voltage (figure 4.3 C). Therefore, such large confidence interval is acceptable considering the low impact of K_x on the model outputs and the complex microbial dynamics. The intervals of confidence estimated for Y and $\mu_{max,e}$ were similar to 0.9 and 3.0 % values estimated by Pinto, Srinivasan, Manuel and Tartakovsky (2010) using voltage measurements obtained during first 20 days of operation (MFC startup).

Table 4.1: CBE model parameters

Parameter	**Symbol**	**Units**	**Notes***	**Simulation CBE**	**Observer based CBE**
Faraday constant	F	A s mol-e^{-1}	Universal	96,485	
Ideal gas constant	R	J K^{-1} mol^{-1}	Universal	8.3145	
Anode Temperature	T	K	Constant	298.15	
Anode volume	V	L	Constant	0.05	
Yield for M_{ox} balance	Y	mg-M mg-S^{-1}	Estimated	41.3	41.2
Substrate consumption rates	$q_{max,e}$	mg-S mg-X^{-1} d^{-1}	Assumed	8.48	
	$q_{max,m}$	mg-S mg-X^{-1} d^{-1}	Assumed	8.20	
Microbial growth rates	$\mu_{max,e}$	d^{-1}	Estimated	1.87	3.59
	$\mu_{max,m}$	d^{-1}	Assumed	0.1	
Steepness	K_X	L mg-X^{-1}	Estimated	0.00077	
	K_r	L mg-X^{-1}	Estimated	0.031	-
Methane yield	Y_{CH4}	mL-CH_4 mg-S^{-1}	Assumed	0.3	
Monod half rates	$K_{S,e}$	mg-S L^{-1}	Assumed	20	
	$K_{S,m}$	mg-S L^{-1}	Assumed	80	
	K_M	mg-M L^{-1}	Assumed	$0.2 \cdot M_{Total}$	
	ε	mg-M L^{-1}	Assumed	$0.0001 \cdot M_{Total}$	
	ξ	mg-S L^{-1}	Assumed	0	
Electrons transferred	m	mol-e^{-1} mol-M^{-1}	Assumed	2	
Molar mass	γ	mg-M mol-M^{-1}	Assumed	663,400	
Mediator fraction	M_{Tot}	mg-M mg-X^{-1}	Assumed	0.05	
Microbial decay rate	$K_{d,e}$	d^{-1}	Assumed	$0.02 \cdot \mu_{max,a}$	
	$K_{d,m}$	d^{-1}	Assumed	$0.02 \cdot \mu_{max,m}$	
Attainable concentration	$X_{max,e}$	mg-X L^{-1}	Assumed	512.5	
	$X_{max,m}$	mg-X L^{-1}	Assumed	525	
Open circuit voltage	E_{min}	V	Measured	0.01	-
	E_{max}	V	Measured	0.40	-
Internal resistance	R_{min1}	Ω	Measured	1.17	-
	R_{min2}	Ω	Measured	5.13	-
	R_{max}	Ω	Measured	2,000	-
Capacitance	C_{min}	F	Measured	0.01	-
	C_{max}	F	Measured	0.95	-

* The “assumed” parameters were taken from Pinto, Srinivasan, Manuel and Tartakovsky (2010). Experimental results obtained from the online estimation procedure described in Coronado, Tartakovsky and Perrier (2013) were used to determine de value of the “measured” parameters.

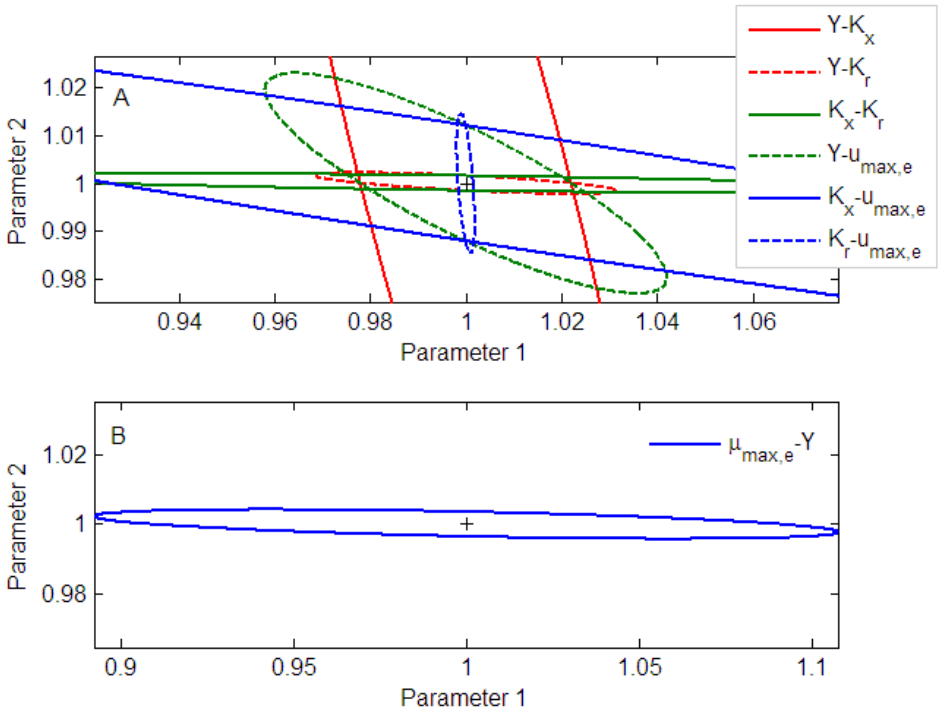

Figure 4.4: 95 % ellipses of confidence for the CBE model considering the "simulation" approach (A) and considering the "parameter observer-based" approach (B).

Parameters included in the empirical equations (4.15 to 4.18) were selected based on the results of the on-line parameter estimation procedure described in the appendix A. Notably, the on-line estimations of E_{oc} were significantly lower than the values estimated during polarization tests (results not shown). This difference can be attributed to higher acetate concentrations in polarization tests, in which E_{oc} values were acquired after 30 min of MFC operation in the open circuit mode. The absence of microbial exoelectricigenic activity during this period led to acetate accumulation and, accordingly, to carbon source non-limiting conditions resulting in higher E_{oc} estimations. Consequently, parameters E_{max} and E_{min} in equation (4.17) were set to 0.4 and 0.01 V, respectively. Parameters R_{max} , R_{min1} and R_{min2} in equations (4.15) and (4.16) were set to 2 000, 1.17 and 5.13 Ω, respectively. Finally, parameters C_{max} and C_{min} in equation (4.18) were set to 0.95 and 0.01 F, respectively, based on the estimated capacitance values obtained during MFC startup and operation. All other parameters were adapted from Pinto, Srinivasan, Manuel and Tartakovsky (2010), as indicated in table 4.1.

Figure 4.5 compares model outputs with the corresponding measurements. Effluent acetate concentrations were accurately described by the model at all influent concentrations (figure 4.5 A). MFC output voltage was observed to depend on the influent acetate concentration (organic load) with voltage drops during low load operation (days 30–35 and 57–59, figure 4.5 B). The model slightly underestimated the output voltage at the highest influent concentration (days 43–50) and overestimated voltage recovery after the second period of MFC operation at low organic load (days 59–63). Nevertheless, effluent acetate and voltage trends were correctly described. The profile of the concentration for the exoelectricigenic bacteria (dotted line in figure 4.5 B) showed a population decrease during the low influent concentration while attaining a plateau during substrate replete conditions. The profile for the methanogenic microorganisms remained negligible during the duration of the simulation, probably due to operational conditions favoring growth of the exoelectricigenic bacteria (Kaur et al., 2014). Additionally, the model provided an adequate description of the short-term output voltage during pulse-width modulated connection of the external resistance, as shown in figure 4.5 C. The concentration of oxidized mediator increased during the short-term closed circuit period and decreased otherwise. This behavior is understandable since during open circuit operation the concentration change of the oxidized form of the intracellular mediator indicates an accumulation of charge within the exoelectricigenic bacteria (biofilm) in the anodic compartment.

In addition to estimating parameters of the "simulation" model, two parameters (Y and $\mu_{max,e}$) were estimated to demonstrate the "parameter observer-based" mode of CBE model application, as described in figure 4.2. The "simulation" model requires values of R_{int}, E_{oc}, and C to be estimated based on the output voltage measurements, e.g. during R-PWM operation. Following the estimation procedure described above, Y and $\mu_{max,e}$ values were estimated to be 41.2 mg-M mg- S^{-1} and 3.59 day^{-1}, respectively. Figure 4.4 B shows the corresponding 95 % confidence ellipse for these two parameters. In this case the two parameters were non correlated with the Pearson's correlation coefficient being close to zero, thus the ellipse of confidence was almost parallel to the horizontal axis. Also, with a 95 % confidence level, the intervals of confidence for Y and $\mu_{max,e}$ were 10.8 and 0.43 %, respectively.

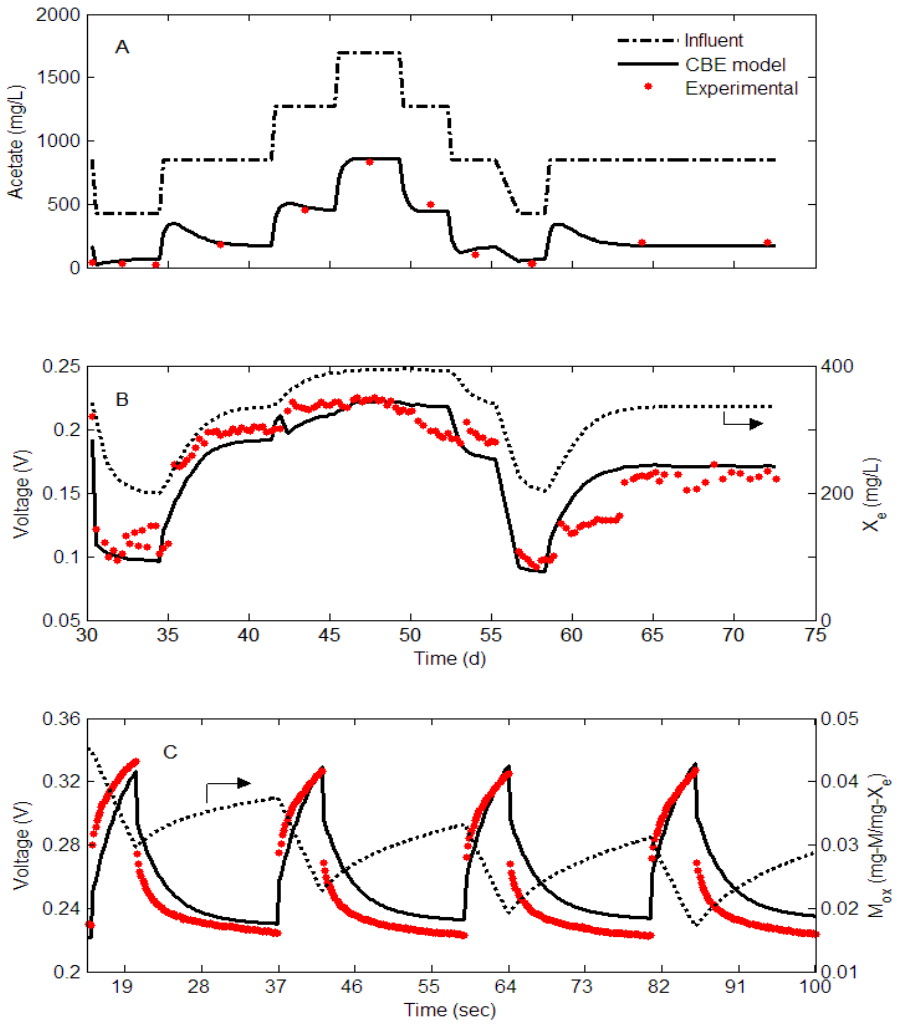

Figure 4.5: Results for the CBE "simulation" model. A comparison of acetate (A) and MFC voltage (B) experimental values with the calculated profiles. Fast-changing concentration of M_{ox} (dotted line) and the corresponding V_{cell} profile are shown for day 48 (C).

Figure 4.6 compares the measured values of voltage and acetate concentration with the corresponding outputs of the "parameter observer-based" model. As expected, the "parameter observer-based" model provided a better fit of the experimental data points, with MSE values of 0.008 and 0.005 for acetate and voltage estimations, respectively (figures 4.6 A and B). As compared to the "simulation" model, the output voltage estimations were particularly improved (figures 4.5 B and 4.6 B), while the acetate estimations were comparable between the two models. Overall, the "parameter observer-based" model proved to be more accurate, in particular, at high values of the influent acetate concentration.

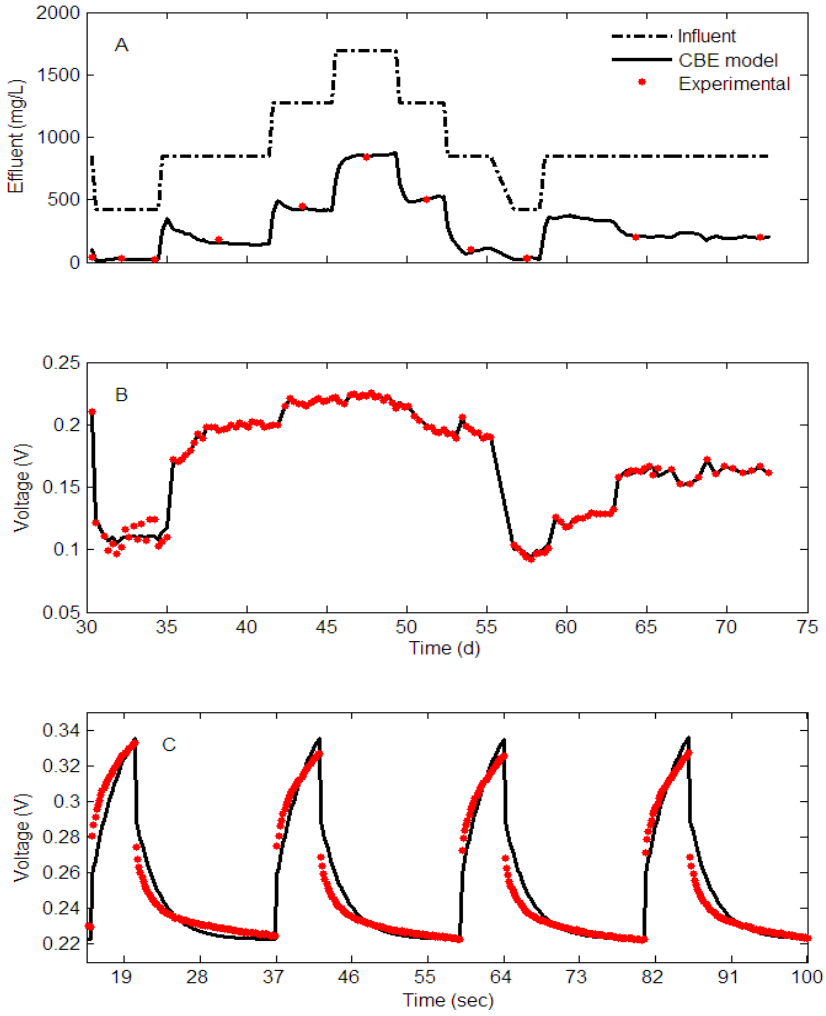

Figure 4.6: Results for the CBE "parameter observer based" model. A comparison of acetate (A) and MFC voltage (B) experimental values with the calculated profiles. Fast dynamics of MFC voltage during R-PWM operation is given for day 48 (C)

4.4 Conclusion

This work presents a combined bioelectrochemical–electrical (CBE) model that takes into consideration the internal capacitance and the nonlinear dynamics of MFCs populated with exoelectricigenic and methanogenic populations. Two approaches for model application were considered. In one approach, model-based simulations required all parameters of the model to be known a priori (e.g. estimated based on the existing experimental results). This "simulation" approach enables a variety of applications such as reactor design, optimization of operating

conditions, etc. An alternative approach requires MFC output voltage to be known or measured in real time thus enabling on-line estimation of certain electrical parameters of the model (E_{oc}, C, R_1 and R_2). While in this "parameter observer-based" approach the model can be only applied to the existing data set or used to accompany an actual process, it provides a better fit, while predicting process variables not measurable in real time, such as effluent carbon source concentration. Both approaches showed acceptable accuracy when describing both fast and slow dynamic behavior during R-PWM operation, while also being able to adequately predict the output substrate concentration. Since on-line measurements of the output substrate concentration are typically unavailable, the CBE model presents a step forward in developing software sensors for on-line MFC monitoring as well as for developing model based process control strategies.

CHAPTER 5 EFFECT OF PERIODIC CONNECTION OF THE EXTERNAL RESISTANCE ON MFC PERFORMANCE

In several recent studies, internal MFC capacitance is exploited to develop novel power management methods (Fradler et al., 2014; Walter, Greenman, & Ieropoulos, 2014). In one approach, by periodically disconnecting the MFC from an electrical load, energy is internally stored and then released to enable a power output burst (Coronado, Perrier, & Tartakovsky, 2013; Grondin, Perrier, & Tartakovsky, 2012). This approach can be used to resolve the problem of mismatch between the external and internal resistances. Significant power losses occur when the internal and external electrical resistances do not match (Pinto, Srinivasan, Guiot, & Tartakovsky, 2011). Furthermore, MFC operation at external resistances below the internal resistance may lead to near permanent loss of performance, including voltage reversal (Oh & Logan, 2007). A more traditional approach to overcome these power losses uses a real-time optimization method which seeks an external resistance that maximizes the power output (Woodward, Perrier, Srinivasan, Pinto, & Tartakovsky, 2010). On the other hand, recent efforts in on-line power output optimization demonstrated that the stability issue can be addressed by MFC operation with periodic connection/ disconnection of the external resistance (Coronado, Perrier, & Tartakovsky, 2013). In one study, stable power output was observed at various organic loads during MFC operation with pulse-width modulated connection of the external resistance (Grondin, Perrier, & Tartakovsky, 2012). Thus, this approach overcomes significant power losses during perturbations in the input substrate concentration.

5.1 Anode capacitance impact on MFC operation

The CBE model can be used as a useful tool to compare different power management approaches as presented in figure 5.1. In this simulation, MFC is assumed to be initially operated at a constant influent carbon source concentration followed by a concentration decrease of 50 %. The three approaches for the operation of the external resistance include using: (1) the perturbation-observation (P/O) algorithm that searches for the optimal R_{ext}^{*} resulting in maximum power output; (2) a fixed external resistance, and (3) an R-PWM operation with a duty cycle of 95 % (the average power output per cycle is shown). The P/O algorithm was simulated following similar operational

conditions as in Woodward, Perrier, Srinivasan, Pinto and Tartakovsky (2010) with a perturbation of 2 Ω and a sampling time of 20 s.

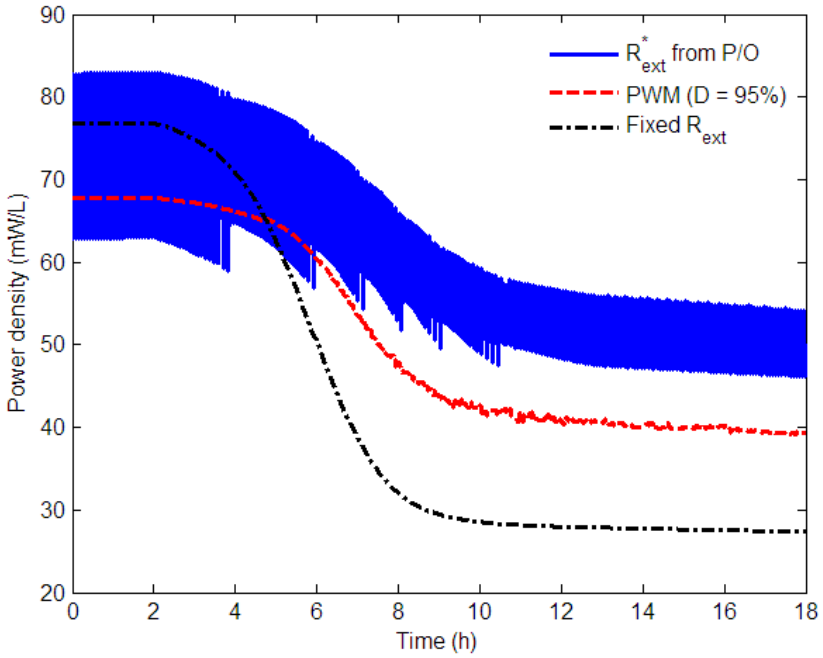

Figure 5.1: MFC power output estimated for three modes of operation, optimal R^*_{ext} calculated using P/O algorithm, fixed R_{ext}, and R-PWM operation at a duty cycle of 95%). A 50 % decrease in the influent concentration was imposed at 2 h.

Clearly, keeping a constant external resistance results in a severe drop in the power produced once the influent carbon source concentration decreases. The P/O algorithm closely follows changes in the internal resistance by adjusting the external resistance thus avoiding such a sharp drop in the MFC power output. Meanwhile, in the R-PWM operation the value of the external resistor remains unchanged at all organic loads and equal to the value used in the case of the constant external resistance, yet the R-PWM operation with a duty cycle of 95 % shows an improvement of the MFC performance when dealing with the sudden influent concentration disturbance. These simulation results agree with the experimental comparison of R-PWM and fixed resistor MFC operation described in (Grondin, Perrier, & Tartakovsky, 2012). Note that in Grondin, Perrier and Tartakovsky (2012) the duty cycle is controlled by selecting upper and lower voltage boundaries that control the intermittent operation which, seems to result in maximum power. That is not the

case in the PWM simulation presented in here and therefore, the power produced is lower than the one obtained with the P/O algorithm. An optimization of the duty cycle and/or the switching frequency might bring the power output closer to the maximum obtained with the P/O algorithm. Yet such optimal R-PWM operation has not been considered in this thesis.

5.2 Effect of Duty Cycle and Switching Frequency

As explained in the state of the art from chapter 2, a few recent publications show experimental results obtained from operating MFCs in an intermittent connection of the external resistance (Coronado, Perrier, & Tartakovsky, 2013; Gardel, Nielsen, Grisdela, & Girguis, 2012; Grondin, Perrier, & Tartakovsky, 2012). Interestingly, in Gardel, Nielsen, Grisdela and Girguis, (2012) microbial communities were found to be unaffected by such periodic operation in a broad range of switching frequencies. At the same time, MFC operation at different values of fixed external resistances was observed to result in different microbial populations (Lyon, Buret, Vogel, & Monier, 2010). Nevertheless, the influence of the periodic connection of the external resistance on the MFC performance still needs a deeper understanding. The CBE model can be used to qualitatively visualize the effect of duty cycle and switching frequency during the PWM operation of the external resistance in the microbial distribution and substrate consumption as well as in the electrical performance of MFCs. All the parameter values are shown in table 7.1 (MFC 1) and the minimum value of the applied external resistance is 5 Ω.

Figure 5.2 shows the average steady-state values of the effluent, exoelectricigenic and methanogenic concentrations as a function of the duty cycle and for two different switching frequencies. Additionally, the upper x-axis represents the apparent external resistance seen by the MFC as if it were operated in a continuous mode. Exoelectricigenic bacteria demonstrate highest concentration at low values of the apparent external resistance (high duty cycles) while methanogenic bacteria proliferate in the regions where the external resistance is at its highest value (low duty cycles). It can be observed that the effluent carbon source concentration presents a maximum (lowest substrate consumption by the microorganisms) at around a duty cycle of 30%, the coexistence region between the two microbial populations. This maximum in substrate effluent concentration was already demonstrated for the continuous operation mode in Pinto, Tartakovsky, Perrier and Srinivasan (2010). An increase of the switching frequency shifts all the profiles toward the left (or always disconnected region), thus expanding the range of apparent external resistances

favorable to the exoelectricigenic bacteria. Consequently, the plateau presenting the lowest value of the effluent concentration observed at high duty cycles (region between 90% to 100%) shifts into lower values of the duty cycle, resulting in a higher substrate consumption by the exoelectricigenic bacteria at higher values of the external resistance.

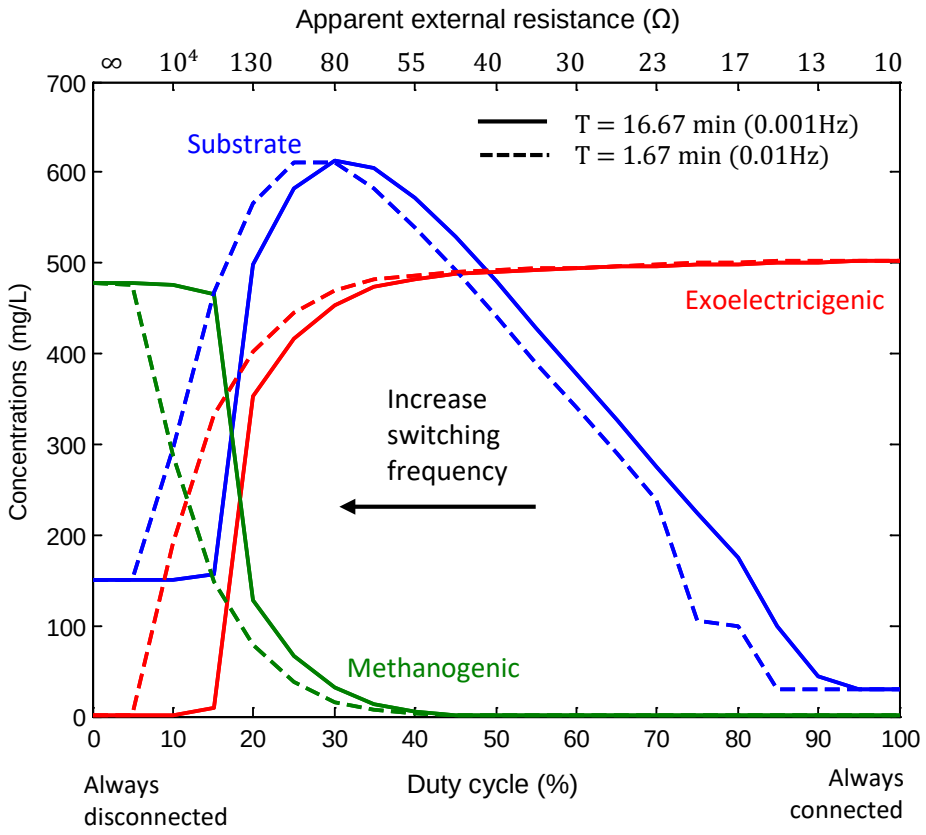

Figure 5.2: Effect of duty cycle and switching frequency on the effluent carbon source, exoelectricigenic and methanogenic microbial concentrations.

The average steady-state values of the output voltage, current and power produced by the MFC under R-PWM operation are shown in figure 5.3. At high values of duty cycle (close to always connected state) the average power output presents the maximum value while average voltage and current values remain similar to their values obtained in the fixed connection. Maximum power extends toward lower duty cycles (around 90%) when increasing the switching frequency. This result corroborates the positive effect of the intermittent operation of the external resistance on the electricity production even during mismatch with the internal resistance value, experimentally

observed in previous works (Coronado, Perrier, & Tartakovsky, 2013; Grondin, Perrier, & Tartakovsky, 2012). On the other hand, maximum voltage corresponding to the open circuit voltage (since current generated is negligible) can be observed at low duty cycles in the region where there still exist exoelectricigenic bacteria present in the microbial community. Once methanogenic are the only microorganisms populating the biofilm, voltage and current drop, as observed for values of the duty cycle around 20 %.

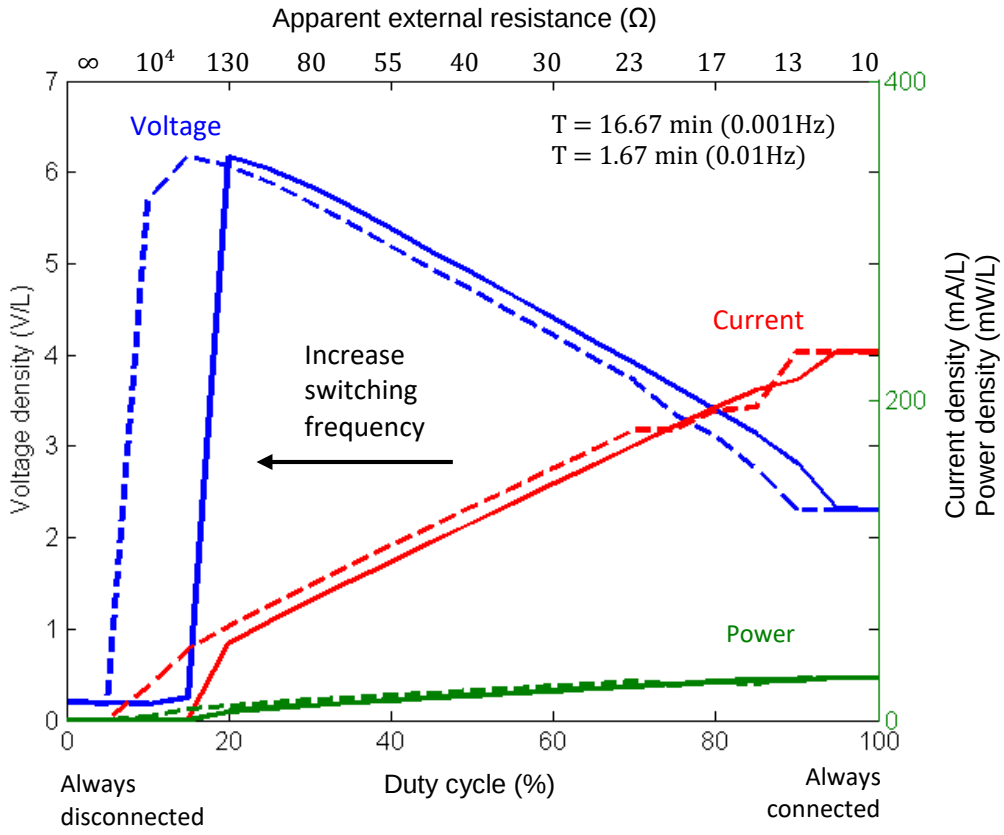

Figure 5.3: Effect of duty cycle and switching frequency on the electrical performance: average voltage, current and power produced by the MFC. Densities are expressed per volume of anodic compartment.

5.3 Conclusion

An experimental study of the effect of the duty cycle and switching frequency on the MFC performance would require a tremendous amount of time because of the major role played by the slow microbial growth dynamics in the overall performance. In such situation, the CBE model adequately describes MFC dynamics under periodic connection of the external resistance and represents a useful engineering tool to study the MFC performance. Exoelectricigenic bacteria demonstrate highest concentration at low values of the apparent external resistance (high duty cycles) while methanogenic bacteria proliferate in the regions of higher values of the apparent external resistance (low duty cycles). The effluent carbon source concentration presents a maximum in the coexistence region between the two microbial populations. An increase on the switching frequency favors the exoelectricigenic population over the methanogenic for higher values of the apparent external resistance. This results in maximum power expanding from 100 % toward lower duty cycles when increasing the switching frequency and corroborates the positive effect of the intermittent operation of the external resistance on the electricity production even during mismatch with the internal resistance value. Unfortunately, because switching frequency or duty cycle do not appear explicitly in the CBE model structure, the existence of an optimum in those two variables cannot be analytically studied and we can only rely on numerical simulations. Besides, those results should be considered cautiously since numerical complications appear when simulating at high values of the switching frequency or duty cycle.

CHAPTER 6 EFFLUENT QUALITY ESTIMATION

Electrical sensors are extensively used in bioreactors to convert available measurements into electrical signals that can be related to the variable of interest. For instance, pH meters correlate the voltage produced by the probe with the pH scale (as a result of a difference in electrical potential between a pH electrode and a reference electrode) and thermocouples generate a temperature-dependent voltage as a result of the thermoelectric effect between two different conductors. In that sense, MFCs naturally generate an electrical voltage signal depending on the carbon source concentration available in the anodic compartment without conversion into any intermediate signal.

Chemical oxygen demand (COD) and biological oxygen demand (BOD_5) are the two most common methods to estimate the concentration of organic pollutants in wastewater. The biodegradable fraction of the organic materials is estimated by measuring BOD5, which is a 5-day test. Results obtained from a COD analysis are also obtained with at least 4-6 h delay. Thus, real-time monitoring of the organic load required to comply with regulatory norms still represents a challenge. Benefiting from the bioelectrochemical nature of MFCs, continuous estimations of the biologically consumable organic fraction in wastewater could be obtained from the electrical measurements in MFCs (Chouler & Di Lorenzo, 2015).

6.1 Simplified mass balance

The lack of observability inherited from the biochemical MFC model eliminates the possibility of designing traditional observers. Consequently, other strategies need to be considered for the estimation of the effluent substrate concentration in MFCs. For instance, the CBE model presented in chapter 4 can be simplified, under certain conditions, to a single equation representing the relationship between substrate concentration and electric current generated by the cell. Thus, assume the following conditions:

(i) operation of the external resistance favoring the absence of methanogenic microorganisms, i.e. $dX_m/dt = 0$;

(ii) fully developed biofilm, i.e. the dynamics of the exoelectricigenic bacteria do not intervene so $dX_e/dt = 0$; and

(iii) steady state conditions for the intracellular mediator, i.e. $dM_{ox}/dt = 0$.

Then, the term related to the substrate consumption by the exoelectricigenic bacteria can be isolated from the mass balance of the intracellular mediator in equation (4.5) and be replaced in the mass balance of the substrate concentration in equation (4.2), resulting in the following simplified expression of the substrate concentration:

$$\frac{dS}{dt} = -\beta I_{cell} + D(S_{in} - S)\ , \tag{6.1}$$

$$\beta = 86\,400\,\frac{\gamma}{mFVY}\ . \tag{6.2}$$

where β is the parameter relating the substrate consumption with the production of electric current in mg-S L^{-1} d^{-1} A^{-1}. Note that, such parameter is assumed to be constant with time according to the CBE model parameters presented in table 4.1.

Equation (6.1) represents a simplified mass balance that only necessitates the estimation of the parameter relating the substrate consumption with the electric current produced by the cell, β. Once parameter β is known, no matter the initial value of the effluent chosen, just from the online measurements of the electric current, equation (6.1) is going to converge to a certain value of the effluent. The higher the dilution rate, the faster it will converge. The accuracy of the estimated effluent concentration will depend upon the accuracy of the estimation of β. A single sample of the effluent carbon source concentration under steady state conditions can be used to determine such parameter as $\beta = \frac{D(S_{in}-S)}{I_{cell}}$.

The simplified mass balance can only be applied to an existing data set or used to accompany an actual process. The estimation of the effluent carbon source concentration continuously necessitates measurements of the electric current generated by the cell, the applied dilution rate and the influent carbon source concentration. Especially, the latter can be challenging in real wastewater treatment plants where the influent carbon source concentration would be considered as an unknown disturbance.

6.2 Algebraic expression for the electric current

Instead of using the differential mass balance from the carbon source, an algebraic relation can be found between effluent concentration and electric current from the kinetics of the exoelectricigenic

population. Thus, replacing the substrate consumption rate q_e (equation 4.7) into the steady state mass balance of the oxidized mediator (equation 4.5), the following relationship can be found:

$$I_{cell} = I_{max}\left(\frac{S}{K_S+S}\right), \tag{6.3}$$

$$I_{max} = \frac{q_{max,e}X_e}{\beta}\left(\frac{M_{ox}}{K_M+M_{ox}}\right), \tag{6.4}$$

were K_S corresponds to the already known half Monod constant for the exoelectricigenic population, $K_{S,e}$.

Typically, the two parameters on the Monod expressions used in the CBE model are considered as constants, and therefore, expression (6.3) would correspond to the positive values of a rectangular hyperbola with an asymptote shifted to the value of I_{max}. However, this is not the actual case. Note that although I_{max} has units of current (mA or A), it does not correspond to any actual available measurement from the MFC and is a function of the intracellular mediator concentration in oxidized form and the concentration of exoelectricigenic bacteria inside the biofilm. Therefore, the value of the asymptote is a function of the effluent concentration, i.e. $I_{max}(S)$, and its variation with time deviates the shape from just a rectangular hyperbola, especially at low effluent concentrations, as shown in figure 6.1 A. Meanwhile, K_S is considered constant and equal to 20 mg L^{-1} according to the CBE model.

The CBE model can be used to visualize the profile between electric current and I_{max} with respect to the effluent concentration (figure 6.1 A and B, respectively). Both profiles are obtained under ideal optimal power operation by externally applying the exact value of the internal resistance at all time ($R_{ext} = R_{int}$), with a sampling time of 15 seconds, an influent concentration of 900 mg L^{-1} and for a decreasing flow rate from 0.5 to 0 L d^{-1}. Especially noticeable is the decrease of I_{max} at low substrate concentrations (figure 6.1 B) due to a decrease in the oxidized mediator concentration available within the cells. Such variation of the asymptote I_{max} modifies the shape of a rectangular hyperbola by presenting a zero derivative at the origin, i.e. $\frac{dI}{dS} = 0$ at $(0,0)$. For an effluent concentration higher than around 28 mg L^{-1}, I_{max} achieves a maximum value. Due to its importance, the effect of the external resistance in the resulting profiles is further discussed in section 6.3.

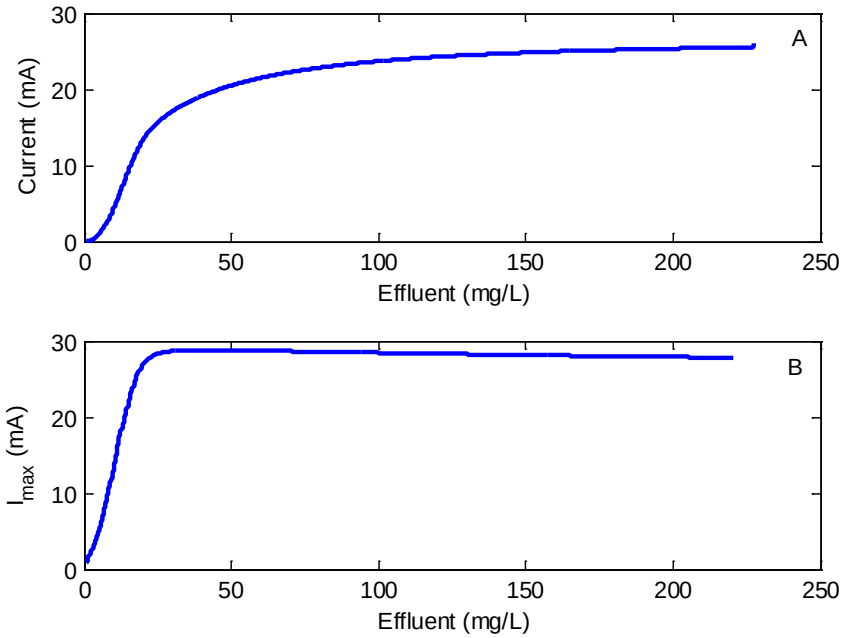

Figure 6.1: Electric current and I_{max} dependence on the effluent substrate concentration using the simulation CBE model under ideal maximum power operation.

Kinetics from the CBE model are useful to find the Monod expression relating the electric current to the effluent carbon source concentration from equation (6.3). Yet, having the asymptote I_{max} as a function of the same effluent carbon source concentration is not a viable approach in order to estimate in real time the effluent quality on MFCs. Adding a limiting term that restrains the current produced at low effluent carbon source concentrations is one possible solution. Thus, equation (6.3) can be modified into the following expression:

$$I_{cell} = I'_{max}\left(\frac{S}{K'_S+S+\frac{K_i}{S^2}}\right), \tag{6.5}$$

where the three parameters, I'_{max} and K'_S are, in this case, constant parameters different from the ones previously found and parameter K_i represents the limitation constant at low effluent carbon source concentrations. Figure 6.2 A shows the profile of the electric current and the Monod expression with limitation compared with the previous simulation from the CBE model. The estimated parameters being 26.9 mA, 13.7 mg-S L^{-1}, and 5 120 mg-S^3 L^{-3}, with confidence intervals

lower than 0.5 for I'_{max}, K'_S and K_i, respectively. MSE calculated is 1.47. Note that the MSE value has been weighted with the normalized values of the effluent carbon source concentrations. Concerning the other electrical variables, power could also be represented by the same expression as the one for the electric current while voltage would present a more complex function featuring higher order polynomials with more parameters, thus resulting too complex.

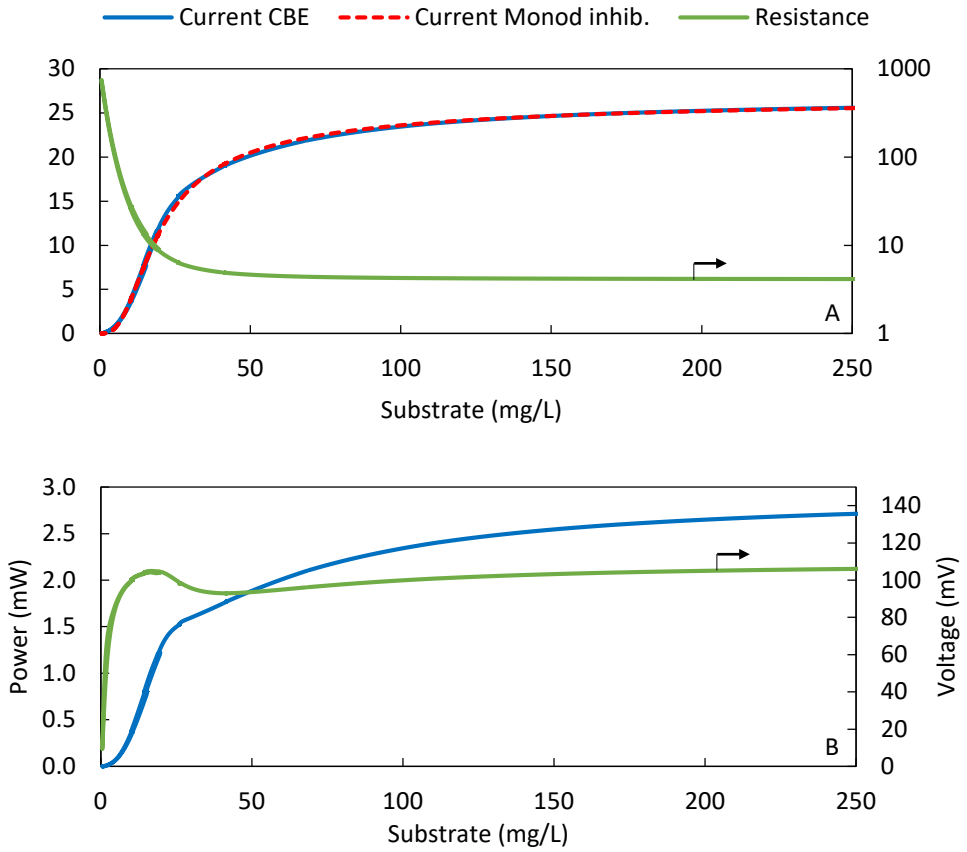

Figure 6.2: Dependence of the electrical variables with respect to the effluent concentration using the CBE model under ideal maximum power operation.

Inflection point from equation (6.3) can be obtained by finding the roots of its second derivative, i.e. finding the roots of the polynomial $K_S S^5 + K_i K_S S^2 + 6K_i S^3 - 3K_i^2$ which can only be computed numerically. Thus, for the previous values of parameters K_S and K_i, the only positive real root would be at an effluent carbon source concentration of 12.7 mg-S L^{-1}.

On the other hand, equation (6.5) can be approximated, at low effluent carbon source concentrations, by a simple cubic polynomial as follows:

$$I_{cell} \cong \frac{S^3}{a}\,, \tag{6.6}$$

$$a = \frac{K_i}{I'_{max}}\,. \tag{6.7}$$

However, by trial and error, it has been found that a third degree hyperbola with a single parameter, b, or even a Monod term with cubic polynomials and only two parameters, I''_{max} and K''_S, such as

$$I_{cell} \cong \sqrt[3]{S^3 + b^3} - b\,, \tag{6.8}$$

$$I_{cell} \cong I''_{max}\left(\frac{S^3}{S^3 + K''_S}\right), \tag{6.9}$$

can be useful for a wider range of low effluent carbon source concentrations. Figure 6.3 shows the cubic, third degree hyperbolic and cubical Monod approximations of the relationship between electric current and effluent carbon source concentrations. Parameter values are 190 mg-S^3 L^{-3} mA^{-1}, 7.94 [-], 19.9 mA, and 4950 mg-S^3 L^{-3}, for a, b, I''_{max} and K''_S, respectively. Note that the cubical Monod expression (equation 6.9) is able to approximate the shape of the current for a wider range of effluent concentrations considering only two parameters, yet the value of the asymptote, I''_{max}, which cannot be measured, is still needed. Experimental validation of the algebraic expressions of the electric current as a function of the effluent concentration is shown later in section 7.2.

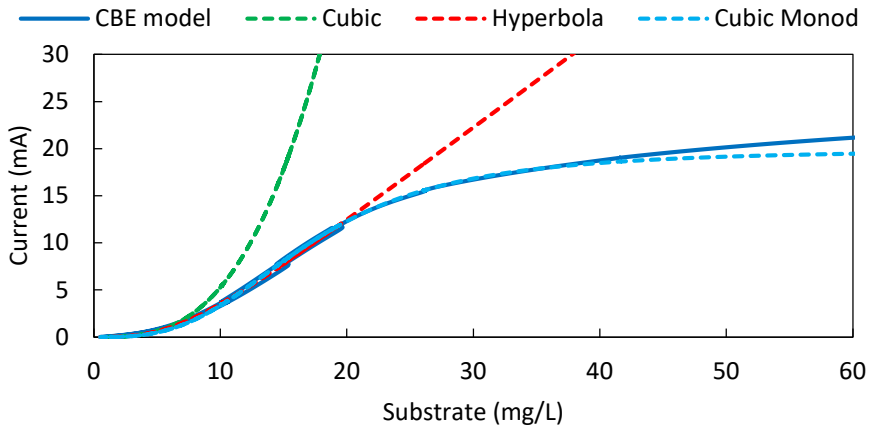

Figure 6.3: Approximations of the simulated electric current at low effluent concentrations.

6.3 Importance of R_{ext} operation

Among the three inputs considered by the CBE model, influent concentration, dilution rate and external resistance, the latter is of key importance in order to obtain the ideal profile shown in figure 6.2 between electric current and effluent carbon source concentration. While changes in S_{in} or D will result in moving along the ideal curve, the operation of the external resistance can actually modify its shape, thus rendering expression (6.5) and its approximations at low effluent concentrations (6.6 to 6.9) inaccurate as shown in figure 6.4.

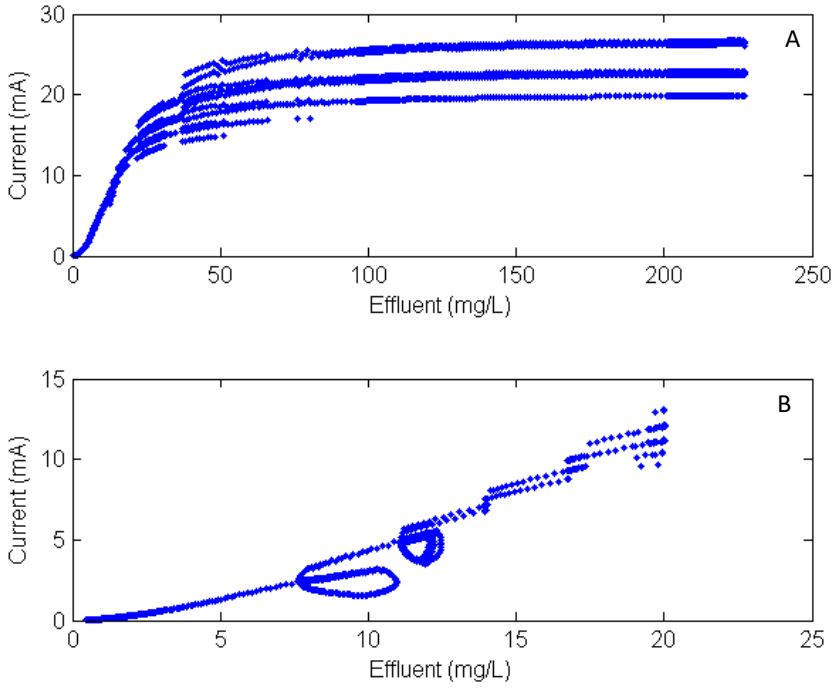

Figure 6.4: Variations in the electric current and effluent substrate concentration profile, due to (A) P/O operation of the external resistance and (B) inadequate sampling time.

Three factors have been found to play a major role for the operation of the external resistance that can heavily influence the shape of the relationship between electric current and effluent substrate concentration: (i) maximum power is required, i.e. tracking R_{int}. Any big mismatch between external resistance and internal resistance results in a loss of shape; (ii) MPPT algorithms that oscillate around the optimum such as P/O, generate multiple profiles simultaneously with different values of I_{max}, one for every value of the external resistance (figure 6.4 A). Adequate filtering of

the measured current should procure the expected ideal shape at the expense of modifying the dynamics; and last, but not least, (iii) discretization time for the external resistance needs to be small enough. When the MPPT algorithm is not able to follow the internal resistance adequately, simulations show a loss in the shape profile for high sampling times, especially at low effluent concentrations where MFCs should operate, e.g. for a simulation in the same conditions as in figure 6.1 A but choosing a sampling time four times superior, 60 seconds (figure 6.4 B).

6.4 Online effluent estimation from the electric current

For an online monitoring of the effluent concentration, the ideal approximation would only involve a single parameter that could be estimated by a single sampling of the effluent substrate concentration. Such is the case of the simplified mass balance (equation 6.1) with parameter β and the hyperbolic approximation of the electric current with parameter b (equation 6.8). Obviously, this is an open loop estimation that cannot guarantee the convergence to the true value.

Thus, providing a seed value of the effluent concentration S_{exp} and a filtered value of the electric current $I_{exp,f}$, parameter b from the third degree hyperbola approximation in equation (6.8) is the positive value of the following expression:

$$b = \frac{-3I_{exp,f}^2 \pm \sqrt{9I_{exp,f}^4 + 12S_{\exp}^3 I_{exp,f}}}{6I_{exp,f}}. \tag{6.10}$$

The estimate is assumed to be constant until a next measure is available to update its value. Such approximation at low effluent concentrations works reasonably well for monitoring the effluent carbon source concentration as shown in figure 6.5. The simulation uses the CBE model for different step changes in the flow rate and the influent concentration during 1 day of operation. Effluent concentrations are typically sampled once a day in wastewater treatment plants which would update the value of the parameter. With time, historical data should be gathered to statistically reduce the effect of a single sample on the value of the parameters.

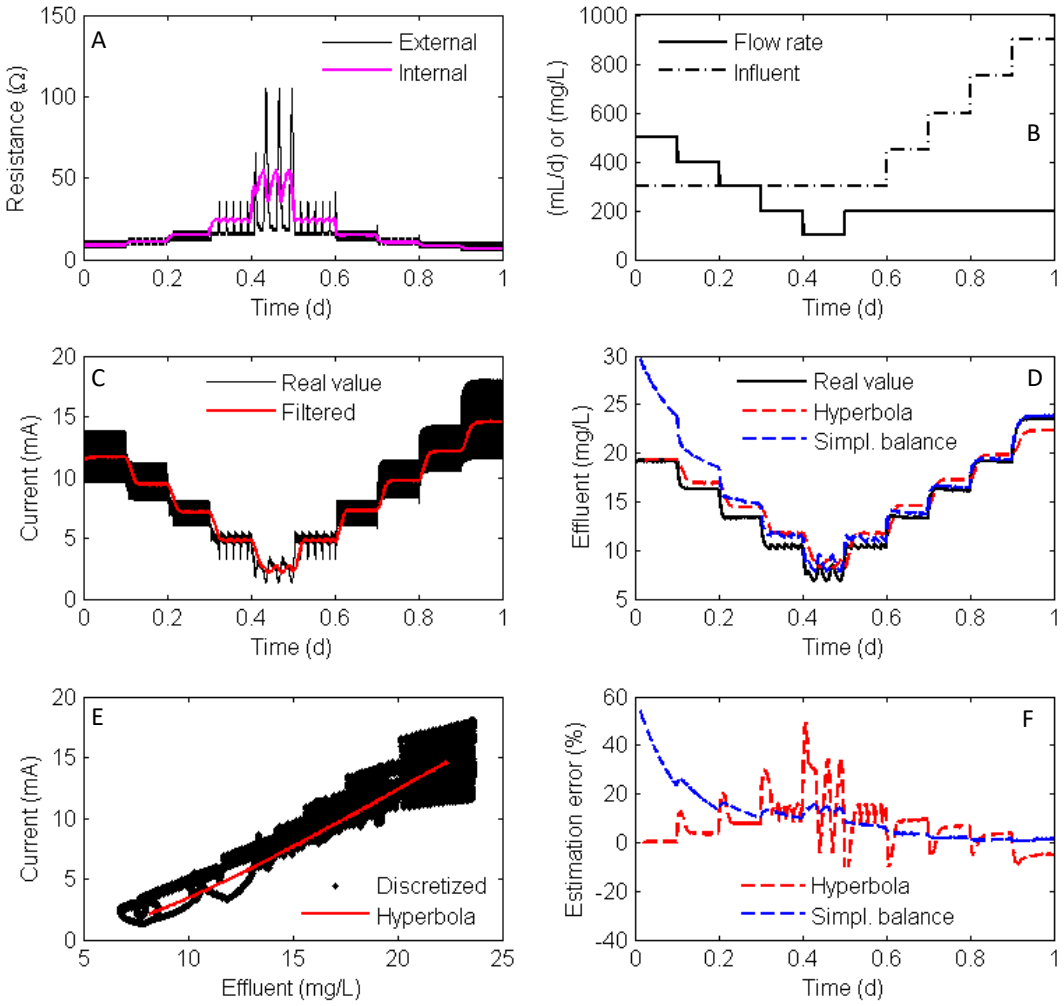

Figure 6.5: Simulation of effluent substrate concentration estimation from the electric current using the CBE model under P/O operation of the external resistance.

Figure 6.5 shows the accuracy of the effluent quality monitoring strategies during one day of operation. Figure 6.5 A shows the P/O operation of the external resistance at a sampling time of 15 seconds and a perturbation of 1.3 Ω together with the evolution of the internal resistance while figure 6.5 B presents the input flow rate profile, ranging from 500 to 100 mL d^{-1} and the influent carbon source concentration profile, ranging from 300 to 900 mg L^{-1}. Notice how the P/O algorithm presents some trouble seeking the maximum in power when the internal resistance

increases since the power curve becomes flatter. The continuous electric current evolution is with its discretized filtered value, obtained applying a moving average within an hour are shown in figure 6.5 C. The evolution of the real effluent carbon source concentration is shown in figure 6.5 D and it is compared with the estimation from the third degree hyperbolic approximation (equation 6.8) and the estimation from the simplified mass balance (equation 6.1). The initial value of the effluent carbon source concentration at steady state is used to calculate parameters b and β, 8.09 [-] and 241 mg-S L^{-1} d^{-1} mA^{-1}, respectively. The estimation error is shown right below in figure 6.5 F. Note the effect of the filtering slowing down the dynamics of the estimated substrate concentration with transient overshoots that can reach up to 50 % at the lowest values of the effluent carbon source concentration. On the other hand, the simplified mass balance is started at a seed effluent carbon source concentration higher than the actual value and its own dynamics bring the estimation to converge close to the true value. This is only because the value of β is very close to the true value of the parameter. Since the dynamic mass balance acts as a low pass filter, the sampled values of the current are directly used in the equation, thus, dynamics are not altered in this approach. Finally, figure 6.5 E presents the measured, or discretized, profile of the electric current against the real values of the effluent carbon source concentration and the profile of the third degree hyperbola approximation. Notice the evident effects of the P/O operation on the profile of the electrical current profile (section 6.3). Nonetheless, averaging the current during an hour of operation counteracts such effect and is able to estimate the effluent concentrations with steady state errors lower than 20 %.

6.5 Conclusion

Current techniques for effluent quality monitoring present a challenge if advanced control strategies are envisioned. Benefiting from the dual electrical and biochemical nature of MFCs to find simple strategies allowing to estimate the effluent carbon source concentration would represent a step forward toward the commercialization of such novel technology. In this sense, this thesis presents two simple ways to estimate the effluent concentration from the measurements of the electric current in MFCs, namely, a simplified dynamic mass balance of the substrate concentration and an algebraic expression describing the electric current as a function of the effluent carbon source concentration. The simplified dynamic approach presents the advantage of being valid within the whole range of effluent concentrations with the knowledge of a single parameter.

Additionally, no filtering of the electric current is needed which does not affect the estimation dynamics. The limiting reason for this solution being the assumed knowledge of the influent carbon source concentration and the need for an effluent carbon source measurement at steady state. Obviously, convergence to the real value is not guaranteed and the estimation is going to be as good as the estimation of the parameter. Nevertheless, the simplified dynamic mass balance is stable. On the other hand, the algebraic approach does not require any knowledge about the MFC inputs but its accuracy greatly depends on the electrical operation of the MFCs. Kinetics suggest the use of a Monod expression with a limitation term at low effluent concentrations. Three parameters need to be estimated in order to adequately describe the electric current in the whole range of effluent concentrations. However, approximations at low effluent concentrations can be found that only require the estimation of a single parameter. The generality of such profile is expected to be independent of the reactor configuration since the structure is derived from kinetics of the exoelectricigenic population.

CHAPTER 7 STAGED MFCS FOR WASTEWATER TREATMENT

Reactor staging benefits systems that are kinetically limited and systems requiring a low effluent composition (Scuras, Jobbagy, & Grady, 2001). It is often used in wastewater treatment with high rates of conversion in CSTRs placed upstream, and polishing the effluent to a specific requirement by those placed downstream. Improved power output and increased efficiency have resulted from connecting series of small MFCs in a hydraulic cascade (Gurung, & Oh, 2012; Ledezma, Greenman, & Ieropoulos, 2013; Winfield, Ieropoulos, & Greenman, 2012; Zhuang et al., 2012). Even, a recent study details the effect on the distribution of the microbial consortia within four staged MFCs treating real wastewater (Hodgson et al., 2016).

7.1 Dynamic modeling using the CBE model

Two MFCs were connected in a hydraulic cascade as shown in figure 3.1. The input flow rate was maintained so that the total hydraulic retention time (HRT) within the two staged MFCs was about 5 h and the input substrate concentration was subjected to step-wise changes (figure 7.1 A). Also, the external resistance was set to 5 Ω for the first MFC and 10 Ω for the second MFC and controlled using the intermittent model of operation (R-PWM) at 0.05 Hz of switching frequency and a duty cycle of 90 %.

The estimation procedure proceeded as detailed in chapter 4 for a single MFC. To estimate model parameters, the difference between model simulations and the corresponding experimentally measured values was minimized. Thus, experimental values for the effluent substrate concentration, S, and output voltage, V_{cell}, were used for parameter estimation (figure 7.1). Additionally, online estimations using the EEC model (Coronado, Tartakovsky, & Perrier, 2013) provided values for the open circuit voltage, E_{OC}, and internal resistance, R_2, (figure 7.3) that were also used during the optimization problem. The first half of the experimental data was used for parameter estimation and the rest for model validation.

Because of the limited number of measurable variables, the confidence intervals obtained from the Fisher information matrix were used to select parameters that can be estimated with an acceptable accuracy. The selected parameters for estimation were Y, $q_{max,e}$, K_r and ξ. It should be mentioned

that no methane production was observed during the experiments due to the operational conditions favoring growth of the electricigenic bacteria (Kaur et al., 2014). Accordingly, equation (4.4) was not considered for parameter estimation and all the parameters related to the methanogenic population were taken from previous experiments where methane production was measurable (Pinto, Srinivasan, Manuel, & Tartakovsky, 2010).

The estimated values of Y in mg-M mg-S^{-1}, $q_{max,e}$ in mg-S mg-X^{-1} d^{-1}, K_r in L mg-X^{-1}, and ξ in mg-S L^{-1} for the models representing the two staged MFCs are 24.7, 16.9, 0.0198, and 14.9, respectively for the first MFC and 73.8, 15.0, 0.027, and 1.91, respectively, for the second MFC (other parameters are indicated in table 7.1). To evaluate the estimation accuracy, the confidence intervals were calculated. Assuming a 95% confidence level, the intervals of confidence were 3.7 %, 3.8 %, 0.039 % and 6.8 % for Y, $q_{max,e}$, K_r and ξ, respectively for the first MFC and 8.5 %, 0.4 %, 0.1 % and 3.7 %, respectively for the second MFC. Such values are acceptable considering the complex microbial dynamics and the relatively small number of estimated model parameters.

On the other hand, parameters included in the empirical equations (4.15 to 4.18) were manually selected based on the results of the online estimation procedure. Accordingly, parameters R_{max}, R_{min1} and R_{min2} in equations (4.15) and (4.16) were set to 1,000 Ω, 0.97 Ω and 3.01 Ω for the first MFC and to 1,000 Ω, 2.27 Ω and 8.64 Ω for the second MFC, respectively. Also, parameters E_{max} and E_{min} in equation (3.17) were set to 0.26 V and 0.01 V for the first MFC and 0.35 V and 0.01 V for the second MFC, respectively. Finally, parameters C_{max} and C_{min} in equation (3.18) were set to 0.61 F and 0.01 F for the first MFC and 0.49 F and 0.01 F for the second MFC, respectively, based on the estimated capacitance values obtained during MFC startup and operation.

Figure 7.1 compares model simulations with the corresponding measurements. The first part of experimental results corresponding to days 0 to 9 of operation was used for parameter estimation and the remaining set of data for model validation. Effluent acetate concentrations were well described by the model at all influent concentrations (figure 7.1 A). MFC output voltage was observed to depend on the influent acetate concentration (organic load) with voltage drops during low load operation (days 7 to 10, figure 7.1 B). Effluent concentrations and voltage trends were correctly described with MSE values of 0.59 and 48.1 for the first MFC and 3.1 and 10.6 for the second MFC, respectively for the effluent concentration and the output voltage experimental profiles, considering the two data sets. Concerning the microbial population, the profile of the

concentration for the exoelectricigenic bacteria showed a population decrease during the low influent concentration while attaining a plateau during substrate-replete conditions (not shown). This effect was especially notable in the case of the second MFC. Additionally, the model provided an adequate description of the intermittent output voltage during pulse-width modulated connection of R_{ext}. Figure 7.1 C shows a zoom of the short-term voltage profile at the end of the day 13.

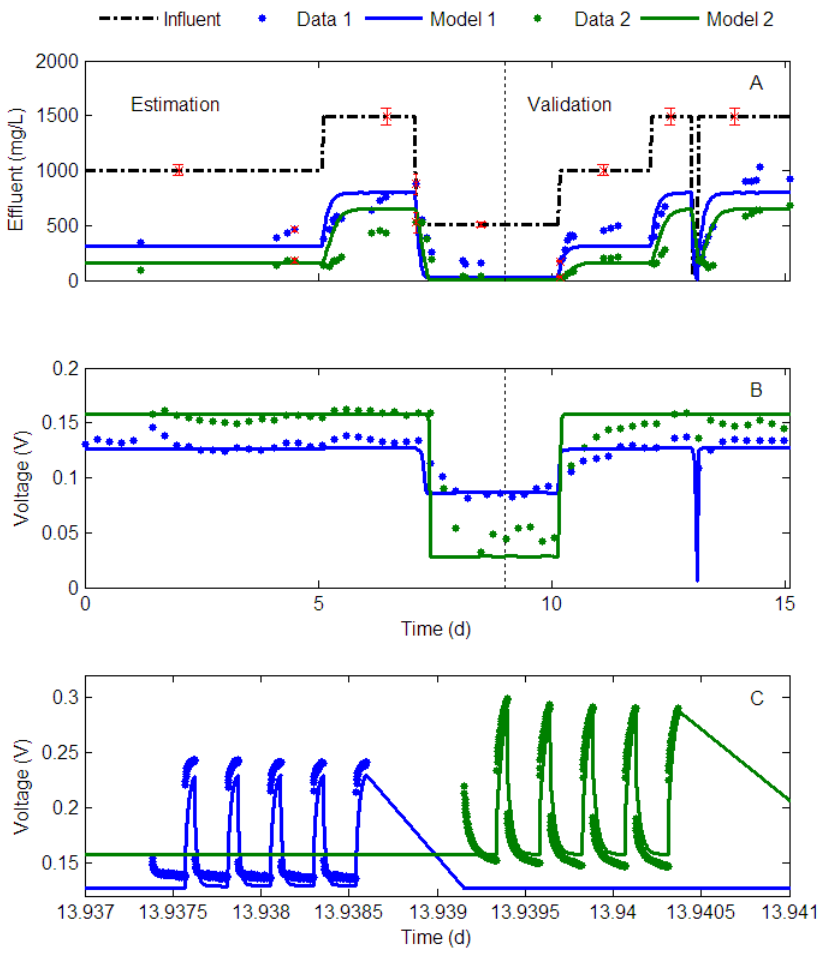

Figure 7.1: Results for the CBE "simulation" model for two staged MFCs. Comparison of effluent concentration (A) and MFC voltage (B) experimental values with the calculated profiles. Fast-changing voltage profile is shown for the end of day 13 in the validation data set (C).

Parameters were also estimated for the "parameter observer-based" CBE model as presented in figure 7.2. The estimated values of Y in mg-M mg-S^{-1}, $q_{max,e}$ in mg-S mg-X^{-1} d^{-1} for the models

representing the two staged MFCs are 26.1 and 19.1, respectively for the first MFC and 40.2 and 6.24, respectively, for the second MFC (units are indicated in table 7.1). Assuming a 95% confidence level, the intervals of confidence were 4.8 % and 14.0 % for Y and $q_{max,e}$, respectively for the first MFC and 8.5 % and 3.7 %, respectively for the second MFC. Such values are acceptable considering the complex microbial dynamics and the relatively small number of estimated model parameters. Again, the two parameters were non correlated with the Pearson's correlation coefficient being close to zero, thus the ellipse of confidence was almost horizontal.

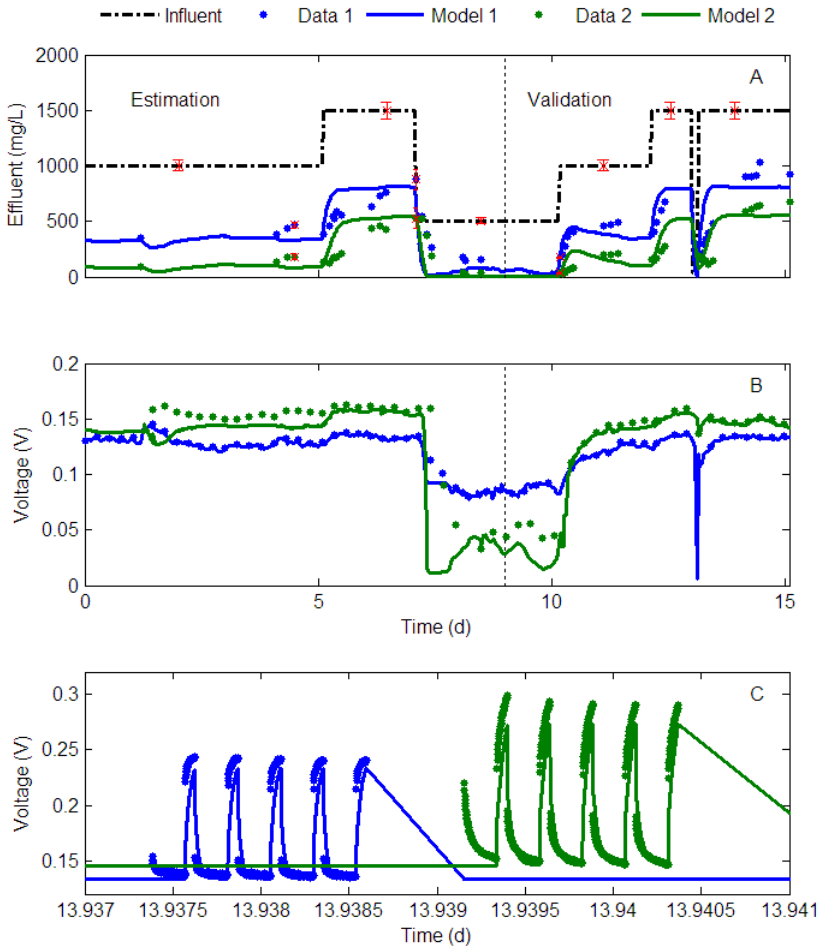

Figure 7.2: Results for the CBE "parameter observer based" model for two staged MFCs. Comparison of effluent concentration (A) and MFC voltage (B) experimental values with the calculated profiles. Fast-changing voltage profile is shown for the end of day 13 (C).

The values of the electrical variables from the EEC model for each MFC are presented in figure 7.3. The effect of substrate deplete conditions can be observed for the second MFC between days 7 and 10 where the influent substrate concentration was at its lowest. The open circuit voltage and capacitance decrease while internal resistance 2 increases. The internal resistance 1 seems to be unaffected by such conditions. Note that by adding the Monod term relating the empirical equations (4.16) to (4.18) with the substrate concentration, the change in open circuit voltage, capacitance and internal resistance 2 is adequately described. Such Monod term was not considered in the estimation from chapter 4 since no effects of the substrate were observed in the online estimated data.

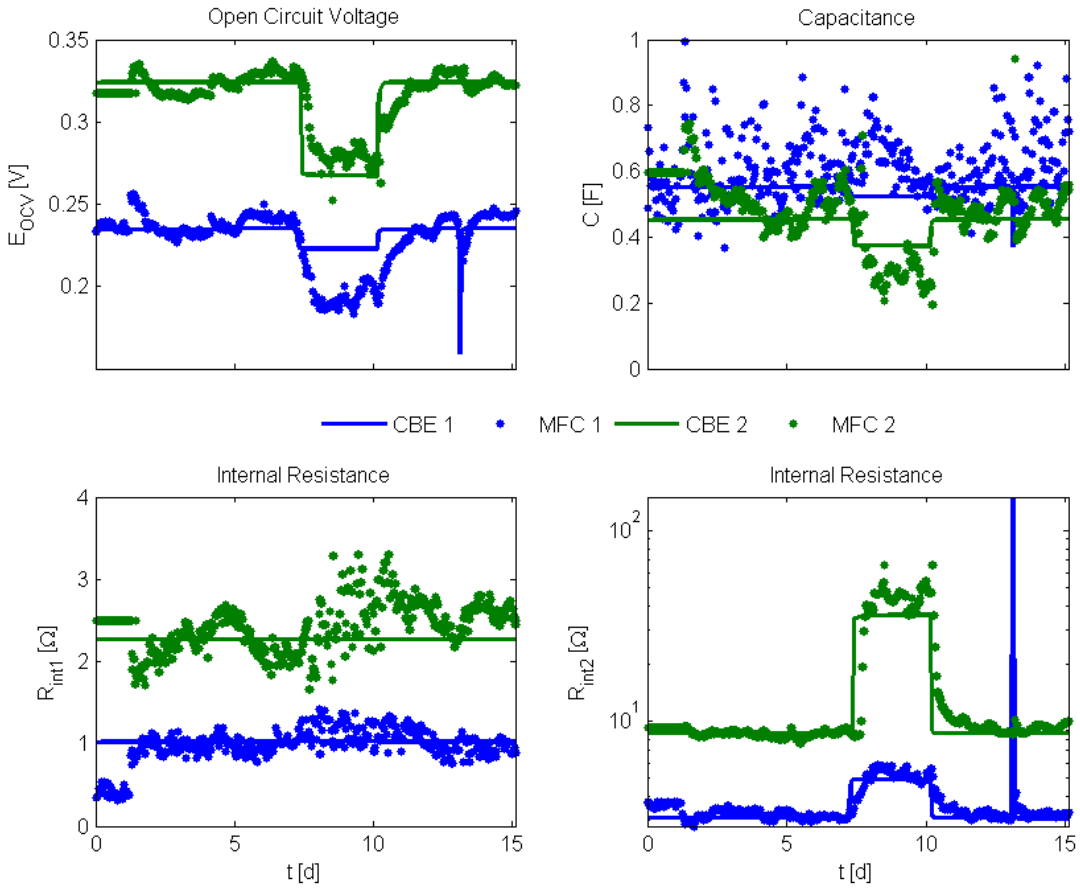

Figure 7.3: Online estimation values for the electrical variables for the two staged MFCs.

Table 7.1: CBE model parameters for the staged MFCs

				Simulation CBE		**Obs. Based CBE**	
Parameter	**Symbol**	**Units**	**Notes***	**MFC 1**	**MFC 2**	**MFC 1**	**MFC 2**
Faraday constant	F	A s mol-e^{-1}	Universal	96,485			
Ideal gas constant	R	J K^{-1} mol^{-1}	Universal	8.3145			
Anode Temperature	T	K	Constant	298.15			
Anode volume	V	L	Constant	0.05			
Yield for M_{ox} balance	Y	mg-M mg-S^{-1}	Estimated	24.7	73.8	26.1	39.6
Substrate consumption rates	$q_{max,e}$	mg-S mg-X^{-1} d^{-1}	Estimated	16.87	15.0	19.1	6.1
	$q_{max,m}$	mg-S mg-X^{-1} d^{-1}	Assumed	8.20			
Microbial growth rates	$\mu_{max,e}$	d^{-1}	Assumed	1.97			
	$\mu_{max,m}$	d^{-1}	Assumed	0.1			
Steepness	K_X	L mg-X^{-1}	Assumed	0.04			
	K_r	L mg-X^{-1}	Estimated	0.0198	0.027	-	
Methane yield	Y_{CH4}	mL-CH_4 mg-S^{-1}	Assumed	0.3			
Monod half rates	$K_{S,e}$	mg-S L^{-1}	Assumed	20			
	$K_{S,m}$	mg-S L^{-1}	Assumed	80			
	K_M	mg-M L^{-1}	Assumed	$0.2 \cdot M_{Tot}$			
	ε	mg-M L^{-1}	Assumed	$0.0001 \cdot M_{Tot}$			
	ξ	mg-S L^{-1}	Estimated	14.85	1.9	-	
Electrons transferred	m	mol-e^{-1} mol-M^{-1}	Assumed	2			
Molar mass	γ	mg-M mol-M^{-1}	Assumed	663,400			
Mediator fraction	M_{Tot}	mg-M mg-X^{-1}	Assumed	0.05			
Microbial decay rate	$K_{d,e}$	d^{-1}	Assumed	$0.02 \cdot \mu_{max,e}$			
	$K_{d,m}$	d^{-1}	Assumed	$0.02 \cdot \mu_{max,m}$			
Attainable concentration	$X_{max,e}$	mg-X L^{-1}	Assumed	512.5			
	$X_{max,m}$	mg-X L^{-1}	Assumed	525			
Open circuit voltage	E_{min}	V	Measured	0.01	0.01	-	
	E_{max}	V	Measured	0.26	0.35	-	
Internal resistance	$R_{min,1}$	Ω	Measured	0.97	2.27	-	
	$R_{min,2}$	Ω	Measured	3.01	8.64	-	
	R_{max}	Ω	Measured	1,000	1,000	-	
Capacitance	C_{min}	F	Measured	0.01	0.01	-	
	C_{max}	F	Measured	0.61	0.49	-	

* The "assumed" parameters were taken from Pinto, Srinivasan, Manuel and Tartakovsky (2010). Experimental results obtained from the online estimation procedure described in Coronado, Tartakovsky and Perrier (2013) were used to determine de value of the "measured" parameters.

7.2 Effluent quality monitoring

Effluent concentration can be monitored using any of the two approaches previously presented in chapter 6, either the simplified mass balance from equation (6.1) or the algebraic relation of the electric current and its approximations from equations (6.5) to (6.9). Experimentally, the two staged MFCs where operated at a variable flow rate from 0 to 0.6 L d^{-1}, which represents a HRT from infinite to 2 h, or a dilution rate between 0 and 12 d^{-1}. The influent concentration for the first MFC was maintained at a constant value of 750 mg-S L^{-1}. The second MFC, however, received a variable influent concentration coming from the first MFC ranging between 25 and 450 mg-S L^{-1} simultaneously with the change in flow rate. Power was maximized by means of a P/O algorithm with a sampling time of 60 s and a resistance perturbation of 1.3 Ω.

The external resistance applied to the staged MFCs and the power and current produced by each cell are shown in figure 7.4 A, B and C, respectively. Note that, an unforeseen error occurred between days 4 and 6 of operation during which the data logging file was corrupted and therefore the data is omitted. Nevertheless, the test was carried out normally during such period. Remark as well, the visible oscillations in the external resistance applied to the second MFC from day 8 of operation. Such behavior is found to appear when the effluent concentration inside the second reactor is low enough which might be translated into a flatter power curve, and therefore, the P/O algorithm finds it more difficult to stay around the optimum. Lowering even further the effluent concentration, the maximum value attainable by the external resistor is achieved at day 12 and that is why the external resistance presents a flat maximum at 133 Ω. The first MFC, on the other hand, does not present any noticeable oscillation during the operation, except the fast inherent oscillations around the maximum power from the P/O algorithm.

Performance of the simplified mass balance (equation 6.1) is presented in figure 7.4 D. The experimental test was initiated at steady state in order to allow for the estimation of parameter β. Thus, using the first effluent substrate concentration, β was found to be 118 and 85.5 mg-S L^{-1} mA^{-1} for the first and second MFCs, respectively. Although a single sample is used to determine the value of the parameter, the performance of the effluent quality monitoring is quite acceptable during the slightly over two weeks of operation of the reactors. Additionally, it should be mentioned the sturdiness of such monitoring approach for direct estimation from the raw electric current values. There is no need to filter the electric current since the differential equation acts as

a low pass filter, thus the dynamics of the effluent concentration estimation are not altered. Only initially, for the estimation of parameter β, the electric current values were filtered for the previous two hours. The highest coulombic efficiency was found to be 83.2 and 95.7 % for the first and second MFCs, respectively.

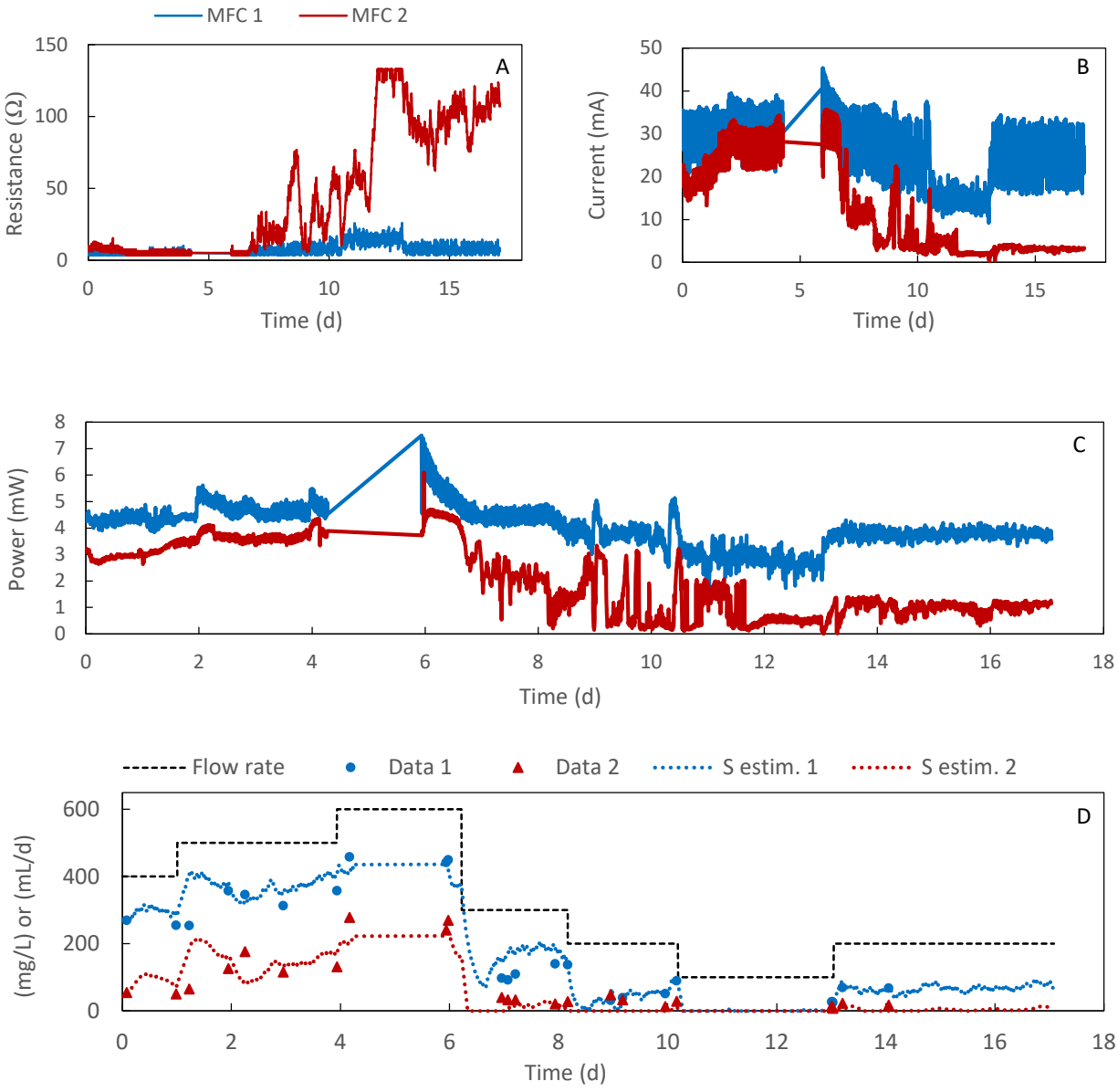

Figure 7.4: Experimental online effluent substrate concentration monitoring in staged MFCs using the simplified mass balance (equation 6.1).

The main advantage of the simplified mass balance for effluent quality monitoring lies in the validity of the estimation over the whole range of operation of the reactors with just a single parameter required. Yet, the need of knowing the influent carbon source concentration at all time may hinder toward its applicability in wastewater treatment applications where such input is considered to be an unknown disturbance. On the other hand, the algebraic expressions describing the electric current as a function of the effluent substrate concentration overcome such limitation and the estimation in staged MFCs becomes independent for each reactor. Additionally, because kinetics of the exoelectricigenic population dictate the profile, it can be assumed general for any kind of reactor, not just for CSTRs. Nevertheless, they require historic records of the electric current and effluent carbon source concentrations in the whole range of operation for the parameters to be estimated prior to the tests.

The performance of the algebraic approaches for the monitoring of the effluent quality is presented in figure 7.5. The Monod expression with limitation (equation 6.5) is used to describe the profile of the electric current as a function of the effluent concentration (figure 7.5 A). The estimated parameters for the first MFC being 38.1 mA, 44.2 mg-S L^{-1}, and 17 400 mg-S^2 L^{-2}, with confidence intervals 5.32, 5.09, and 8.46 % for I'_{max}, K'_S and K_i, respectively, and for the second MFC being 32.7 mA, 29.2 mg-S L^{-1}, and 63 500mg-S^2 L^{-2}, with confidence intervals 4.27, 6.85, and 9.52 for I'_{max}, K'_S and K_i, respectively. Note that the MSE is weighted with the normalized experimental values of the effluent substrate concentration in order to counteract the lack of more experimental values at higher concentrations. MSE calculated is 51.9 and 66.8 for the first and second MFCs, respectively. Cubic, third degree hyperbolic and cubical Monod approximations at low effluent concentrations are also shown in figure 7.5 B and C. Parameter values for the first MFC are 457 mg-S^2 L^{-2} mA^{-1}, 19.1 [-], 25.8 mA, and 28 600 mg-S L^{-1}, with confidence intervals 8.03, 7.53, 12.3 and 4.76 %, for a, b, I''_{max} and K''_S, respectively, and for the second MFC are 1 940 mg-S^2 L^{-2} mA^{-1}, 30.87 [-], 22.8 mA, and 48 200 mg-S L^{-1}, with confidence intervals 9.61, 8.43, 15.5 and 7.14 %, for a, b, I''_{max} and K''_S, respectively.

Note that the estimated parameters from the experimental values are much higher than the values estimated from the simulation using the CBE model in section 6.2. Parameters in the CBE model were calculated using a relatively young MFC, barely three months since the inoculation, while the experimental data from figure 7.5 was obtained after six months of operation. This might suggest a variation in the electric current profile with time, thus time dependent parameters.

Considering the staged MFCs fed with acetate as the ideal scenario, a more realistic feeding medium, such as wastewater, would probably present a higher value of the limitation parameter K_i, which would translate into a wider range of low effluent concentrations for the algebraic approximations to be valid. The reasons for the increase in such parameter probably being caused by increasing diffusion difficulties of both substrate and electrons/mediators through the biofilm.

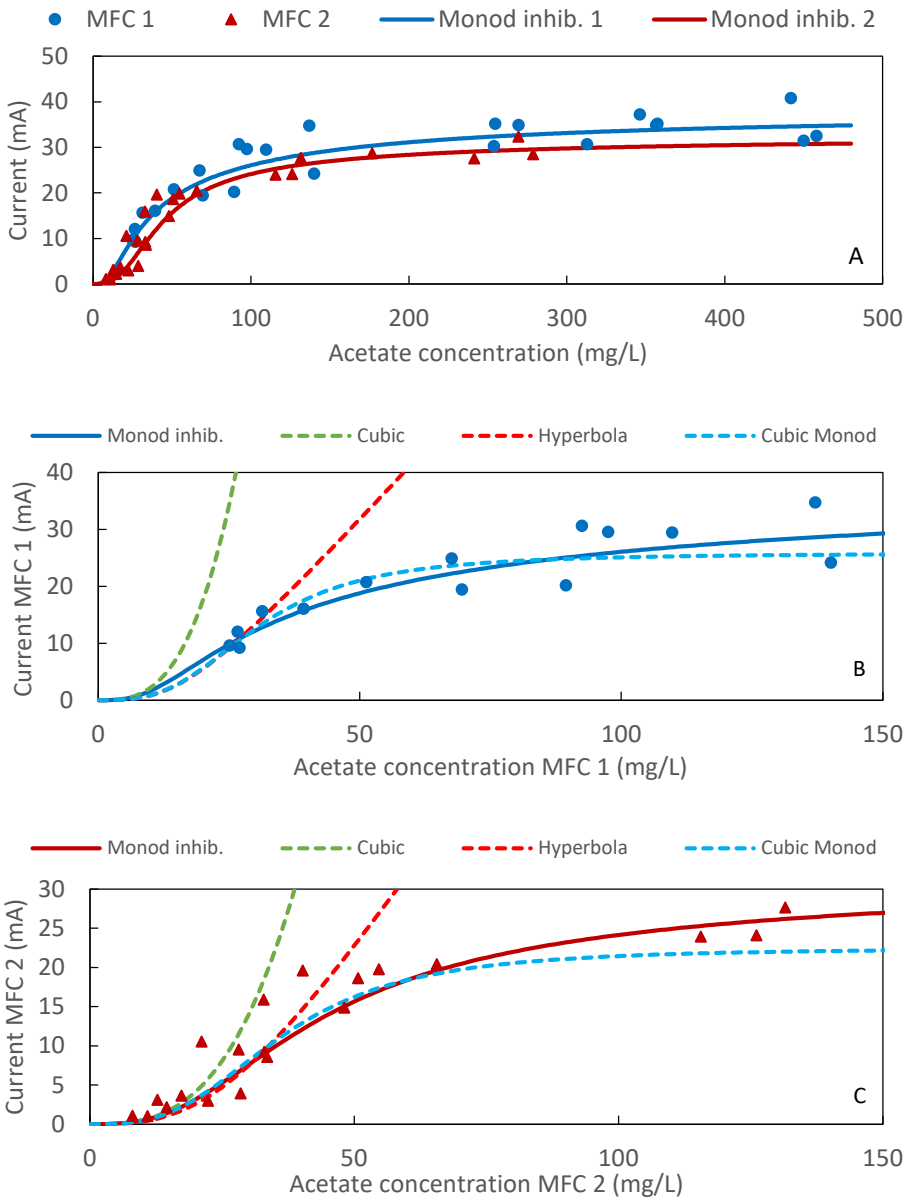

Figure 7.5: Experimental values of electric current as a function of the effluent concentration described using a Monod expression with limitation (A) and its approximations at low effluent concentrations for the first MFC (B) and for the second MFC (C).

A final observation that can be made with the experimental data at hand is that, looking at the values for the Monod expression with limitation, the second MFC presents a lower value of I_{max} and a higher value for the limitation constant K_i, which indicates a poorer electrical performance when compared with the first MFC. This can also be observed in the simplified mass balance when comparing the β parameters. The first MFC always presents a higher value for β which indicates a higher substrate consumption rate per unit of electric current generated. This is the case when the two staged MFCs are fed directly with acetate and the first cell produces the higher power output. However, feeding the MFCs in series with real wastewater will result in the opposite situation, since different microbial populations intervene in each reactor to decompose such complex substrate into the acetate required by the exoelectricigenic microorganisms mainly present in the last reactor of the series (Hodgson et al., 2016).

7.3 Effluent quality control

In parallel to investigating MFC staging, control strategies need to be developed in order for the process to counteract the unpredictable fluctuations in the environment that can directly affect its performance (Oh et al. 2010). Current control strategies only deal with the control of the electrical component in MFCs (Wang, Park, & Ren, 2015) while completely disregarding the treatment performance of MFCs. Their application to staged MFCs could result in failure of the process due to downstream MFC starvation. Control strategies dealing both with electrical and treatment performances of staged MFCs are expected to ensure a more stable operation.

Cascade PIDs is a well known control strategy for staged reactors and can be easily applied to the MFCs operated with the P/O algorithm. Such decentralized control configuration treats the electrical and treatment performances separately and it would be one of the first control approaches to try (figure 3.1 B). A block diagram for such control configuration is shown in figure 7.6. The desired effluent concentration, S_2^{ref}, is set on the master control loop (PID 1). This is compared to the effluent concentration from the second MFC, and the master's PID output is used to set the effluent concentration set point, S_1^{ref}, to the slave controller (PID 2). Then, the slave sets the flow rate for the cascade of reactors. Each PID is described by its incremental form from (equation 3.7). The simplified mass balance (equation 6.1) is used to estimate the effluent substrate concentration for each reactor, $\hat{S}_1$ and $\hat{S}_2$.

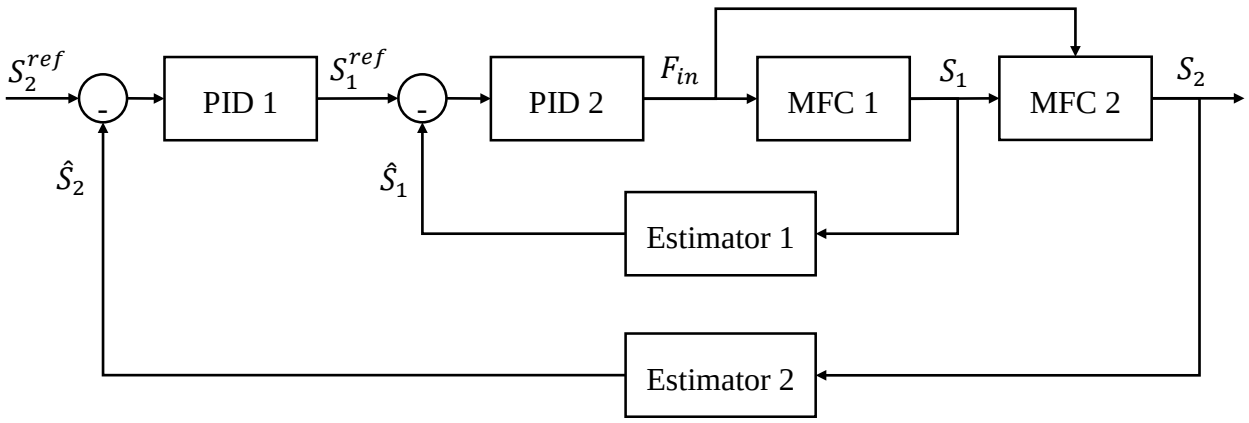

Figure 7.6: Block diagram for the hydraulic cascade control configuration for two staged MFCs.

The performance of the cascade control strategy shown in figure 7.6 was evaluated after a sudden drop in the influent substrate concentration from 1 200 to 800 mg-S L^{-1} after 1.7 days of steady state operation. Power was maximized by means of a P/O algorithm with a sampling time of 60 s and a resistance perturbation of 1.3 Ω. The desired effluent concentration was set to 100 mg-S L^{-1} although typical effluent substrate concentrations for wastewater treatment plants would be even lower than 25 mg-S L^{-1}. Such high value was chosen to avoid the oscillations caused by the low effluent concentrations. Parameters K_c and τ_I were tuned, respectively, at 0.25 [-] and 600 min for of the master PID, and 2 mL L d^{-1} mg-S^{-1} and 200 min for the slave PID. No derivative term was needed. Using the first effluent concentration, β was found to be 211 and 141 mg-S L^{-1} mA^{-1} for the first and second MFCs, respectively. The sampling time for the PIDs was set to 20 min and the manipulated flow rate had a minimal physical constraint at 10 mL d^{-1}. The coulombic efficiency at the beginning of the test was 62.9 and 95.1 % for the first and second MFCs, respectively.

After the sudden drop in the influent substrate concentration at 1.7 d, the internal resistances increase and so are tracked by the external resistances while the generated currents slightly decrease (figure 7.7 A and B). The disturbance rejection is tackled by the PID cascade configuration by presenting and overshoot of almost 80 % in the input flow rate 12 hours after the influent change, (figure 7.7 C). The steady state value at the end of the test corresponds to around 430 mL d^{-1} which represents around 23 % increase with respect to the initial flow rate. Similarly, the effluent substrate concentration for the second MFC presents an overshoot of a 119 % with respect to the desired effluent substrate concentration of 100 mg-S L^{-1} and the effect of the disturbance lasts over 2 days.

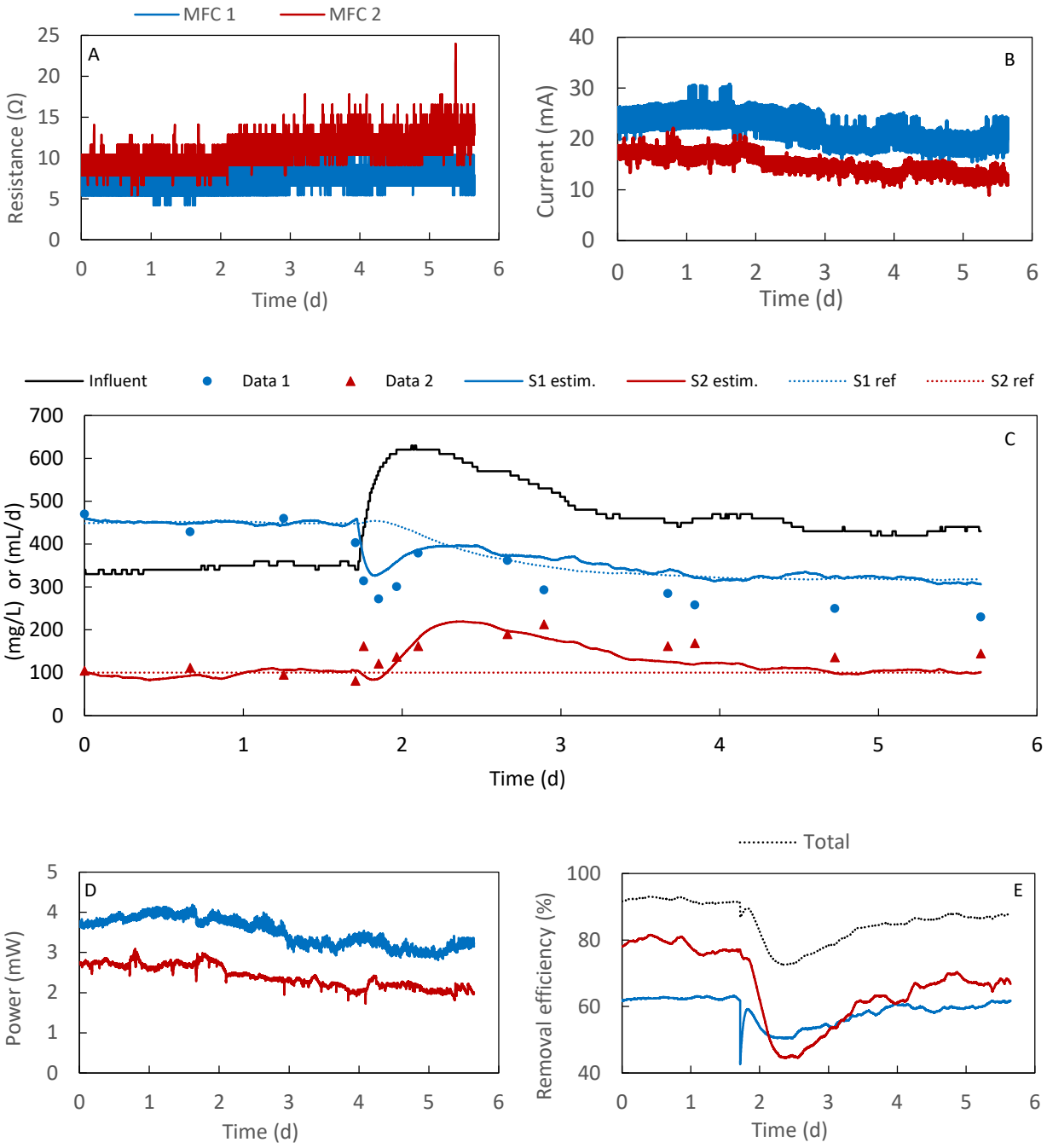

Figure 7.7: Performance of staged MFCs operated with P/O and a PID cascade control configuration after a sudden drop in the influent substrate concentration from 1 200 to 800 mg-S L^{-1} after 1.7 days of steady state operation.

Although the estimation of the effluent concentration holds at the beginning of the test, experimental values seem to drift from the estimation by the end, getting to a maximum error of a

37 % overestimation and 31 % underestimation for the first and second MFCs, respectively. In general terms, removal efficiency is kept close to 90 % between the two MFCs, except during the disturbance effect where attains the lowest value at 73 % (figure 7.7 D). Overall, the cascade PID control configuration is able to reject the sudden decrease in the influent concentration at the expense of increasing the flow rate. Such scenario might not be feasible in wastewater treatment plants so an alternative control strategy would need to be developed.

Benefiting from the electrical nature of MFCs, the PID cascade control strategy could be replaced by an even simpler control strategy whose performance results in a treated flow rate without overshoot and that only requires the tuning of a single PID. Thus, a very simple control strategy (Figure 7.8) to ensure the effluent quality control in two staged MFCs would consist of: (i) A PID controller that manipulates the treatment flow, and (ii) an ON/OFF controller that manipulates the duty cycle, DC, in MFC 1 by switching from connected at a 90 % duty cycle to fully disconnected. Both controllers consider the error with respect to the desired effluent concentration as shown in the block diagram in figure 7.9.

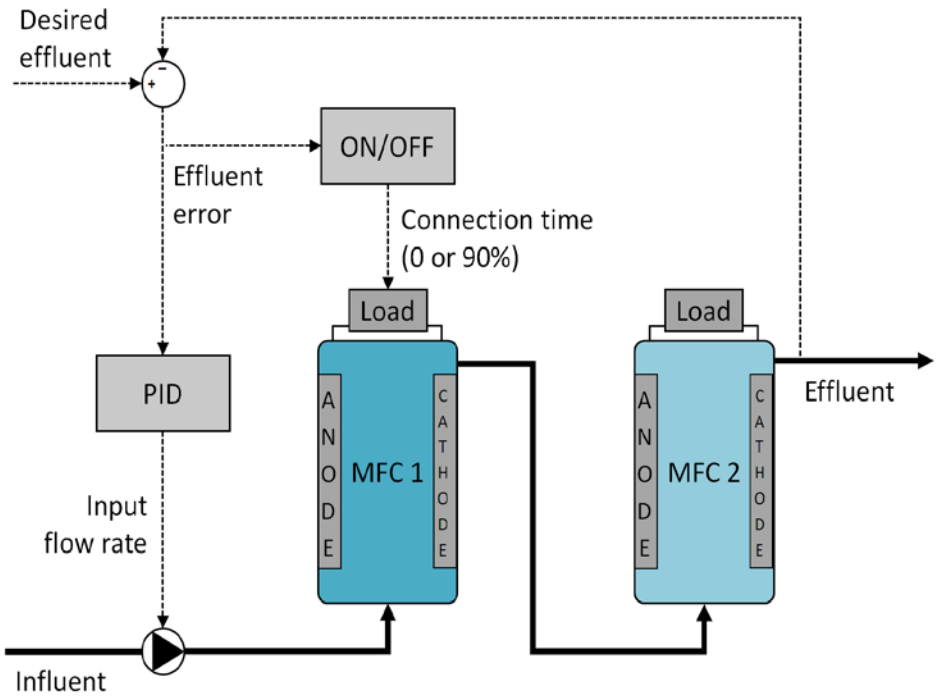

Figure 7.8: Simple effluent quality control strategy for staged MFCs in wastewater treatment applications. Each MFC is represented using the CBE model.

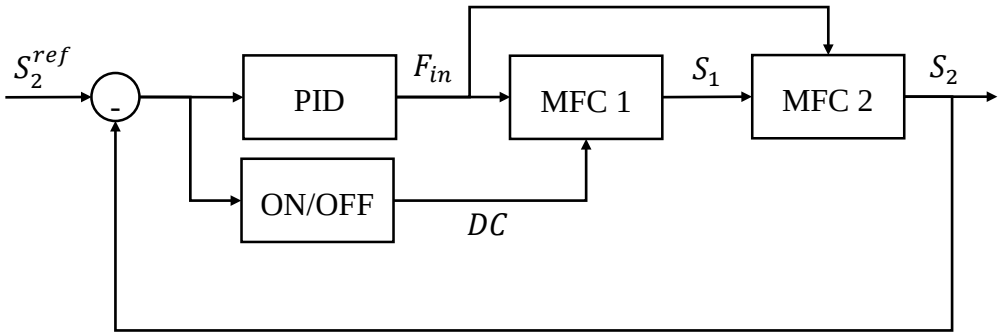

Figure 7.9: Block diagram for the PID and ON/OFF control configuration for two staged MFCs.

The operational conditions and the parameters presented in table 7.1 are used for the simulation. Under no other ground than to speed the simulation, a switching frequency of 0.1 Hz is used. The two controllers are discretized with sampling periods of 5 min for the ON/OFF controller and 10 min for the PID controller. The PID controller is used in discrete incremental form tuned at 2.5 mL d^{-1}, 240 min and 0 min for K_c, τ_I and τ_D, respectively. The treatment flow presents lower and upper boundaries set at 0.1 L d^{-1} and 0.5 L d^{-1}, respectively. Remark that the ON/OFF controller only acts when the error in the desired effluent is positive. Otherwise the effect of the ON/OFF controller would contribute to increase the error because an electrical disconnection of the first MFC results in a greater amount of substrate going into the second MFC.

Figure 7.10 shows a simulation of the performance of such control strategy after a sudden decrease of 33% in the influent concentration followed by an increase of 100% of the effluent desired concentration (set-point). It can be observed that the effect of the ON/OFF controller introduces oscillations in the effluent concentration with respect to the set point (lower than a 5 % variation) but improves dramatically the disturbance rejection capability (between 5-25 h) and increases the response speed during regulation (at 30 h). Additionally, the treatment flow remains closer to the initial value which is desirable in wastewater treatment applications.

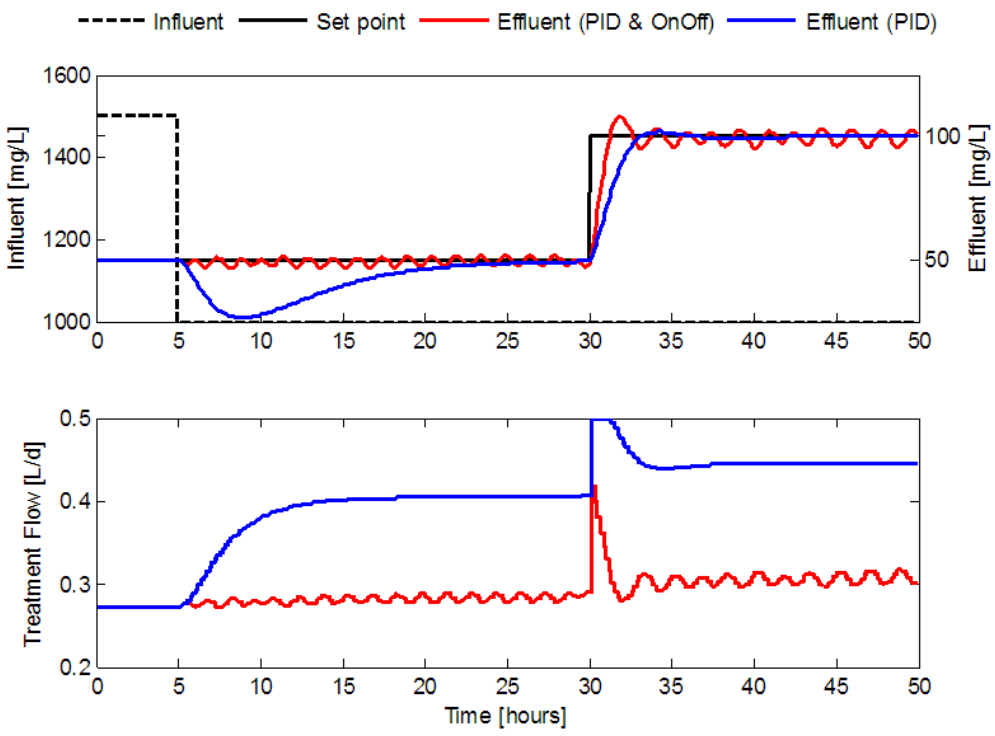

Figure 7.10: Comparison of the effluent quality control performance on two staged MFCs using a PID to manipulate the treatment flow alone (blue) or with the help of an ON/OFF controller to manipulate the connection time in MFC 1 (red).

7.4 Conclusion

MFC staging is a practical way to meet the stringent norms required for wastewater treatment. Using the CBE model to describe the dynamics of staged MFCs is straight forward as expected from a single MFC, although the numerical parameter estimation becomes more difficult, in practical terms, with the increasing number of units. The CBE model adequately describes MFC dynamics under periodic connection/disconnection of the external resistance and when combined with real time estimation of the EEC model parameters allows the best fitting especially of the output voltage while predicting effluent substrate concentration accurately.

Effluent quality monitoring in staged MFCs could favor the use of algebraic expressions to describe the electrical current as a function of the effluent concentration. The reason being the interconnection between the reactors. While the simplified version of the mass balance introduces

the possibility of online monitoring of the effluent quality that only needs for a single parameter to be estimated, it requires the knowledge of the influent substrate concentration at every time instant and steady state operation for the initial effluent sampling. On the other hand, algebraic expressions of the electric current as a function of the effluent concentration overcome such limitations but require for more parameters to be estimated, among which the value of an asymptote representing the maximum current that cannot be measured by any means. Such parameters can only be estimated from historical records of the whole range of effluent concentration operation.

Cascade PID configuration is a well known control strategy for staged reactors. Nevertheless, better alternatives to the cascade PID configuration for staged MFCs can be found by tackling the electrical operation as well. A simple control configuration including a PID to control the flow rate and an On/OFF controller to adjust the connection of the external resistance in the first MFC results in a quicker flow rate control with no overshoot and the ability to cope with disturbances in the influent concentration, whilst keeping the effluent concentration within acceptable tolerances.

CHAPTER 8 CONCLUSION, SCIENTIFIC CONTRIBUTION AND PERSPECTIVES

8.1 Conclusion

First, this thesis presents a dynamic model able to describe the internal capacitance and the nonlinear dynamics of MFCs populated with exoelectricigenic and methanogenic populations. Two approaches of the CBE model are considered depending on the purpose and available experimental data. On the one hand, a "simulation" approach, that requires all parameters of the model to be known, can be used for reactor design, optimization of operating conditions, etc. This work uses the "simulation" CBE model to describe the dynamic behavior of staged MFCs under intermittent operation of the external resistance and, additionally, studies the effect of such electrical operation on MFC performance. The apparent external resistance obtained by changing the duty cycle and the switching frequency has been found to affect the distribution of the substrate concentration and microbial populations as well as the electrical performance. An increase on the switching frequency favors the exoelectricigenic population over the methanogenic for higher values of the apparent external resistance. This results in maximum power expanding from 100 % toward lower duty cycles when increasing the switching frequency and corroborates the positive effect of the intermittent operation of the external resistance on the electricity production even during mismatch with the internal resistance value. Experimentally, such study would require a tremendous amount of time because of the major role played by the slow microbial growth dynamics in the overall MFC performance which proves the utility of the "simulation" CBE model. On the other hand, an alternative approach requires the MFC output voltage to be available in real time thus enabling on-line estimation of certain electrical parameters of the model (E_{oc}, C, R_1 and R_2). This CBE "parameter observer-based" approach runs in parallel with already existing data by incorporating the electrical parameters as actual inputs, thus providing a better fit while predicting process variables not measurable in real time, such as effluent carbon source concentration. Both approaches showed acceptable accuracy when describing both fast and slow dynamic behavior, while also being able to adequately predict the output substrate concentration. Since on-line measurements of the output substrate concentration are typically unavailable, the CBE model presents a step forward in developing software sensors for on-line MFC monitoring.

Second, this thesis opens the door to the online estimation of the effluent carbon source concentration. Under adequate conditions, MFCs naturally generate an electrical voltage signal depending on the carbon source concentration available in the anodic compartment. Benefiting from such electrochemical nature, continuous estimations of the biologically consumable organic fraction in wastewater could be obtained in real time. Electrical measurements in MFCs are sensitive to changes in the effluent concentration, being especially responsive at low effluent concentrations, the ideal range for wastewater treatment applications. This work presents two simple ways to monitor the effluent quality in MFCs. The first way benefits from the dynamic modeling of MFCs and simplifies the CBE model to a single equation that incorporates the electric current as an input into the substrate mass balance. This dynamic approach is valid in the whole range of effluent concentrations, requires the estimation of a single parameter relating the current produced to the substrate consumed, and represents a natural low-pass filter that doesn't affect the output dynamics. Yet, its practical application to staged MFCs relies on assuming the influent concentration to be measurable and the need to estimate the parameter under steady state conditions. Obviously, although the simplified dynamic mass balance is stable, convergence to the real value is not guaranteed and the estimation is going to be as good as the seed measurement. The second approach overcomes such limitations by directly describing the electric current only as a function of the effluent concentration. Kinetics of the CBE model suggest a Monod expression with a diffusion limitation term at low effluent concentrations. Only measurements of the electric current are required to estimate the effluent concentration, however, three parameters need to be estimated for each reactor, I'_{max}, K'_S and K_i, which necessitate from historical records. Yet, a third degree hyperbolic approximation at low effluent concentrations can be found that only requires the estimation of a single parameter. Unfortunately, because all the strategies are based on open-loop estimations, convergence to the true value is not guaranteed. Nevertheless, results encourage further research so that MFC effluent quality monitoring reaches a sufficient level of maturity to be incorporated as sensors into advanced control configurations.

Third, this work compares two control configurations suitable for effluent quality control in staged MFCs. A more traditional decentralized control strategy uses cascade PIDs with P/O electrical operation and a simpler centralized configuration that takes advantage of the dual electrical and biochemical nature of MFCs. The centralized control configuration consists of a PID to control the flow rate and an ON/OFF controller to adjust the connection of the external resistance in the first

MFC. In both cases, the electrical operation of the staged MFCs is kept independent between the cells. Experimental results show a big overshoot in the manipulated flow rate when using the decentralized cascade PIDs while simulations of the centralized PID-ON/OFF control configuration results in a quicker flow rate control with no overshoot and the ability to cope with disturbances in the influent concentration whilst keeping the effluent concentration within acceptable tolerances. Wastewater treatment applications would require control configurations that are not demanding on changes in the input flow rate, thus keeping it as close to the nominal point of operation as possible which is obtained with the centralized control strategy. Basically, the ON/OFF controller uses the external resistance as an electrical equivalent to hydraulically bypassing the first cell when substrate deplete conditions occur in the second cell.

And last but not least, this final paragraph is to reclaim attention to the stability, endurance and robustness of the two staged MFCs that have been operating nonstop so that experimental results could be incorporated into this thesis. During all those years, the cells have suffered from multiple accidents, e.g. from damaged heaters that boiled the second reactor, to electrical surges that stop the feeding pumps, to computer updates that stopped the electrical operation, to unstable controllers that dangerously increased the flow rate, etc. and yet, they were able to easily recover. Unlike other bioreactors, staged MFCs require minimal maintenance. Both P/O algorithm and R-PWM electrical operation proved to be long term effective strategies keeping the reactors producing electricity for several months without showing visible signs of either treatment or electrical performance loss. Hopefully, all those advantages will overcome their limitations and translate into a bright future for MFCs in the domain of wastewater treatment.

8.2 Scientific contribution

The scientific contribution behind this PhD thesis can be summarized in the following points, in order of importance:

1. Development and experimental validation of a CBE model able to describe the internal capacitance and nonlinear dynamics resulting from an R-PWM operation of the external resistance in staged MFCs. Furthermore, the CBE model has been used to qualitatively study the effect of duty cycle and switching frequency on the MFC microbial community and electrical performance.

2. Development and experimental validation of open loop monitoring approaches for the continuous estimation of the effluent substrate concentration in staged MFCs. The originality lies in finding suitable correlations between the output electrical current and the effluent carbon source concentration.
3. Suggestion of a simple centralized control strategy suitable for wastewater treatment applications that benefits from the dual electrical and biochemical nature in MFCs and results in a manipulated flow rate without overshoot while dealing with variations in the influent substrate concentration.
4. Presentation of an exhaustive review about the current dynamic modeling trends and the emerging areas of BES real-time monitoring, control and optimization, which deals with unpredictable external disturbances and maximizing energy production. Previous reviews did not focus on such emerging research areas or even in fast process dynamics.

Consequently, this thesis resulted in the following scientific publications:

1. Recio-Garrido, D., Perrier, M., & Tartakovsky, B. (2014, June). Parameter estimation of a microbial fuel cell process control-oriented model. In *Control and Automation (MED), 2014 22nd Mediterranean Conference of* (pp. 918-923). IEEE.
2. Recio-Garrido, D., Perrier, M., & Tartakovsky, B. (2016). Combined bioelectrochemical–electrical model of a microbial fuel cell. *Bioprocess and biosystems engineering*, *39*(2), 267-276.
3. Recio-Garrido, D., Perrier, M., & Tartakovsky, B. (2016). Modeling, optimization and control of bioelectrochemical systems. *Chemical Engineering Journal*, *289*, 180-190.
4. Recio-Garrido, D., Tartakovsky, B., & Perrier, M. (2016). Staged microbial fuel cells with periodic connection of external resistance. *IFAC-PapersOnLine*, *49*(7), 91-96.
5. Staged microbial fuel cells for wastewater treatment (in preparation, *Biochemical Engineering Journal*).
6. Model-based approaches for online effluent quality monitoring in microbial fuel cells (in preparation, *Biosensors and Bioelectronics*).

Additionally, results from this PhD thesis have been presented in the following international conferences:

- 4th North American Regional Meeting of the International Society for Microbial Electrochemistry and Technology (NA-ISMET). Conference held at The Pennsylvania State University (USA) in May 2014. Poster and oral presentation.
- 22nd Mediterranean Conference on Control and Automation (MED). Conference held at the University of Palermo (Italy) in June 2014. Oral presentation.
- 5th North American Regional Meeting of the International Society for Microbial Electrochemistry and Technology (NA-ISMET). Conference held at The Arizona State University (USA) in October 2015. Poster presentation.
- 11th IFAC Symposium on Dynamics and Control of Process Systems, including Biosystems (DYCOPS-CAB). Conference held at the Norwegian University of Science and Technology (Norway) in June 2016. Oral presentation.

8.3 Perspectives and recommendations

The discovery of mediator-less BESs created an opportunity for developing a number of novel technologies for sustainable energy or resource production from sustainable energy sources such as organic wastes. However, many BES technologies remain in the early development stages with a number of obstacles still to be resolved before progressing towards industrial applications. This transition from discovery to technology implementation can be accelerated by merging the knowledge of BES microbiology, electrochemistry and operating know-how into mathematical models suitable for process design, control and optimization.

In general terms, several areas of interest for applying model-based optimization and control techniques can be pointed out. BES models can be used for optimizing design and configuration of MFCs and MECs. Biofilm models, which account for the properties of anodophilic biofilms containing multiple microbial populations, can be most useful in this regard. Other BES optimization studies can address issues of optimal connection of multiple units. Development of software sensors (observers) capable of real-time estimation of key process parameters is another potentially promising research area. On-line monitoring strategies, which provide timely

information on the state of BESs might be instrumental in stabilizing performance and averting process failures due to unpredictable variations in the influent stream composition.

More in particular, following the results presented in this PhD thesis, a number of new research opportunities might be further investigated and analysed in the fields of dynamic BESs dynamic modeling, effluent quality monitoring and control.

<u>BESs dynamic modeling and monitoring:</u>

1. *Fast numerical solution for the CBE model:* Integrating the set of stiff differential equations from the CBE model under R-PWM using the predetermined solvers from Matlab such as the *ode15s* takes too long. Thus, finding a fast numerical solution for the CBE is required, e.g. orthogonal collocation that translates the differential equations into sets of algebraic equations.
2. *CBE model for MECs:* Analogous to the work performed with MFCs, an EEC could be developed for MECs under PWM operation of the applied electric voltage. Furthermore, a similar strategy as the one used to estimate the EEC parameters in MFCs, could be developed for MECs. Research is ongoing on this aspect with the idea of developing a CBE model for MECs as well.
3. *Observer-based estimation of β:* Research is ongoing on the use of fluorometry to estimate COD values in real time in wastewater treatment applications. Measurements using such technique could be used to estimate online the value of β by means of an observer-based estimator.
4. *(Bio)cathode reaction modeling:* Opportunities for improved predictive capacity of BES models include cathodic reaction modeling, and modeling of oxygen diffusion through the air-breezing cathode. Also, while some models describe electrochemical reactions associated with Me-based catalysts, none consider biocathodes or microbially catalyzed electrosynthesis. This lack of cathode (bio)reaction modeling becomes more important with the advance of microbial electrosynthesis

<u>BESs optimization and control:</u>

1. *Optimization of the duty cycle and/or the switching frequency during PWM:* Experimental results with MFCs might suggest the existence of an optimum in power as a function of the

operational condition in the PWM. The CBE model developed in chapter 4 is unable to reproduce such experimental observations and research is ongoing to experimentally study the existence of such optimum and the factors involving its existence in MECs. Additionally, this effect could be incorporated into the CBE model.

2. *Development of a cascade/supervisory control strategy dealing with the dual electrical and biochemical nature in MFCs:* Overall, it can be suggested that large differences between the electrical and bioelectrochemical dynamics can be tackled by a cascade/supervisory control strategy. An example of such control system is shown in figure 8.1. In such an approach, one controller directly tackles fast process dynamics (short-term control), while the second (long-term) controller tackles slow process dynamics and provides reference values to the first controller.

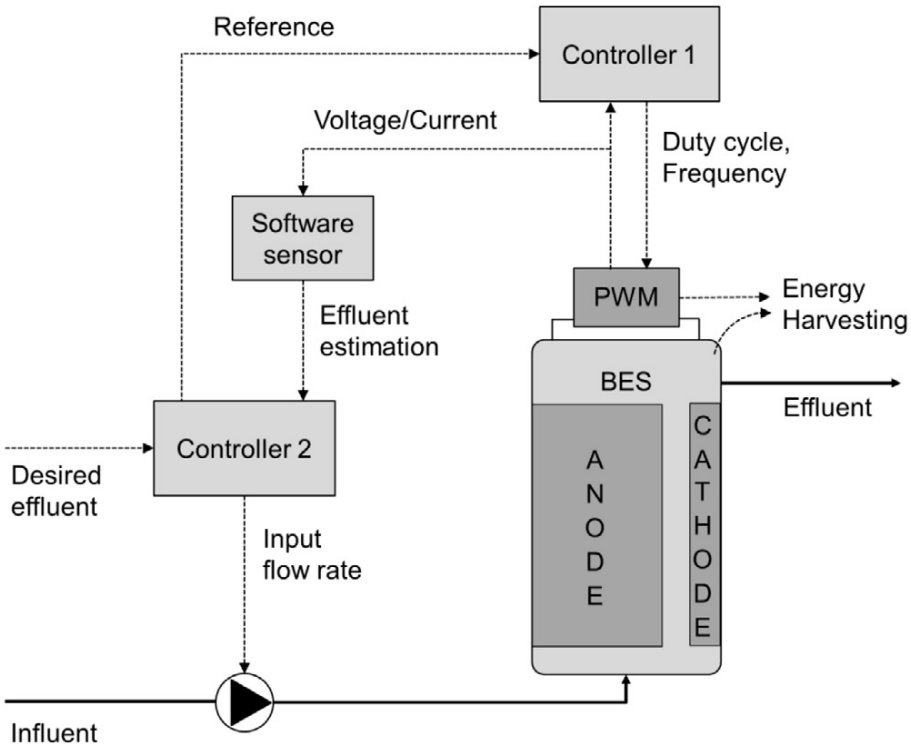

Figure 8.1: Process control diagram showing a cascade/supervisory control system with a master controller tackling slow microbial dynamics and a slave controller tackling fast electrical dynamics.

BIBLIOGRAPHY

Andersen, S. J., Pikaar, I., Freguia, S., Lovell, B. C., Rabaey, K., & Rozendal, R. A. (2013). Dynamically adaptive control system for bioanodes in serially stacked bioelectrochemical systems. *Environmental science & technology*,*47*(10), 5488-5494.

Attarsharghi, S., Woodward, L., & Akhrif, O. (2012, October). An improved maximum power extraction scheme for microbial fuel cells. In *IECON 2012-38th Annual Conference on IEEE Industrial Electronics Society* (pp. 910-915). IEEE.

Babauta, J., Renslow, R., Lewandowski, Z., & Beyenal, H. (2012). Electrochemically active biofilms: facts and fiction. A review. *Biofouling*, *28*(8), 789-812.

Batstone, D. J., Keller, J., Angelidaki, I., Kalyuzhnyi, S. V., Pavlostathis, S. G., Rozzi, A., ... & Vavilin, V. A. (2002). The IWA anaerobic digestion model no 1 (ADM1). *Water Science and Technology*, *45*(10), 65-73.

Boghani, H. C., Kim, J. R., Dinsdale, R. M., Guwy, A. J., & Premier, G. C. (2013). Control of power sourced from a microbial fuel cell reduces its start-up time and increases bioelectrochemical activity. *Bioresource technology*,*140*, 277-285.

Boghani, H. C., Papaharalabos, G., Michie, I., Fradler, K. R., Dinsdale, R. M., Guwy, A. J., ... & Premier, G. C. (2014). Controlling for peak power extraction from microbial fuel cells can increase stack voltage and avoid cell reversal. *Journal of Power Sources*, *269*, 363-369.

Chaudhuri, S. K., & Lovley, D. R. (2003). Electricity generation by direct oxidation of glucose in mediatorless microbial fuel cells. *Nature biotechnology*, *21*(10), 1229-1232.

Chouler, J., & Di Lorenzo, M. (2015). Water quality monitoring in developing countries; can microbial fuel cells be the answer?. *Biosensors*, 5(3), 450-470.

Clauwaert, P., Aelterman, P., De Schamphelaire, L., Carballa, M., Rabaey, K., & Verstraete, W. (2008). Minimizing losses in bio-electrochemical systems: the road to applications. *Applied Microbiology and Biotechnology*, *79*(6), 901-913.

Coronado, J., Perrier, M., & Tartakovsky, B. (2013). Pulse-width modulated external resistance increases the microbial fuel cell power output. *Bioresource technology*, *147*, 65-70.

Coronado, J., Tartakovsky, B., & Perrier, M. (2013). On-line Monitoring and Parameter Estimation of a Microbial Fuel Cell Operated with Intermittent Connection of the External Resistor. *IFAC Proceedings Volumes*, *46*(31), 233-237.

del Campo, A. G., Cañizares, P., Lobato, J., Rodrigo, M., & Morales, F. F. (2014). Effects of External Resistance on Microbial Fuel Cell's Performance. In *Environment, Energy and Climate Change II* (pp. 175-197). Springer International Publishing.

Dochain, D. (2003). State and parameter estimation in chemical and biochemical processes: a tutorial. *Journal of process control*, *13*(8), 801-818.

Dochain, D. (2013). *Automatic control of bioprocesses*. John Wiley & Sons.

Du, Z., Li, H., & Gu, T. (2007). A state of the art review on microbial fuel cells: a promising technology for wastewater treatment and bioenergy. *Biotechnology advances*, *25*(5), 464-482.

Esram, T., & Chapman, P. L. (2007). Comparison of photovoltaic array maximum power point tracking techniques. *IEEE Transactions on Energy Conversion EC*, *22*(2), 439.

Fan, L., Zhang, J., & Shi, X. (2015). Performance Improvement of a Microbial Fuel Cell Based on Model Predictive Control. *Int. J. Electrochem. Sci*, *10*, 737-748.

Fang, F., Zang, G. L., Sun, M., & Yu, H. Q. (2013). Optimizing multi-variables of microbial fuel cell for electricity generation with an integrated modeling and experimental approach. *Applied energy*, *110*, 98-103.

Fradler, K. R., Kim, J. R., Boghani, H. C., Dinsdale, R. M., Guwy, A. J., & Premier, G. C. (2014). The effect of internal capacitance on power quality and energy efficiency in a tubular microbial fuel cell. *Process Biochemistry*, *49*(6), 973-980.

Gardel, E. J., Nielsen, M. E., Grisdela Jr, P. T., & Girguis, P. R. (2012). Duty cycling influences current generation in multi-anode environmental microbial fuel cells. *Environmental science & technology*, *46*(9), 5222-5229.

Grondin, F., Perrier, M., & Tartakovsky, B. (2012). Microbial fuel cell operation with intermittent connection of the electrical load. *Journal of Power Sources*,*208*, 18-23.

Gurung, A., & Oh, S. E. (2012). The improvement of power output from stacked microbial fuel cells (MFCs). *Energy Sources, Part A: Recovery, Utilization, and Environmental Effects*, *34*(17), 1569-1576.

Hamelers, H. V., Ter Heijne, A., Stein, N., Rozendal, R. A., & Buisman, C. J. (2011). Butler–Volmer–Monod model for describing bio-anode polarization curves. *Bioresource technology*, *102*(1), 381-387.

Ha, P. T., Moon, H., Kim, B. H., Ng, H. Y., & Chang, I. S. (2010). Determination of charge transfer resistance and capacitance of microbial fuel cell through a transient response analysis of cell voltage. *Biosensors and Bioelectronics*, *25*(7), 1629-1634.

He, Z., Wagner, N., Minteer, S. D., & Angenent, L. T. (2006). An upflow microbial fuel cell with an interior cathode: assessment of the internal resistance by impedance spectroscopy. *Environmental science & technology*,*40*(17), 5212-5217.

Hodgson, D. M., Smith, A., Dahale, S., Stratford, J. P., Li, J. V., Grüning, A., ... & Rossa, C. A. (2016). Segregation of the anodic microbial communities in a microbial fuel cell cascade. *Frontiers in microbiology*, *7*.

International Energy Agency (2012). *World Energy Outlook*. Available online at: http://www.iea.org/publications/freepublications/publication/WEO2012_free.pdf

Janicek, A., Fan, Y., & Liu, H. (2014). Design of microbial fuel cells for practical application: a review and analysis of scale-up studies. *Biofuels*, *5*(1), 79-92.

Jayasinghe, N., Franks, A., Nevin, K. P., & Mahadevan, R. (2014). Metabolic modeling of spatial heterogeneity of biofilms in microbial fuel cells reveals substrate limitations in electrical current generation. *Biotechnology journal*,*9*(10), 1350-1361.

Kato Marcus, A., Torres, C. I., & Rittmann, B. E. (2007). Conduction-based modeling of the biofilm anode of a microbial fuel cell. *Biotechnology and Bioengineering*, *98*(6), 1171-1182.

Kaur, A., Boghani, H. C., Michie, I., Dinsdale, R. M., Guwy, A. J., & Premier, G. C. (2014). Inhibition of methane production in microbial fuel cells: operating strategies which select electrogens over methanogens. *Bioresource technology*, *173*, 75-81.

Kelly, P. T., & He, Z. (2014). Nutrients removal and recovery in bioelectrochemical systems: a review. *Bioresource technology*, *153*, 351-360.

Kravaris, C., Hahn, J., & Chu, Y. (2013). Advances and selected recent developments in state and parameter estimation. *Computers & chemical engineering*, *51*, 111-123.

Kundu, A., Sahu, J. N., Redzwan, G., & Hashim, M. A. (2013). An overview of cathode material and catalysts suitable for generating hydrogen in microbial electrolysis cell. *international journal of hydrogen energy*, *38*(4), 1745-1757.

Ledezma, P., Greenman, J., & Ieropoulos, I. (2013). MFC-cascade stacks maximise COD reduction and avoid voltage reversal under adverse conditions. *Bioresource technology*, *134*, 158-165.

Lefebvre, O., Uzabiaga, A., Chang, I. S., Kim, B. H., & Ng, H. Y. (2011). Microbial fuel cells for energy self-sufficient domestic wastewater treatment—a review and discussion from energetic consideration. *Applied microbiology and biotechnology*, *89*(2), 259-270.

Liu, H., Cheng, S., & Logan, B. E. (2005). Production of electricity from acetate or butyrate using a single-chamber microbial fuel cell. *Environmental science & technology*, *39*(2), 658-662.

Logan, B. E. (2008). *Microbial fuel cells*. John Wiley & Sons.

Logan, B. E. (2009). Exoelectrogenic bacteria that power microbial fuel cells. *Nature Reviews Microbiology*, *7*(5), 375-381.

Logan, B. E. (2010). Scaling up microbial fuel cells and other bioelectrochemical systems. *Applied microbiology and biotechnology*, *85*(6), 1665-1671.

Logan, B. E., Call, D., Cheng, S., Hamelers, H. V., Sleutels, T. H., Jeremiasse, A. W., & Rozendal, R. A. (2008). Microbial electrolysis cells for high yield hydrogen gas production from organic matter. *Environmental Science & Technology*, *42*(23), 8630-8640.

Logan, B. E., & Regan, J. M. (2006). Microbial fuel cells-challenges and applications. *Environmental science & technology*, *40*(17), 5172-5180.

Lovley, D. R. (2008). The microbe electric: conversion of organic matter to electricity. *Current opinion in Biotechnology*, *19*(6), 564-571.

Lyon, D. Y., Buret, F., Vogel, T. M., & Monier, J. M. (2010). Is resistance futile? Changing external resistance does not improve microbial fuel cell performance. *Bioelectrochemistry*, *78*(1), 2-7.

Merkey, B. V., & Chopp, D. L. (2012). The performance of a microbial fuel cell depends strongly on anode geometry: a multidimensional modeling study. *Bulletin of mathematical biology*, *74*(4), 834-857.

Molognoni, D., Puig, S., Balaguer, M. D., Liberale, A., Capodaglio, A. G., Callegari, A., & Colprim, J. (2014). Reducing start-up time and minimizing energy losses of microbial fuel cells using maximum power point tracking strategy. *Journal of Power Sources*, *269*, 403-411.

Oh, S. T., Kim, J. R., Premier, G. C., Lee, T. H., Kim, C., & Sloan, W. T. (2010). Sustainable wastewater treatment: how might microbial fuel cells contribute. *Biotechnology advances*, *28*(6), 871-881.

Oh, S. E., & Logan, B. E. (2007). Voltage reversal during microbial fuel cell stack operation. *Journal of Power Sources*, *167*(1), 11-17.

Oliveira, V. B., Simões, M., Melo, L. F., & Pinto, A. M. F. R. (2013a). A 1D mathematical model for a microbial fuel cell. *Energy*, *61*, 463-471.

Oliveira, V. B., Simões, M., Melo, L. F., & Pinto, A. M. F. R. (2013b). Overview on the developments of microbial fuel cells. *Biochemical Engineering Journal*,*73*, 53-64.

Ortiz-Martínez, V. M., Salar-García, M. J., De Los Ríos, A. P., Hernández-Fernández, F. J., Egea, J. A., & Lozano, L. J. (2015). Developments in microbial fuel cell modeling. *Chemical Engineering Journal*, *271*, 50-60.

Pathapati, P. R., Xue, X., & Tang, J. (2005). A new dynamic model for predicting transient phenomena in a PEM fuel cell system. *Renewable energy*, *30*(1), 1-22.

Picioreanu, C., Head, I. M., Katuri, K. P., van Loosdrecht, M. C., & Scott, K. (2007). A computational model for biofilm-based microbial fuel cells. *Water research*, *41*(13), 2921-2940.

Picioreanu, C., Katuri, K. P., van Loosdrecht, M. C., Head, I. M., & Scott, K. (2010). Modelling microbial fuel cells with suspended cells and added electron transfer mediator. *Journal of applied electrochemistry*, *40*(1), 151-162.

Picioreanu, C., Katuri, K. P., Head, I. M., van Loosdrecht, M. C., & Scott, K. (2008). Mathematical model for microbial fuel cells with anodic biofilms and anaerobic digestion. *Water science and technology*, *57*(7), 965-971.

Picioreanu, C., Kreft, J. U., & van Loosdrecht, M. C. (2004). Particle-based multidimensional multispecies biofilm model. *Applied and environmental microbiology*, *70*(5), 3024-3040.

Picioreanu, C., van Loosdrecht, M. C., Curtis, T. P., & Scott, K. (2010). Model based evaluation of the effect of pH and electrode geometry on microbial fuel cell performance. *Bioelectrochemistry*, *78*(1), 8-24.

Pinto, R. P., Srinivasan, B., Escapa, A., & Tartakovsky, B. (2011). Multi-population model of a microbial electrolysis cell. *Environmental science & technology*, *45*(11), 5039-5046.

Pinto, R. P., Srinivasan, B., Guiot, S. R., & Tartakovsky, B. (2011). The effect of real-time external resistance optimization on microbial fuel cell performance. *Water research*, *45*(4), 1571-1578.

Pinto, R. P., Srinivasan, B., Manuel, M. F., & Tartakovsky, B. (2010). A two-population bio-electrochemical model of a microbial fuel cell. *Bioresource technology*, *101*(14), 5256-5265.

Pinto, R. P., Tartakovsky, B., Perrier, M., & Srinivasan, B. (2010). Optimizing treatment performance of microbial fuel cells by reactor staging. *Industrial & Engineering Chemistry Research*, *49*(19), 9222-9229.

Pinto, R. P., Tartakovsky, B., & Srinivasan, B. (2012). Optimizing energy productivity of microbial electrochemical cells. *Journal of Process Control*,*22*(6), 1079-1086.

Premier, G. C., Kim, J. R., Michie, I., Dinsdale, R. M., & Guwy, A. J. (2011). Automatic control of load increases power and efficiency in a microbial fuel cell. *Journal of Power Sources*, *196*(4), 2013-2019.

Ramasamy, R. P., Ren, Z., Mench, M. M., & Regan, J. M. (2008). Impact of initial biofilm growth on the anode impedance of microbial fuel cells. *Biotechnology and bioengineering*, *101*(1), 101-108.

Recio-Garrido, D., Perrier, M., & Tartakovsky, B. (2016). Combined bioelectrochemical–electrical model of a microbial fuel cell. *Bioprocess and biosystems engineering*, *39*(2), 267-276.

Ren, Z., Yan, H., Wang, W., Mench, M. M., & Regan, J. M. (2011). Characterization of microbial fuel cells at microbially and electrochemically meaningful time scales. *Environmental science & technology*, *45*(6), 2435-2441.

Rozendal, R. A., Hamelers, H. V., Euverink, G. J., Metz, S. J., & Buisman, C. J. (2006). Principle and perspectives of hydrogen production through biocatalyzed electrolysis. *International Journal of Hydrogen Energy*, *31*(12), 1632-1640.

Schröder, U. (2007). Anodic electron transfer mechanisms in microbial fuel cells and their energy efficiency. *Physical Chemistry Chemical Physics*, *9*(21), 2619-2629.

Schrott, G. D., Bonanni, P. S., Robuschi, L., Esteve-Nuñez, A., & Busalmen, J. P. (2011). Electrochemical insight into the mechanism of electron transport in biofilms of Geobacter sulfurreducens. *Electrochimica Acta*, *56*(28), 10791-10795.

Sedaqatvand, R., Esfahany, M. N., Behzad, T., Mohseni, M., & Mardanpour, M. M. (2013). Parameter estimation and characterization of a single-chamber microbial fuel cell for dairy wastewater treatment. *Bioresource technology*,*146*, 247-253.

Sirinutsomboon, B. (2014). Modeling of a membraneless single-chamber microbial fuel cell with molasses as an energy source. *International Journal of Energy and Environmental Engineering*, *5*(2-3), 1-9.

Scuras, S. E., Jobbagy, A., & Grady, C. L. (2001). Optimization of activated sludge reactor configuration: kinetic considerations. *Water research*, *35*(18), 4277-4284.

Sun, M., Sheng, G. P., Mu, Z. X., Liu, X. W., Chen, Y. Z., Wang, H. L., & Yu, H. Q. (2009). Manipulating the hydrogen production from acetate in a microbial electrolysis cell–microbial fuel cell-coupled system. *Journal of Power Sources*, *191*(2), 338-343.

Tartakovsky, B., Manuel, M. F., Neburchilov, V., Wang, H., & Guiot, S. R. (2008). Biocatalyzed hydrogen production in a continuous flow microbial fuel cell with a gas phase cathode. *Journal of Power Sources*, *182*(1), 291-297.

Tartakovsky, B., Mehta, P., Santoyo, G., & Guiot, S. R. (2011). Maximizing hydrogen production in a microbial electrolysis cell by real-time optimization of applied voltage. *International journal of hydrogen energy*, *36*(17), 10557-10564.

Torres, C. I., Marcus, A. K., Parameswaran, P., & Rittmann, B. E. (2008). Kinetic experiments for evaluating the Nernst− Monod model for anode-respiring bacteria (ARB) in a biofilm anode. *Environmental science & technology*, *42*(17), 6593-6597.

Wagner, N. (2002). Characterization of membrane electrode assemblies in polymer electrolyte fuel cells using ac impedance spectroscopy. *Journal of Applied Electrochemistry*, *32*(8), 859-863.

Walter, X. A., Greenman, J., & Ieropoulos, I. A. (2014). Intermittent load implementation in microbial fuel cells improves power performance. *Bioresource technology*, *172*, 365-372..

Wang, L., Lin, Q., Zhang, J., Wang, J., Zhou, Y., & Feng, X. N. (2014). New Progress in Microbial Fuel Cells and its Outlook. In *Advanced Materials Research*, *860*, 816-821. Trans Tech Publications.

Wang, H., Park, J. D., & Ren, Z. (2012). Active energy harvesting from microbial fuel cells at the maximum power point without using resistors. *Environmental science & technology*, *46*(9), 5247-5252.

Wang, H., Park, J. D., & Ren, Z. J. (2015). Practical energy harvesting for microbial fuel cells: a review. *Environmental science & technology*, *49*(6), 3267-3277.

Wang, H., & Ren, Z. J. (2013). A comprehensive review of microbial electrochemical systems as a platform technology. *Biotechnology advances*,*31*(8), 1796-1807.

Wang, H., Ren, Z., & Park, J. D. (2012). Power electronic converters for microbial fuel cell energy extraction: Effects of inductance, duty ratio, and switching frequency. *Journal of Power Sources*, *220*, 89-94.

Watson, V. J., & Logan, B. E. (2011). Analysis of polarization methods for elimination of power overshoot in microbial fuel cells. *Electrochemistry Communications*, *13*(1), 54-56.

Woodward, L., Perrier, M., Srinivasan, B., Pinto, R. P., & Tartakovsky, B. (2010). Comparison of real-time methods for maximizing power output in microbial fuel cells. *AIChE Journal*, *56*(10), 2742-2750.

Woodward, L., Tartakovsky, B., Perrier, M., & Srinivasan, B. (2009). Maximizing power production in a stack of microbial fuel cells using multiunit optimization method. *Biotechnology progress*, *25*(3), 676-682.

Yahya, A. M., Hussain, M. A., Wahab, A., & Khairi, A. (2015). Modeling, optimization, and control of microbial electrolysis cells in a fed-batch reactor for production of renewable biohydrogen gas. *International Journal of Energy Research*, *39*(4), 557-572.

Yan, M., & Fan, L. (2013). Constant voltage output in two-chamber microbial fuel cell under fuzzy PID control. *International Journal of Electrochemical Science*, *8*, 3321-3332.

Yang, Y., Xu, M., Guo, J., & Sun, G. (2012). Bacterial extracellular electron transfer in bioelectrochemical systems. *Process Biochemistry*, *47*(12), 1707-1714.

Zeng, Y., Choo, Y. F., Kim, B. H., & Wu, P. (2010). Modelling and simulation of two-chamber microbial fuel cell. *Journal of Power Sources*, *195*(1), 79-89.

Zhang, X. C., & Halme, A. (1995). Modelling of a microbial fuel cell process. *Biotechnology Letters*, *17*(8), 809-814.

Zhuang, L., Zheng, Y., Zhou, S., Yuan, Y., Yuan, H., & Chen, Y. (2012). Scalable microbial fuel cell (MFC) stack for continuous real wastewater treatment. *Bioresource technology*, *106*, 82-88.

Appendix A – Online parameter estimation procedure for the equivalent electrical circuit

This appendix summarizes the on-line parameter estimation procedure developed by Coronado, Tartakovsky and Perrier (2013) to estimate the parameters of the EEC model for a MFC.

Voltage dynamics at the capacitor (V_c) of the EEC shown in figure A.1 can be described by the following first order differential equation:

$$\frac{dV_c}{dt} = \frac{\mathrm{E_{OC}}}{C(R_1+R_{ext})} - \frac{R_1+R_2+R_{ext}}{R_2C(R_1+R_{ext})}V_c \ . \tag{A.1}$$

By applying Kirchhoff's law and solving equation (A.1), the analytical solution of MFC output voltage, V_{cell}, is obtained in the following form:

$$V_{cell} = E_{OC} - \left[U_{c,final} + \left(U_{c,initial} - U_{c,final}\right)e^{-\frac{t}{\tau}}\right]\frac{R_{ext}}{R_1+R_{ext}}, \tag{A.2}$$

where $U_{c,initial}$ and $U_{c,final}$ are the initial and final voltage values shown in figure A.1.

First, R_1 estimation is obtained during MFC operation at a high frequency (e.g. 100 Hz) from the following equation:

$$R_1 = R_{ext}\frac{U_{high}-U_{low}}{U_{low}}, \tag{A.3}$$

where U_{high} and U_{low} are the high and low output voltage levels measured in the experiment (figure A.1). Subsequently, E_{oc} estimation is obtained by operating the MFC at a low frequency (e.g. 1.0 Hz) and low duty cycle. It is assumed that U_{oc} is equal to the voltage at the end of the open circuit part of the cycle:

$$U_{OC} = \max(U_{MFC}), \tag{A.4}$$

Finally, R_2 and C estimations are obtained using voltage measurements at a low operating frequency. It is assumed that V_{cell} reaches a steady-state value at the end of the closed circuit part of each cycle. In figure A.1 this value is denoted as U_{final}.

The value of R_2 is estimated as:

$$R_2 = U_{final}\frac{R_1+R_{ext}}{U_{OC}-U_{final}}, \tag{A.5}$$

The value of C is calculated as

$$C = \frac{\tau}{R_2}\frac{R_1+R_2+R_{ext}}{R_1+R_{ext}}, \tag{A.6}$$

where τ is the time constant shown in figure A.1.

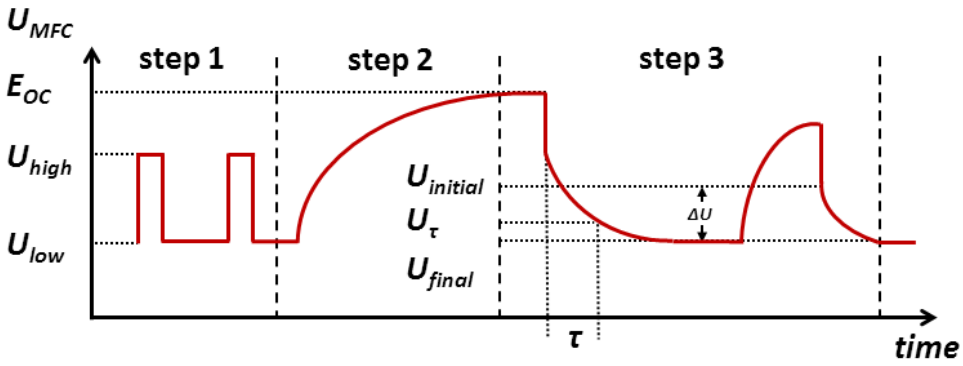

Figure A.1: U_{MFC} profiles at low and high operating frequencies used for online parameter estimation. Operating modes used to estimate R_1, E_{OC}, R_2 and C, are shown as steps 1, 2 and 3, respectively